

THE UNIVERSITY OF MANITOBA

**THE EFFECT OF PROCESS PARAMETERS ON
MICROSTRUCTURE OF TRANSIENT LIQUID PHASE BONDED
SUPERALLOYS INCONEL 738 AND WASPALOY**

BY

NATHAN P. WIKSTROM

A thesis submitted to the Faculty of Graduate Studies in partial fulfillment of the
requirements for the degree of Master of Science

**DEPARTMENT OF MECHANICAL AND MANUFACTURING ENGINEERING
WINNIPEG, MANITOBA
DECEMBER 2006**

THE UNIVERSITY OF MANITOBA
FACULTY OF GRADUATE STUDIES

COPYRIGHT PERMISSION

**THE EFFECT OF PROCESS PARAMETERS ON MICROSTRUCTURE OF TRANSIENT
LIQUID PHASE BONDED SUPERALLOYS INCONEL 738 AND WASPALOY**

by

Nathan P. Wikstrom

A Thesis/Practicum submitted to the Faculty of Graduate Studies of The University of

Manitoba in partial fulfillment of the requirement of the degree

of

Master of Science

Nathan P. Wikstrom © 2006

Permission has been granted to the Library of the University of Manitoba to lend or sell copies of this thesis/practicum, to the National Library of Canada to microfilm this thesis and to lend or sell copies of the film, and to University Microfilms Inc. to publish an abstract of this thesis/practicum.

This reproduction or copy of this thesis has been made available by authority of the copyright owner solely for the purpose of private study and research, and may only be reproduced and copied as permitted by copyright laws or with express written authorization from the copyright owner.

ACKNOWLEDGMENT

I would like to acknowledge my supervisors Dr. M.C. Chaturvedi and Dr. O.A. Ojo whose help and counseling has been paramount in my understanding, and whose advice and support has guided me through this journey. I would also like to thank Dr. N.L. Richards, Dr. J.R. Cahoon, Dr. R. Sidhu, Mr. Seun Idowu, Mr. Dotun Akinlade, Ms. Krutika Vishwakarma, and all members of the Materials group at the University of Manitoba for their many useful discussions.

I acknowledge the financial support for this research by Standard Aero Ltd., Bristol Aerospace, Boeing Canada Technologies Ltd., Manitoba Aerospace Association, and NSERC. I would like to also thank John Van Dorp, Dan McCooeye, Don Mardis, and Mike Boskwick for their technical assistance. Finally, I would like to thank my parents, Mr. Terry and Mrs. Debbie Wikstrom, whose love and support is unquestionably the reason for all of my successes.

ABSTRACT

This dissertation reports the results of an investigation on the effect of process parameters on microstructure of transient liquid phase (TLP) bonded nickel-base superalloys Inconel 738 and Waspaloy. 6.0 x 6.0 x 12.0 mm coupons of superalloy samples were bonded using DF-3 and NB 150 filler alloys in a high vacuum brazing furnace at temperatures ranging from 1100°C to 1225°C for varying lengths of time. Standard metallographic techniques were utilized to prepare and examine the microstructure of the bonded joints by the use of optical and scanning electron microscope techniques.

The effect of bonding temperature and time on microstructure of TLP joints of Inconel 738LC and Waspaloy were investigated. In Inconel 738LC that was bonded with Amdry DF-3, a centerline eutectic was observed to have formed along the joint centerline when an insufficient time was available for a complete isothermal solidification at the brazing temperatures. In the specimens bonded at temperatures between 1120°C and 1175°C, the eutectic width decreased with an increase in the bonding temperature for a constant hold time. Conventional TLP models predict a decrease in bonding time with an increase in temperature, however a deviation from these models was observed in samples bonded above 1175°C. The rate of isothermal solidification was observed to have substantially reduced at these and higher brazing temperatures, and resulted in the formation of a different type of centerline eutectic microconstituent than that formed at lower temperatures.

Although Waspaloy was bonded with a different type of filler alloy, viz., NB 150, the results were similar to those observed in IN738/DF3 system in terms of the formation and width of the eutectic with change in the bonding temperature, and the occurrence of decreased rate of isothermal solidification at temperatures above 1175°C. A Ni-Ti intermetallic phase was observed to have formed in centerline bonded region in both IN 738 and Waspaloy systems that were bonded above 1175°C. It is suggested that a considerable enrichment of the liquated insert with Ti atoms diffusing from the base alloy could be a probable factor contributing to the change in the isothermal solidification rate for both the base-filler alloy systems. This is in agreement with the suggestion by Sinclair et al. that diffusion of a slower second solute out of liquated insert towards the base metal may contribute to the reduction in isothermal solidification rate.

Nevertheless, a notable observation was made in Waspaloy joint bonded at 1175°C, 1200°C, and 1225°C for 6hrs and longer. Boride particles were observed as a part of the centerline eutectic microconstituent, which were completely absent in joints prepared at a lower temperature of 1145°C for 6hrs and longer. This suggests that diffusion of boron out of liquated insert was reduced at higher temperatures. Also, the average eutectic thickness did not decrease with an increase in the bonding temperature from 1175°C to 1225°C. Both of these factors imply that in contrast to the suggestion by Sinclair et al, diffusion of second solute (Ti) might not be the main factor controlling the isothermal solidification stage at higher temperatures where a reduction in the solidification rate was observed. Based on some preliminary work reported in this dissertation it is suggested that instead of the diffusion of second solute, like Ti, certain fundamental diffusion

conceptual factors may be involved. An increase in diffusivity and decrease in solubility of MPD with increase in temperature, as stated in Fick's 2nd law of diffusion, are suggested to be important factors contributing to the reduction in isothermal solidification rate observed at higher temperatures in the present work

TABLE OF CONTENTS

ACKNOWLEDGEMENT	i
ABSTRACT	ii
TABLE OF CONTENTS	v
LIST OF FIGURES	viii
LIST OF TABLES	xi
CHAPTER 1 – INTRODUCTION	1
CHAPTER 2 – LITERATURE REVIEW	4
2.1 Inconel 738	5
2.2 Waspaloy	5
2.3 Alloying and Trace Elements	6
2.4 Microstructure of Cast Inconel 738 and Wrought Waspaloy	8
2.4.1 Gamma (γ) Matrix	8
2.4.2 Gamma Prime (γ') Precipitates	9
2.4.3 Carbides	11
2.5 Joining and Repair of Ni-base Superalloy Components	12
2.5.1 Fusion Welding	13
2.5.2 Brazing	15
2.5.2.1 Advantages of Brazing	16
2.5.3 Transient Liquid Phase (TLP) Bonding	16
2.5.3.1 Advantages and Disadvantages of TLP Bonding	18
2.5.3.2 Joining Atmosphere	19

2.5.3.3	Surface Preparation	21
2.5.3.4	Filler Alloys	22
2.5.4	TLP Bonding Control Mechanisms	24
2.5.4.1	Stage 1 – Heating and Melting of Interlayer	24
2.5.4.2	Stage 2 – Base Metal Dissolution	26
2.5.4.3	Stage 3 – Isothermal Solidification	28
2.5.4.4	Stage 4 – Joint Homogenization	32
2.5.5	Selection of Bonding Parameters (Temperature, Time, Gap Size)	34
2.5.6	Grain Boundaries	36
2.5.7	Transient Liquid Phase Bonding Applications and Anomalies	39
2.5.8	Scope of the Present Investigation	43
CHAPTER 3 – EXPERIMENTAL TECHNIQUES		45
3.1	Materials	45
3.2	Sample Preparation	45
3.3	Microscopic Examination	47
CHAPTER 4 – RESULTS AND DISCUSSION		48
4.1	TLP Bonding of Inconel 738 With Amdry DF-3	48
4.1.1	Microstructure of As-Received Inconel 738 Base Alloy	48
4.1.2	Effect of Diffusion Time on Bond Microstructure	48
4.1.3	Effect of Gap Size on Bond Microstructure	59
4.1.4	Effect of Diffusion Temperature on Bond Microstructure	61
4.1.5	Interface Precipitates	69

4.2	TLP Bonding of Waspaloy with Nicrobraz 150	72
4.2.1	Microstructure of As-Received Waspaloy Base Alloy	72
4.2.2	Effect of Diffusion Time on Bond Microstructure	72
4.2.3	Effect of Diffusion Temperature on Bond Microstructure	75
4.3	Effect of Pre-Bond Heat Treatment of Waspaloy	83
4.4	High Temperature Isothermal Solidification Kinetics	86
CHAPTER 5 – SUMMARY AND CONCLUSIONS		95
CHAPTER 6 – SUGGESTIONS FOR FUTURE WORK		98
REFERENCES		100
CONTRIBUTIONS TO RESEARCH FROM THE PRESENT DISSERTATION		106

LIST OF FIGURES

Figure 2.1	Plot of relative weldability vs. Al and Ti content for a number of Ni-based superalloys [31, 32, 33].	14
Figure 2.2	Stages during TLP bonding process: (a) initial condition (b) dissolution (c) isothermal solidification (d) completion of isothermal solidification (e) solid state homogenization and (f) final condition [46].	25
Figure 3.1	TLP bonding cycle used for all samples.	46
Figure 4.1	Optical micrograph of as-received Inconel 738 showing dendritic structure (X50 mag).	49
Figure 4.2	SEM micrograph of as-received Inconel 738 showing uniformly dispersed γ' particles within γ matrix and MC carbide.	49
Figure 4.3	SEM micrograph of Inconel 738 bonded with Amdry DF-3 at 1120°C for 30 minutes at (a) X800 and (b) X4500.	50
Figure 4.4	SEM micrograph of Inconel 738 bonded with Amdry DF-3 at 1120°C for (a) 290 minutes and (b) 420 minutes.	51
Figure 4.5	SEM micrograph of Inconel 738 bonded with Amdry DF-3 at 1160°C for (a) 30 minutes (b) 290 minutes and (c) 420 minutes.	52
Figure 4.6	EDS spectra of Cr-rich boride particle at bond centerline for (a) entire spectra and (b) boron peak.	55
Figure 4.7	EDS spectra of Ni-rich boride particle at bond centerline for (a) entire spectra and (b) boron peak.	56
Figure 4.8	EDS spectra of γ solid solution phase at bond centerline for (a) entire spectra and (b) absence of boron peak.	57
Figure 4.9	SEM micrograph of Inconel 738 bonded with Amdry DF-3 at 1100°C for 1 hour at a gap size of (a) 100 μ m and (b) 200 μ m.	60
Figure 4.10	SEM micrograph of Inconel 738 bonded with Amdry DF-3 at 1175°C for (a) 290 minutes and (b) 420 minutes.	62

Figure 4.11	SEM micrograph of Inconel 738 bonded with Amdry DF-3 at 1190°C for (a) 290 minutes and (b) 420 minutes.	63
Figure 4.12	(a) SEM micrograph of Inconel 738 bonded with Amdry DF-3 at 1190°C for 290 minutes showing phases present and (b) EDS spectra of Ni-Ti rich phase.	66
Figure 4.13	Fine γ' particles formed within γ matrix Inconel 738 bonded with Amdry DF-3 at 1190°C for 290 minutes	68
Figure 4.14	Variation in concentration of Ti and microhardness of centerline region of bonded region with temperature.	68
Figure 4.15	SEM micrograph of Inconel 738 bonded with Amdry DF-3 for 720 minutes (12 hours) at (a) 1175°C and (b) 1225°C.	70
Figure 4.16	Optical micrograph of as-received Waspaloy showing grain extension in rolling direction (X50 mag).	73
Figure 4.17	SEM micrographs of (a) as-received Waspaloy showing primary and secondary γ' within γ matrix (b) MC carbide in as-received Waspaloy showing reduction in γ' particles immediately adjacent to carbide and (c) heat treated Waspaloy at 1200°C for 30 minutes showing extensive grain growth.	73
Figure 4.18	SEM micrograph of Waspaloy bonded with Nicrobraz 150 at 1100°C for (a) 30 min (b) 360 min and (c) 480 min.	76
Figure 4.19	SEM micrograph of Waspaloy bonded with Nicrobraz 150 at 1145°C for 360 min.	79
Figure 4.20	SEM micrograph of Waspaloy bonded with Nicrobraz 150 for 360 min at (a) 1175°C and (b) 1225°C.	80
Figure 4.21	SEM micrograph of Waspaloy bonded with Nicrobraz 150 at 1175°C for 1 hour with (a) pre-bond heat treatment and (b) as-received.	84
Figure 4.22	SEM micrograph of as-received Waspaloy for 360 minutes at (a) 1200°C and (b) 1225°C.	85
Figure 4.23	SEM micrograph of Waspaloy bonded with Nicrobraz 150 at 1175°C for (a) 10 min (b) 60 min and (c) 360 min.	87

Figure 4.24	SEM micrograph of Waspaloy bonded with Nicrobraz 150 for 360 minutes at (a) 1200°C and (b) 1225°C.	89
Figure 4.25	EDS spectra of eutectic cross section of Waspaloy bonded at 1175°C for 6 hours showing existence of Cr, Mo rich boron containing phase.	90
Figure 4.26	Phase diagram of nickel-boron system showing small solid solubility region of boron in nickel [67].	93
Figure 4.27	Effect of bonding temperature and solubility on total time for complete isothermal solidification for different eutectic systems [39].	93

LIST OF TABLES

Table 2.1	Nominal composition of base metal Inconel 738 and Waspaloy [8, 15].	7
Table 3.1	Composition of interlayer filler alloys (wt. %).	46
Table 4.1	Composition of eutectic phases present for Inconel 738 joints bonded at 1120°C and 1160°C.	58
Table 4.2	Composition of Ni-Ti rich phase present at 1190°C.	67
Table 4.3	Composition of eutectic phases present in Waspaloy joints.	78

CHAPTER 1

INTRODUCTION

Current aero and industrial gas turbine engine designs are formulated to perform effectively within stringent operating conditions, and to render the highest realizable efficiencies and desired outputs. In order to meet the requirements vital for operation of these engines the design criteria demands suitable material selection. A group of high strength alloys known as nickel-base superalloys have found place in a variety of gas turbine engine component applications. Inconel 738LC, which is a γ' ($\text{Ni}_3\text{Al,Ti}$) precipitation strengthened nickel-base superalloy is extensively used as turbine material for hot sections of these engines due to its excellent elevated temperature strength and corrosion resistance [1]. Waspaloy, also a γ' strengthened nickel-base superalloy, has found application in less demanding sections of the engine such as rotors and disks [2]. The demand for higher efficiencies, which require the turbine engine to operate at higher temperatures, has led to increased and faster degradation of certain components through higher levels of creep, fatigue and oxidation. In most situations it is economically more feasible to refurbish damaged components in lieu of complete replacement. As such, a significant amount of work has been done on a number of different types of repair schemes for these alloys including conventional methods such as fusion welding. Although this process can be effective for a number of alloys, those nickel-base superalloy that contain a significant amount of Ti and Al have been found to be difficult to weld due to their high susceptibility to hot cracking during welding or post-weld heat treatment [3]. A process known as transient liquid phase (TLP) bonding [4] has evolved

into an attractive alternative joining technique for these difficult to weld alloys due to a number of technological and economical advantages.

In the TLP bonding process, an interlayer alloy melts between the two base metals to be joined, which involves base alloy dissolution, and forms a liquid phase. This phase rapidly attains equilibrium with the solid base metal. Subsequent to this, due to the interdiffusion of alloying elements between the base metal and the liquid, the melting point of the interlayer liquid at the liquid-solid interface starts to increase and isothermal solidification of the liquid at the interface begins. As the melting point depressing (MPD) solute diffuses continuously into the base metal, the volume of liquid that can be maintained at equilibrium decreases, causing solidification to proceed towards the center of the joint from the mating solid surfaces. If sufficient time for complete isothermal solidification is not allowed at the bonding temperature, formation of eutectic microconstituents could occur along the braze centerline. It is normally the goal to prevent the formation of these microconstituents as they have been found to be deleterious to the mechanical properties of bonded superalloys [5]. Therefore, a proper selection of various process parameters is important in achieving reliable TLP bonded joints in both Inconel 738LC and Waspaloy systems. A number of TLP bonding models, which are normally based on binary alloy systems, have been developed to explain the TLP process mechanisms. However, the phase relationships that are actually encountered in commercial joining of complex multicomponent alloys may not always lend themselves to an extrapolation of binary analysis. Recent studies [6, 7] have suggested that the presence of a second solute either within the original filler metal or

through introduction of dissolved/diffused base metal element may affect isothermal solidification kinetics. Furthermore, certain fundamental diffusion conceptual factors, which have not been generally considered, may also be involved.

In view of this, the objective of the present study was to investigate the effect of bonding parameters, namely temperature, time and gap size, on microstructure developed during bonding of nickel-base superalloys Inconel 738LC and Waspaloy. Similarities in isothermal solidification behavior between each system was evaluated and discussed.

The goal of the work was to provide a better understanding of isothermal solidification rate due to changes in various bonding parameters and to attempt to explain possible factors contributing to the observed solidification behavior encountered during bonding at relatively high temperatures. It is hoped that this work would serve as a basis for further quantitative studies on the seemingly anomalous phenomena observed. In this dissertation, a number of physical metallurgical aspects of both Inconel 738LC and Waspaloy are reviewed, followed by an explanation of the processes involved during TLP bonding. Results and discussions of the purposed investigations will be presented next.

CHAPTER 2

LITERATURE REVIEW

Superalloys can generally be described as a group of alloys developed for use in high-temperature environments under stress, where surface stability, creep strength, and thermomechanical fatigue resistance are imperative. These alloys are generally based on either Fe, Co, or Ni systems and find application in industrial gas turbine and aero-engine turbine components. Intensive compositional, microstructural, and process development of Ni-base alloys over the past few decades has resulted in alloys that can withstand ever increasing temperatures and corrosive environments experienced in today's turbine engines. The superalloy Waspaloy is a widely used wrought alloy for disk and rotor applications, development of which can be traced back to the 1950's. Inconel 738 is a cast alloy having excellent high temperature creep strength and the ability to withstand long times in corrosive environments. Both alloys obtain their high temperature strength through ordered intermetallic $\text{Ni}_3(\text{Al,Ti})$ -type γ' precipitate within γ solid solution matrix. Due to their use in stringent environments, superalloy turbine components often suffer degradation over time. A number of processes for component repair have been used, however difficulties encountered in conventional weld repair processes have resulted in the development of an alternative refurbishment procedure called Transient Liquid Phase (TLP) bonding. During this process a number of bonding parameters can influence the resultant microstructure, and thus the mechanical properties of the joint. This section will attempt to overview the materials used in this study as well as the mechanisms and parameters controlling the final microstructure of the TLP bonded joints.

2.1 Inconel 738

Inconel 738 is a vacuum melted and cast precipitation hardened nickel-base superalloy which possesses excellent high temperature creep-rupture strength combined with hot corrosion resistance. Components manufactured from this alloy can be used in applications requiring service temperatures of up to 980°C [8]. Typical usages include turbine blades, guide vanes, and other hot section components [9]. Inconel 738 obtains its high temperature strength primarily by the presence of 40 % volume fraction of ordered $L1_2$ -type intermetallic $Ni_3(Al,Ti)$ based γ' precipitates within a γ solid solution matrix. It is usually available in either a high or low carbon version, both of which are vacuum cast. The low carbon version (IN 738 LC) also contains a smaller amount of Zr which increases the castability of larger sections [8].

2.2 Waspaloy

Waspaloy is a wrought nickel-base superalloy which possesses excellent high temperature strength and good corrosion resistance up to around 700°C for critical rotating components and up to 870°C for less demanding applications [10, 11]. The alloy was originally developed for use as a turbine blade material, however progressive development of new alloys capable of handling stringent conditions experienced in today's turbine engines has rendered it more suitable as a material for disk and rotor applications [2]. Waspaloy obtains its strength through mechanisms similar to those that govern the strength of Inconel 738, but has a much lower volume fraction of γ'

strengthening phase, normally around 20-30% [12, 13, 14]. Table 2.1 shows the nominal composition of both Inconel 738 and Waspaloy [8, 15].

2.3 Alloying and Trace Elements

Alloying and trace elements in superalloys play an integral role in the optimization of their varying properties. Many elements have a high solubility in nickel and can change its properties depending on the type and amount of element added. Mo, Ta, W, Cr, Co, Re can be added for solid solution strengthening. Oxidation resistance can be increased through Al and Cr additions. While Co increases the upper temperature limit to which an alloy can be used, it can also increase the ability of the alloy to form γ' phase, which itself is obtained through Al and Ti additions [16]. Certain trace elements may be added or excluded based on their metallurgical effects and on properties. It has been reported [17, 18, 19] that residual gases and minor elements such as S and P should be limited in superalloy development. Formation of voids can be initiated through gas introduction, while certain elemental additions can form brittle phases as well as low melting eutectics. B and Zr can also be added for major improvements in creep properties and hot workability, while it has been shown that the addition of B to Waspaloy can significantly improve creep resistance [20]. Recently P has been shown to improve creep properties of some nickel-base superalloys [21] but is harmful to their weldability [22]. Zr, and possibly Hf, have a high affinity for S and can also minimize grain boundary embrittlement caused by this element [17].

Table 2.1: Nominal composition of base metal Inconel 738 and Waspaloy [8, 15].

Element	Inconel 738 (wt%)	Waspaloy (wt.%)
Ni	Bal.	Bal.
Cr	15.84	18.36
Co	8.50	14.02
Mo	1.88	3.73
W	2.48	0.02
Nb	0.92	0.02
Al	3.46	1.49
Ti	3.47	3.12
Fe	0.07	0.61
Ta	1.69	-
C	0.11	0.032
B	0.012	0.005
Zr	0.04	-
S	0.001	0.003

2.4.2 Gamma Prime (γ') Precipitates

The major contributor to high strength in Inconel 738 and Waspaloy is the ordered FCC $L1_2$ -type $Ni_3(Al,Ti)$ based γ' phase particles. This phase forms in Ni-base alloys that contain Ti and Al in amounts exceeding their solubility in Ni. It has been suggested [24] that the composition of γ' in Inconel 738 is $(Ni_{.922}Co_{.058}Cr_{.017}Mo_{.002}W_{.002})_3(Al_{.518}Ti_{.352}Ta_{.046}Nb_{.041}W_{.014}Cr_{.020})$. γ' has an ordered FCC structure with a lattice parameter very close to that of γ matrix. The similarity in unit cell dimensions allows the γ' precipitate to be coherent with the matrix, however small differences between the lattice parameter between the two phases can often render morphological changes in γ' . It has been observed that γ' will form spherically for a 0-0.2% mismatch, develops into a cuboidal shape for 0.5-1% mismatch, and can become plate like above a 1.25% mismatch [16].

Fayman reported, using analytical transmission electron microscope studies of thin foils and extraction replicas, that as received Waspaloy contained two distinct size distributions of γ' , each of which was a different composition [25]. Primary γ' , represented as γ'_p , was found to have a diameter of 194 ± 39 nm and comprised between 3-5% of the total γ' precipitation, while secondary γ' (γ'_s) had a diameter of 44 ± 11 nm. They found that γ'_p was rich in Ni, Co, Ti, and Al, whereas γ'_s contained slightly increased amounts of Cr, Mo, and Fe. Precipitate size and distribution was found to be a function of heat treatment temperature and time. The amount, or volume fraction, of γ' present within the alloy can significantly affect mechanical properties of these alloys. Increasing the Al + Ti content in Waspaloy has been shown [14, 15] to increase both the

yield and tensile strengths at a cost of decrease in ductility. Chang [14] also showed that an increase of 4.5 to 7.5 wt.% of Al + Ti increased the volume fraction of γ' in Waspaloy from 30 to 50 %.

Strengthening due to γ' particles is due to (1) lattice mismatch between γ' and γ , (2) precipitate order (3) precipitate size and (4) volume fraction [16]. As mentioned earlier, a change in lattice mismatch can have an effect on morphology of γ' precipitate which can directly influence the mechanical strength of superalloys [26]. A coherent particle whose lattice parameter differs from the matrix phase induces an elastic strain field around the particle which can contribute a hardening effect due to the dislocation interaction with the field. Particles of γ' possess an ordered atomic structure of preferred atomic positions in of which increases the energy required for dislocations to pass through it. These precipitates possess an energy known as antiphase domain boundary energy which represents the extra energy associated with ordered positions of atoms rather than random ones [16]. Finally, it is well known that dislocations may either bow around precipitates or cut through them. When the precipitates are too small dislocations may not be hindered adequately, however if they are too large dislocations tend to bow around the particles. The optimal strength is thus obtained when the interparticle spacing is just small enough to prevent dislocations from bowing [23].

2.4.3 Carbides

Carbon levels in cast superalloys such as Inconel 738, nominally 0.11 wt%, are normally higher than those of the wrought variety (0.10 wt% max in Waspaloy). Carbides can be formed when carbon combines with a number of refractory elements such as Ti, Mo, Ta, W and Nb to form what are known as MC carbides, and normally form on cooling as discrete particles during the original alloy melting stage. MC carbides usually form in a coarse globular or blocky morphology with a cubic lattice structure, and can exist in either intergranular or intragranular positions. Carbides in general may provide a limited amount of matrix strengthening if their size is small enough, however grain size control and grain boundary strengthening are more palpable traits.

Some MC carbides can transform to $M_{23}C_6$ carbides after exposure to high temperatures during service or through heat treatment operations. The transformation occurs as a reaction between MC and γ such that: $MC + \gamma \rightarrow M_{23}C_6 + \gamma'$ [27]. M_6C may also transform from $M_{23}C_6$ depending on the composition of the superalloy and heat treatment. It has been reported that the formation of $M_{23}C_6$ and M_6C generally occurs in superalloys that contain larger amounts of Cr, and as such deplete the regions immediate adjacent to the carbide which may act as initiation points for stress corrosion cracking [28]. In Waspaloy Fayman [25] reported that the approximate composition of MC and $M_{23}C_6$ carbides were $(Ti_{0.57}Mo_{0.23}Ni_{0.15}Cr_{0.03}Al_{0.02})C$ and $(Cr_{0.80}Ni_{0.09}Mo_{0.08}Co_{0.03})_{23}C_6$, respectively. He suggested that the $M_{23}C_6$ carbides contained significant amounts of Cr while the MC carbides had high levels of Ti and Mo. Due to the large amounts of Ti in

MC carbide it was also found that the matrix adjacent to these particles was denuded of γ' precipitates [25].

The mechanical properties of nickel-base superalloys can be strongly affected by the morphology and distribution of carbides. Script type MC carbides along grain boundaries can lower ductility, acting as a crack initiation site and crack-propagation path if the distribution is continuous [29]. This continuous network of carbides will enhance crack propagation by decohesion between the carbide and matrix. However, discrete and disconnected grain boundary $M_{23}C_6$ carbides can strengthen the grain boundary by the prevention of grain boundary sliding and permit stress relaxation [16]. Carbides can also tie up certain elements that could cause phase instability during service.

2.5 Joining and Repair of Ni-base Superalloy Components

Due to increase in part complexity and cost, joining and repair procedures have become an economical alternative in lieu of complete replacement of Ni-base superalloy turbine engine components. The need for effective repair schemes has led to a large amount of research work on the joining and repair of these alloys. Certain alloys, such as Inconel 738 and to a lesser extent Waspaloy, are known to be difficult to repair by conventional welding techniques, and as such several restoration methods have been employed as appropriate alternatives. The ultimate goal of any repair technique is to obtain a joint with microstructural and mechanical properties that are similar to that of the parent materials being joined. Some processes such as diffusion bonding and diffusion brazing have been used to obtain joints with excellent properties, however, processes involved in

their application may be costly, difficult to prepare, or only applicable to certain material combinations. A number of factors can determine the appropriate repair scheme including service environment, temperature of use, mechanical property requirements, cost, ease of use, etc. Two of the most common methods for the repair of Ni-base superalloys are by either fusion welding or diffusion brazing, also known as transient liquid phase bonding (TLP).

2.5.1 Fusion Welding

Fusion welding refers to the joining of two surfaces by the formation of a liquid phase through localized heating and subsequent cooling of the liquid region. Welding is generally done such that the base material is at or near room temperature and involves significant temperature gradients between weld pool and base material. Some types of fusion welding of superalloys include tungsten inert gas (TIG), electron beam, plasma arc, and laser. Welding can be done with or without filler metals, with the advantage of using fillers allowing more ductility at the bond area as well as the ability to produce welds of variable widths. Fusion welding has been used extensively in the repair of certain superalloy materials, however its use in Ni-base superalloys containing significant amounts of Ti and Al has been restricted due to their high susceptibility to heat affected zone (HAZ) cracking during welding and post weld heat treatments [3]. The cracking probability is normally related to the volume fraction (V_f) of γ' phase present in the alloy [30]. A general relation between the amount of Ti and Al, and thus V_f of γ' phase, is shown in Figure 2.1 [31, 32, 33]. It can be seen that Inconel 738 is generally considered difficult to weld while Waspaloy sits on the periphery of weldable superalloys.

2.4 Microstructure of Cast Inconel 738 and Wrought Waspaloy

Both Inconel 738 and Waspaloy can have complex microstructures owing to the inherently large amount of alloying elements present in them, manufacturing and fabrication process used, and thermal exposure during heat treatments and processing. The most obvious effects of these on microstructures involve the precipitation of γ' , formation of carbides, and possible formation of certain detrimental topologically close packed (TCP) phases such as σ . These phases exist within the γ matrix which is an FCC nickel-base phase containing a number of solid-solution elements.

2.4.1 Gamma (γ) Matrix

The matrix of both Inconel 738 and Waspaloy is FCC nickel-base phase containing a relatively large amount of elements Co, Fe, Cr, Mo, W, etc. in solution. The solubility of elements in nickel can be assessed by Hume-Rothery rules, one of which is based on atomic size factor. Appreciable solubility is obtained when the difference in atomic diameter of the solute and solvent is less than 15 % [23]. The γ matrix acts as a medium for the dispersion of the ordered $\text{Ni}_3(\text{Al,Ti})$ -type γ' precipitates as well as for any formed carbides or other phases. The γ matrix also gains some of its strength by solid solution strengthening, which can be related to the increase in resistance to dislocation motion due to the distortion imparted to the lattice. Lattice distortion is due to the atomic size difference between nickel and the solute atoms and can be determined by the change in lattice parameter of the nickel-rich matrix caused by alloying [23].

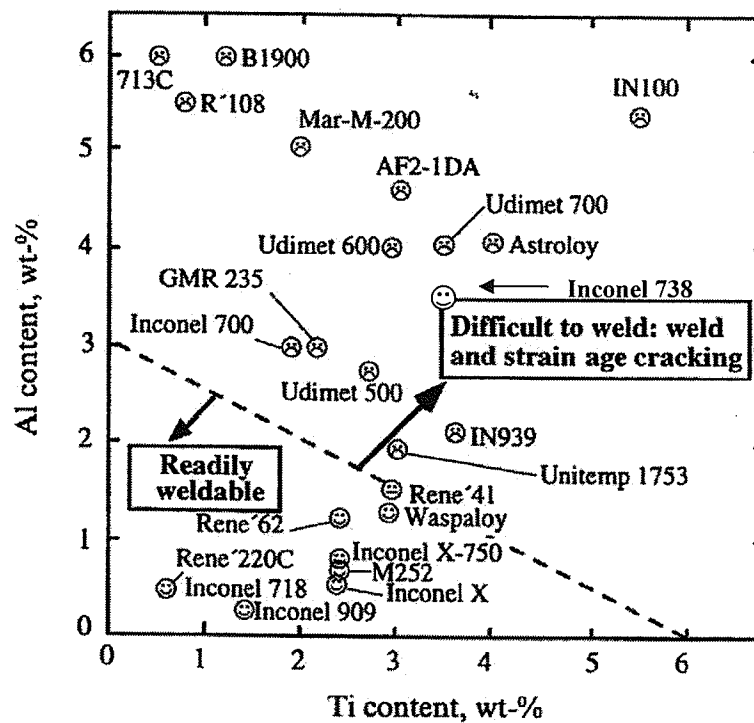


Figure 2.1: Plot of relative weldability vs. Al and Ti content for a number of Ni-based superalloys [31, 32, 33].

The use of fusion welding as a feasible repair technique for Ni-base superalloys can be hindered by a number of factors. The inherent processing steps during welding involves rapid heating and cooling of the part, which can have detrimental effects on the microstructure and properties of the joint. Considerable heat gradients are experienced within the HAZ, and cracking normally occurs in this region. Stresses within the HAZ can develop due to the rapid precipitation of γ' phase during cooling from welding temperature as well as thermally induced due to the difference in temperature between weld pool and component. It has recently been found that HAZ cracking occurred in TIG welded Inconel 738 [34, 35] due to a mechanism involving the constitutional liquation of the γ' phase. Laser welding of Waspaloy has also been shown to be limited by its susceptibility to post weld heat treatment cracking. It was found that cracking during welding of Waspaloy could effectively be controlled by an overaging pre-weld heat treatment and optimization of welding speed and post-weld heat treatments [36].

2.5.2 Brazing

Conventional brazing is a joining technique analogous to soldering but done above temperatures of about 425°C. During brazing a filler metal is placed between two pieces of the material to be joined and the assembly is heated above the liquidus temperature of the filler metal. The filler metal liquates and is held in place by the surface tension between the liquid and solid base metal. A metallurgical bond is then produced between the two pieces upon cooling to the solid state. Typically brazing times are short, on the order of minutes, such that relatively low amounts of solid state diffusion of elements

may occur between liquated filler metal and base alloy. Conversely, a process known as diffusion brazing usually allows for longer brazing times such that significant elemental diffusion could take place. Conventional brazing of nickel-base superalloys and other high temperature materials can lead to inadequate mechanical properties and as such diffusion brazing techniques are often utilized.

2.5.2.1 Advantages of Brazing

Brazing techniques can be used in the aerospace industry for joining difficult to weld materials including Ti, Ni, and Al based alloys. The flexibility of the process allows it to be used for the joining of both cast and wrought products, dissimilar metals, and powder processed metals. A typical requirement of the brazing process is that a vacuum environment is needed, thus, clean superior brazes can be produced due to the elimination of oxygen and other volatile substances from the process. The brazing process is also inherently more accessible as compared to fusion welding, and as such components with complex or varying sections can be easily joined. Since the brazing process requires the entire assembly to be brought up to processing temperature, there is no heat gradient produced in the sections unlike those produced in the HAZ during welding. This can also be an advantageous time and money saver if subsequent heat treatment or aging processes are done in conjunction with the actual brazing cycle.

2.5.3 Transient Liquid Phase (TLP) Bonding

Transient Liquid Phase (TLP) Bonding, also known as Activated Diffusion Brazing (ADB), is a process first developed by Duvall et al. [4] which combines the features of

liquid phase joining and diffusion bonding techniques without the use of large external pressure. Joint microstructures can be produced whose characteristics resemble that of the base materials being joined if the brazing parameters are properly selected. Simple and complex shapes can be joined with relatively easy surface preparation and cleaning techniques. The process has the advantage of economically producing high strength diffusion bonds in certain difficult to join alloys, such as nickel-base superalloys. Its largest application in recent years has been the repair of aero-engine turbine blades and joining of disk to blade assemblies.

In TLP bonding process a thin interlayer material of a specific composition and melting point is placed between two parts to be joined. An interlayer with a composition similar to that of the alloys being joined, but containing a certain melting point depressant (MPD), is normally used. The base metal / interlayer assembly is then placed within a vacuum or inert gas atmosphere, where the interlayer melts at the bonding temperature (which is less than the melting point of the base metal). Normally the brazing temperature and interlayer composition are selected such that minimal dissolution of the base metal is experienced. While at bonding temperature, rapid interdiffusion of elements occurs between liquid layer and solid base metal (changing the composition of the liquid and solid phases) such that equilibrium is established at the joint interface. After this initial equilibrium process, continual diffusion of MPD element out of the liquid phase will cause the joint to isothermally solidify (due to increase in melting point of the liquid phase) from the solid/liquid interface towards centerline. Complete isothermal solidification may occur if enough holding time is allowed at bonding

temperature. After a complete isothermal solidification, a homogenization process can be employed in order to obtain a bond region with characteristics similar to that of base metal. It should be noted that if sufficient time is not allowed for complete isothermal solidification, any residual liquid will solidify to a eutectic-type constituent.

2.5.3.1 Advantages and Disadvantages of TLP Bonding

The use of TLP bonding has provided an alternative method for joining and repair of difficult to weld alloys, including nickel-base superalloys containing higher amounts of Ti and Al. It has an advantage over other alternative joining techniques such as diffusion bonding for the reason that high pressure and complex fixturing are not required. Similar to conventional brazing, TLP bonding can be utilized for complex shaped parts or for bonds with variable thicknesses as well as in different base alloy combinations. Process costs can be reduced due to the ability to braze large numbers of parts at one time, as well as the economic savings induced through smaller refurbishment costs as those compared to total component replacement. Microstructure and mechanical properties of bonding materials can be greatly improved such that properties similar to those of the base metal may be achieved.

Although the TLP process possesses many attractive qualities for the repair and refurbishment of aero-engine components, there are some limitations to its commercial application. The main solidification process can take large amounts of time (on the order of hours) because the process is controlled by the solid-state diffusion of MPD. Because of this many vendors may choose to limit the amount of time at bonding temperature,

thus negating the positive effects of complete isothermal solidification. It has also been found in a number of studies that incomplete isothermal solidification of the liquid insert will form eutectic-type constituents at bond centerline. These microconstituents have been found to be brittle in nature and have generally been assumed to be detrimental to mechanical properties of TLP joints. Diffusion of MPD into base metal substrate has also been shown to precipitate unwanted second phase particles, with potential harmful effect, at braze joint / interlayer interface as well as along grain boundaries. Finally, although setup fixturing is relatively simple compared to diffusion bonding, joints bonded using TLP can often under-perform due to improper fit-up, loss of liquid at joint edge, and poor vacuum status. These and other key parameters of TLP bonding are discussed in the following sections.

2.5.3.2 Joining Atmosphere

TLP bonding of nickel-base superalloys is done at elevated temperatures, normally higher than about 1000°C. At these high temperatures the tendency of the base metal to oxidize is very high, and as such bonding in an appropriate atmosphere is required. Hydrogen type atmospheres can be used as protective environments as hydrogen dissociates oxides developed at high temperatures during bonding. However, its effectiveness does not include alloys containing Ti and Al, such as nickel-base superalloys. Inert atmospheres such as helium and argon may also be employed. The inert atmosphere eliminates any gases, such as oxygen, that may react with the braze assembly. Effective multiple inert gas purging followed by furnace vacuuming can also create a region almost free of any gases during vacuum furnace brazing.

The most common and effective method of diffusion brazing is performed in a vacuum furnace. Nickel-base superalloys and other oxide-susceptible alloys have been successfully bonded using this method. A vacuum system is used to achieve sufficient vacuum in the furnace before actual brazing cycle begins and is maintained throughout the process in order to remove any evolved gas. The vacuum system is normally a stage type system utilizing low vacuum mechanical pump and supplementary high vacuum pump. Low vacuum pump consists of an eccentric that is rotated by an electric motor within an air tight housing partially filled with vacuum pump oil. A spring loaded valve rests against the edge of the rotating eccentric and maintains an air tight seal. Combination of the rotation and the spring loaded valve continuously pulls air out of the vacuum chamber and is expelled through a non-returning valve. Mechanical pumps can usually be employed to reach vacuums of around $10^{-2} - 10^{-3}$ torr. High vacuum can be achieved by a diffusion pump which is an oil based pump in which a tubular barrel of refined diffusion pump oil is boiled by an electric heating element. The vapor produced is then directed up a funneled baffle where it is then directed downwards against the water cooled walls of the pump. When the oil vapor is condensed back to liquid there is a considerable reduction in volume which pulls gas away out of the chamber. It is imperative that the oil not be allowed to contaminate the chamber and also a backing mechanical pump is employed and stabilized before the diffusion pump is engaged.

Some of the advantages of using a vacuum atmosphere include reduction in certain oxides, maintenance of furnace heating coils, and elimination of volatile gases and

impurities. The vacuum atmosphere also eliminates the requirement of using high volumes of special inert or hydrogen type atmospheres. The elimination of any additional gas usage can decrease process costs as well as eliminate the need to use dangerous gases such as hydrogen that can require expensive safety procedures.

2.5.3.3 Surface Preparation

Surface preparation and cleanliness is one of the most important steps in obtaining good quality TLP joints. However, during service the component surface integrity can be compromised by oxidation, debris build up, and combustion products. It is therefore important that any residual films, grease, or oils be removed before brazing cycle is to be attempted. Often times this may require removal of some beneficial coating that may have been applied to the component to increase its resistance to corrosive environment. A good brazing surface should have a sufficient surface roughness and good wettability by the filler alloy which itself should have a relatively low viscosity to allow for good flow and adhesion in the joint. Clean surfaces are normally obtained by mechanical surface removal or chemical cleaning such as fluoride ion cleaning among others.

Mechanical cleaning is normally used when there is a large amount of surface oxide, the oxides are easily accessible, and when the surface to be joined must be of a specific shape or completely flat. The mechanical cleaning process can consist of grit blasting, grinding, brushing or filing. The advantage of this process is that the cleaning process is normally simple, inexpensive, and allows for some level of required surface roughness. Chemical methods normally employ hot vapor soaking and rinsing cycles until the

required cleanliness is achieved. Fluoride cleaning methods offer a quality method to effectively clean narrow thermal fatigue cracks for in service components. This method of cleaning normally involves heating of the part to be joined in a hydrogen rich environment wherein fluorocarbon gas is introduced to reduce surface oxides.

2.5.3.4 Filler Alloys

Brazing filler alloys containing boron, silicon, and/or phosphorus as MPDs have been used extensively in the repair and refurbishment of nickel-base superalloy components used in aero-engine and land based turbine engines. The characteristics of these alloys are very important in the production of high quality TLP bonded joints. It is therefore imperative that filler alloy chemistry, physical shape, and dimensions be optimized for the required interlayer / base metal system.

The main and most obvious requirement of any filler alloy is for it to have a chemical composition similar and with a liquidus less than the solidus of the base metal. For brazing of nickel-base superalloys this is obtained by using a nickel based filler metal with an addition of boron, silicon, or phosphorus MPD. These elements can be added in specific amounts to reduce the melting temperature such that their composition is usually close to a eutectic point. Filler alloys that have compositions close to a eutectic will also experience less dissolution of base metal than those of non-eutectic composition and lower minimum temperature requirement for brazing. The MPD should also have an appreciable solubility and/or diffusivity in the base alloy. Boron is normally considered to diffuse in nickel-base alloys by an interstitial mechanism and thus exhibits a high

diffusion coefficient. However, the solubility of boron in pure nickel is quite low at a value of around 0.3 at. % [37]. Elements such as carbon, titanium, and aluminum are also normally deliberately excluded from filler metals due to their tendency to form undesirable stable phases during bonding that have a tendency to embrittle the joint [3].

The composition of the braze filler alloy is an important factor if the joined component is to be reinstated back into service. It is imperative that the properties of the joint region be close or the same as those of the base alloy such that mechanical properties and oxidation resistance are maintained. Because of this elements such as Cr can be added to nickel-base filler alloys in significant amounts mainly to increase oxidation and corrosion resistance. Additional alloying to braze filler alloys may not be required depending on the braze and homogenization stages used during processing. General compositional similarity of the bond region can be obtained even without the addition of secondary base alloy elements if thin gap sizes are used and sufficient time is allowed during homogenization stage.

The filler alloys are used in varying forms including tape, powder/paste, amorphous foil, and rapidly solidified sheet. Thin foils ($\leq 50\mu\text{m}$) are normally produced by rapid solidification whereas larger thickness fillers tend to be tapes formed by accumulation of powdered particles maintained by a rigid binder. Another approach is the use of a cored interlayer with a dissimilar surface. The interlayer exists as a base material, such as pure nickel with a surface enriched with MPD by a diffusion treatment.

2.5.4 TLP Bonding Control Mechanisms

TLP bonding is a relatively simple process that involves the use of a filler metal or interlayer of specific composition placed between the two metals to be joined and the whole assembly is heated to a specific bonding temperature and held for a certain duration of time. A significant number of models have been developed to explain the mechanisms controlling each stage during TLP bonding. Conventional models [38, 39] are based on binary alloy-liquid systems where the interlayer may be of a single composition (type I) or close to eutectic composition (type II). Duvall et al [4] originally defined three stages of TLP bonding, namely, base metal dissolution or erosion, isothermal solidification of liquated interlayer, and homogenization of bond region. Tuah-Poku et al [39] added melting of filler alloy and homogenization of liquid to the list of TLP stages, while MacDonald and Eagar [40] also considered a “stage 0” which involved heating rate effects during initial stages heating above interlayer liquidus to bonding temperature. Stages of TLP bonding process for an interlayer with composition close to eutectic are shown schematically in Figure 2.2.

2.5.4.1 Stage 1 – Heating and Melting of Interlayer

This initial heating stage of TLP bonding covers the first part of stage 1 where the bond assembly is heated up from room temperature to the melting point of interlayer (T_M). This is then followed by initial melting of the interlayer above T_M . The interlayer may melt over a range of temperatures but is normally assumed to be close to the terminal eutectic composition and thus possessing one finite melting point. During melting the interlayer should wet the solid base metal surface and flow throughout the joint.

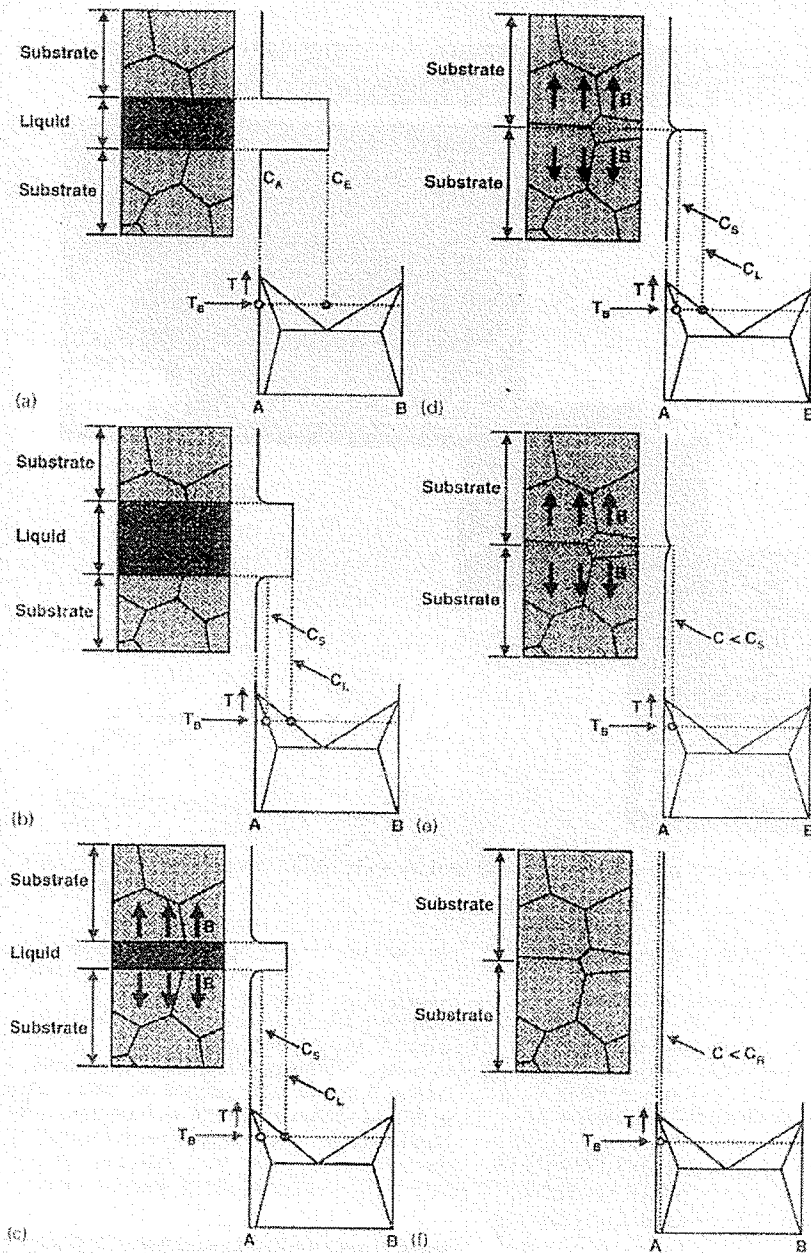


Figure 2.2: Stages during TLP bonding process: (a) initial condition (b) dissolution (c) isothermal solidification (d) completion of isothermal solidification (e) solid state homogenization and (f) final condition [46].

Wetability of the base metal surface will depend on the surface energy of both the liquid and solid as well as the viscosity of the liquid. In general, liquid metals do not wet oxidized surfaces therefore underscoring the need for a clean brazing surface.

2.5.4.2 Stage 2 – Base Metal Dissolution

Base metal dissolution stage occurs immediately after liquation of filler metal and will progress during heating from T_M to bonding temperature (T_B). During dissolution stage the composition of the MPD in the liquid will vary along the liquidus line towards its equilibrium value at temperature T_B . This may occur rapidly if T_B is reached very quickly or may involve continual modification as the bonding temperature is increased from T_M to T_B . The composition of MPD in solid state will also modify in a similar manner along the solidus line reaching an equilibrium value correspondingly at T_B . In order for the liquid to modify its composition according to the phase diagram, the width of the liquid will have to grow in order to effectively reduce its MPD concentration. The maximum width of liquid, or maximum dissolution width, will be reached at some time after reaching T_B . Nakao et al [41] suggested that the dissolution phenomenon could be modeled on the basis of the Nerst-Brunner theory such that:

$$\frac{dC}{dt} = K \left(\frac{A}{V} \right) \cdot (C_s - C_t) \quad (1)$$

where, C_s is the solute concentration of MPD at saturated state, C_t is the instantaneous value of solute concentration, A is the surface area of the solid, V is the volume of the liquid phase, and K a constant. Assuming that the system being used can form a eutectic then the values for C_s and C_t can be easily found by the equations:

$$C_i = \left[\frac{ph}{x + ph} \right] C_i \quad , \quad C_s = \left[\frac{ph}{x_s + ph} \right] C_i \quad (2)$$

where, C_i is the initial concentration of MPD in interlayer, p is equal to ρ_l/ρ_s , ρ_l is the density of the liquid interlayer, ρ_s is the density of the base material, $2h$ is the initial thickness of the interlayer, x is the instantaneous dissolution width, and x_s is the maximum dissolution width at saturated state. From this a distribution parameter P can be determined by the following such that:

$$P = Kt = h \left\{ \ln \frac{x_s(x + ph)}{ph(x_s - x)} \right\} \quad (3)$$

Nakao et al [41] showed that there was a linear relationship between this dissolution parameter P and the holding time. Time required for dissolution was usually of the order of seconds or minutes, and did not normally play a significant role in the total time required for bonding which is usually of the order of hours. However, it has been reported [42, 43] that during bonding with very thin filler metals ($<5\mu\text{m}$) the isothermal solidification stage could commence at temperatures below T_B during dissolution. This phenomenon may be more readily experienced with the use of MPD with high diffusivities and the use of slow heating rates reaching bonding temperatures far above the melting point of the interlayer material. This could hypothetically lead to a complete isothermal solidification of joint area preceding the completion of dissolution stage for very thin initial interlayer gap sizes.

In another approach Zhang and Shi [44] developed a quantitative model for base metal dissolution. Since this stage normally happens very quickly and does not significantly increase total time for bonding, its kinetics may become secondary to its effect. Zhang

and Shi [44] developed a model to more adequately determine base metal dissolution thickness as compared to earlier approximations based on phase diagram considerations only. They developed an equation based on work by Lashko [45] such that the maximum dissolution thickness, W_t , could be determined from:

$$W_t = C_L W_B \left(\frac{\rho_L}{\rho_m} \right) \left[1 - e^{\left(\frac{\alpha t}{W_B} \right)} \right] \quad (4)$$

where, C_L is the solubility coefficient, α is the dissolution coefficient (where both C_L and α vary with temperature and pressure), ρ_L and ρ_m are the densities of the liquid and base metal respectively, and t is the time variation. Their work found that there was a difficulty in obtaining accurate dissolution and solubility parameters due to the complexity of chemical compositions of most base metals and interlayers. However, good agreement was found between predicted and experimental results. Their findings showed that the initial interlayer thickness and temperature (C_L and α) had a strong influence on base metal dissolution.

2.5.4.3 Stage 3 – Isothermal Solidification

In conventional TLP bonding theory, isothermal solidification stage is assumed to commence after the dissolution stage has completed. This stage occurs at a constant temperature, T_B , where the liquid is assumed to be of equilibrium liquidus composition ($C_{L\alpha}$), and the solid immediately adjacent to the solid/liquid interface to be of equilibrium solidus composition ($C_{\alpha L}$). At a constant bonding temperature, continual diffusion of MPD element out of the liquid into the solid base material will cause the compositional equilibrium state to shift. A decrease in the amount of liquid that can be maintained at

constant temperature due to the loss of MPD will cause isothermal solidification to occur at the liquid/solid interface, which will cause it to move towards the centerline of the liquated interlayer. The only phase that can form is the solid solution phase because no solute rejection into the liquid may occur at the interface. This solidification stage could occur quite slowly because it is controlled by solid-state diffusion of MPD into base metal. The isothermal solidification stage is considered complete once the entire joint region has solidified and the local composition of the joint centerline has reached a value of $C_{\alpha L}$. Because of the relatively slow nature of the isothermal solidification stage it is normally considered to be the most important stage as it controls the total bonding time.

A number of models have been developed and proposed to explain the isothermal process controlling mechanisms. These models are normally based on a number of fundamental assumptions. The assumption of local equilibrium condition, based on the phase diagram, existing at the solid/liquid interface at bonding temperature is integral to the modeling process. However, a recent review by Gale and Butts [46] has revealed that there is a body of recent discussion over the extent to which this local equilibrium is maintained under classical conditions. Secondly, the effect of convection in the liquid is negligible due to the thickness of the interlayer and the composition of the liquid is uniform. Finally, the interdiffusion coefficients in both the solid and liquid phase are assumed to be independent of composition and the base metal can be assumed to be semi-infinite.

A number of analytical [39, 40, 41, 47, 48, 49] and numerical [50, 51, 52, 53, 54] approaches to the modeling of isothermal solidification stage during TLP bonding have been developed. TLP bonding is a diffusion based process and is governed by Fick's first and second diffusion laws:

$$F = -D \frac{\partial C}{\partial x} \quad , \quad \frac{\partial C}{\partial t} = \frac{\partial}{\partial x} D \frac{\partial C}{\partial x} \quad (5)$$

where, F is the rate of transfer per unit area section, C is the concentration of diffusing element, x is the distance of travel through the section, D is the diffusion coefficient, and t is time. Tuah-Poku [39] using derivations by Shewman [55] showed that the solute distribution in semi-infinite base metal can be given by the following error function:

$$C(x, t) = C_{al} + (C_M - C_{al}) \operatorname{erf} \left[\frac{x}{\sqrt{4Dt}} \right] \quad (6)$$

where, C_M is the initial solute concentration in base metal, D_s is the solute diffusion coefficient in base metal, C_{al} is the equilibrium solidus composition existing in the base metal immediately adjacent to the liquid/solid interface, x is the distance along the specimen length from the surface, t is the time. This model considers the braze assembly to be a half semi-infinite base metal with stationary interface where solute concentration is maintained at C_{al} . Integration of Fick's first law coupled with the derivative of equation (6) yields the total amount of solute, M_t , entering the base material as represented by:

$$M_t = 2(C_{al} - C_M) \sqrt{\frac{Dt}{\pi}} \quad (7)$$

If the amount of total solute present is assumed constant during the brazing process it can be shown that:

$$M_i = \frac{C_0 W_0}{2} \quad (8)$$

where, C_0 is the initial solute concentration in the interlayer and W_0 is the initial width of the interlayer. By substituting equation (8) for M_i in equation (7) and rearranging for time, t , Tuah-Poku et al. [39] developed an equation to express the time required to complete the isothermal solidification stage:

$$t = \left(\frac{\pi}{16D} \right) \frac{C_0^2 W_0^2}{(C_{al} - C_M)^2} \quad (9)$$

The above equation assumed a single phase model based on a stationary solid/liquid interface. Further work on two phase systems was systematically done by Ramirez and Liu [47], Liu et al [48], Lesoult [49] and Zhou [52] among others and found similar but more accurate results than those yielded by equation (9). Specifically Zhou [52] found that:

$$t = \frac{W_{\max}^2}{16K^2 D} \quad (10)$$

where, K is a constant, W_{\max} is the maximum liquid width and can be approximated by:

$$W_{\max} = \frac{C_0 W_0}{C_{L\alpha}} \quad (11)$$

and K can be computed numerically by solving:

$$\frac{C_{al} - C_M}{C_{L\alpha} - C_{al}} = \sqrt{\pi} \left[\frac{K(1 + \operatorname{erf}(K))}{\exp(-K^2)} \right] \quad (12)$$

Earlier work by Tuah-Poku et al [39] was based on a single phase solution and reported that estimates of isothermal solidification time were very high. They suggested that actual solidification conditions may not be as those assumed including complexities due to a moving boundary surface and curved surfaces due to liquation of grain boundaries.

However, later work showed that the use of migrating solid/liquid interface based models tended to more closely represent actual bonding conditions.

Recent work done by Ojo et al [56] compared models based on this migrating solid/liquid interface as well as a different approach developed by Gale and Wallach [57, 58]. They suggested in their work that base metal dissolution and isothermal solidification stage could occur simultaneously instead of sequentially in contrast to earlier researchers. The solid base material and liquid interlayer were subsequently treated as a continuum where the time required for complete isothermal solidification could be estimated by:

$$C_{\alpha L} - C_M = (C_0 - C_M) \left[\operatorname{erf} \left(\frac{W}{\sqrt{4Dt}} \right) \right] \quad (13)$$

where, $C_{\alpha L}$ is the equilibrium solidus solute concentration, C_M is the initial solute concentration in the base metal, C_0 is the initial solute concentration in the interlayer, W is the initial half thickness of the interlayer, D is the diffusion coefficient, and t is the time required for complete a isothermal solidification. Ojo et al [56] using IN 738LC superalloy and Ni-Cr-B filler alloy found that this method and those based on the moving solid/liquid interface could be used to reasonably predict the time required for a complete isothermal solidification to occur. The predicted times from the two different models were comparable and were in good agreement with experimentally determined values.

2.5.4.4 Stage 4 – Joint Homogenization

Homogenization stage is generally assumed to follow the completion of isothermal solidification stage and is usually done at a temperature below that of brazing temperature. With increasing time at homogenization temperature, MPD element

concentration will decrease at bond centerline in addition to increased diffusion of base metal solute elements towards the bond centerline. The goal of the homogenization process is to obtain a joint with chemistry and microstructure similar or identical to that of the base metal.

Modeling of homogenization stage has been done by a number of workers [47, 59]. Ramirez and Liu [47] showed that the time required to reduce the concentration of MPD solute at centerline down to a required level, C_r , can be determined by:

$$t = \left(\frac{1}{k_2^2} - \frac{1}{k_1^2} \right) \frac{(2h)^2}{16D} \quad (14)$$

where, h is the original half thickness of the interlayer, D is the solute diffusion coefficient, and where C_r is the final desired concentration and constants k_1 and k_2 can be determined from:

$$\frac{C_{al}}{C_0} = \text{erf}(k_1) \quad , \quad \frac{C_r}{C_0} = \text{erf}(k_2) \quad (15)$$

Ramirez and Liu's work however was based on diffusion of MPD out of the bond region into base metal region. It is normally advantageous in certain systems to allow for diffusion of base metal elements during homogenization. Often times certain elements, such as Ti and Al, are specifically avoided in interlayer chemistry because they have been found to form very stable interfacial phases during bonding [4]. Homogenization allows for the diffusion of these elements towards the solidified joint region. In view of this, Ikawa [59] used an equation based on Fick's Law to represent solute concentration at the bond centerline:

$$C_r = C_M + (C_0 - C_M) \operatorname{erf} \left[\frac{h}{4\sqrt{Dt}} \right] \quad (16)$$

where, C_r is the required concentration of base metal solute at the bond centerline, C_M is the initial concentration of the diffusing solute in base metal, C_0 is the initial solute concentration in the interlayer region, h is the maximum half thickness of liquated region, D is the diffusion coefficient of solute, and t is the time required for homogenization. In their work, Nakao et al [60] using aluminum distribution during homogenization of a nickel base superalloy, found close agreement between the results yielded by this equation and their experimental results.

2.5.5 Selection of Bonding Parameters (Temperature, Time, Gap Size)

Proper selection of bonding parameters during TLP bonding of nickel-base superalloys is principal to achieving a sound and reliable joint for use in high temperature applications. The brazing temperature can have a significant effect on the joint microstructure and the subsequent mechanical properties. Bonding is normally done at temperatures just above the liquidus temperature of the interlayer, so as to minimize heat effects on base metal microstructure and dissolution. This approach can be beneficial because less energy would be required at lower temperatures and extensive grain growth can be prevented.

An increase in temperature would be required for the use of higher melting point interlayers containing certain beneficial secondary elements (W, rare earth elements, etc.). Furthermore, the use of higher temperature during brazing would increase the diffusion coefficient of the MPD into the base metal in any system, and would thus tend to increase the rate of isothermal solidification. Since the increased rate of isothermal

solidification would reduce the time required for bonding, the use of higher temperatures may be economically attractive. Use of higher temperature would also increase the rate of bond homogenization after isothermal solidification of joint region is completed.

The effect of brazing time at a specific brazing temperature is also very important in the bonding process. For a complete isothermal solidification to take place, sufficient time at brazing temperature is required to allow for diffusion of MPD into base alloy. In situations where sufficient hold time is not allowed, any residual liquid at centerline could transform during cooling to a eutectic-type solidification product. It is generally known that this eutectic product would be brittle and could have detrimental effects on mechanical properties of the joint. The time required for a complete isothermal solidification would depend on both diffusivity and solubility of MPD in the base metal, which are in turn influenced by the bonding temperature.

At a constant temperature the amount of diffused MPD for any given time period should be independent of differences in the initial interlayer gap size. It stems from this that longer time would be required for larger initial gap sizes to complete the isothermal solidification step, since they contain more MPD compared to smaller gap sizes. Therefore, the width of residual liquid, which transforms during cooling into centerline eutectic, would be expected to decrease with a decrease in the initial filler gap size. Larger initial interlayer thicknesses could also lead to a prolongation of homogenization stage due to increase in the required base metal element diffusion distance.

2.5.6 Grain Boundaries

Grain boundaries can have a number of effects on elemental diffusion during heat treatments as well as during TLP bonding process. Assuming that the lattice diffusion distance is much larger than the grain size, such as that found in many wrought superalloys, the grain boundary can have a large effect on the diffusion of different species through the substrate. Under this condition grain boundary diffusion can be orders of magnitude faster than lattice diffusion. With increasing holding time at elevated temperature diffusion mechanism may change due to the effects of grain growth and grain boundary migration. Mishin and Razumovskii [61] indicated that moving grain boundaries intensively absorb diffusant elements and can spread them in a relatively thin layer near the grain surface, thus increasing the effective diffusion rate. Suto and Sato [62] also reported that effective solubility of boron in nickel could be increased in fine grained condition as compared to single crystal. They reported that the apparent solubility of boron in polycrystalline nickel increased remarkably with decrease in grain size, and attributed the increase to more trapping of B atoms at grain boundaries.

Ikeuchi et al [63] reported that grain boundaries can affect TLP bonding kinetics by a number of factors including (1) high diffusivity in the grain boundary region, (2) the balance between grain boundary energy and liquid/solid interfacial energy, (3) the interfacial energy due to the curvature of the liquid/solid interface, and (4) diffusional flow along the solid liquid interface caused by factors (2) and (3). While brazing pure nickel with Ni-P filler alloy, they reported that liquid penetration occurred at grain boundary sites during isothermal solidification with a greater fraction occurring at high

angle random grain boundaries. Through extensive modeling Ikeuchi et al [63] showed that in order for isothermal solidification process to progress the amount of MPD must be reduced in the liquid. They also found that significant liquation of grain boundary regions were evident in base metal regions immediately adjacent to liquated interlayer region. They theorized that rapid diffusion of MPD out of liquated region into base metal grain boundaries would effectively reduce the composition of MPD in the local area of liquid immediately adjacent to the grain boundary region. This in effect would cause solidification in a direction towards the centerline of the joint and not liquation in a direction towards the base metal. In effect the higher diffusivity in grain boundary regions would displace the liquid/solid interface in a direction opposite of what is normally observed (liquation along grain boundaries in a direction away from the centerline of the joint). Therefore, the effect of higher diffusivity along grain boundaries causes a decrease in the amount of liquid present at the grain boundary. Ikeuchi et al [63] subsequently showed that by considering the balance between grain boundary energy and liquid/solid interfacial energy, the rate of isothermal solidification of the liquid as a whole was increased, and the shape of liquid penetration was towards the base metal and agreed with their observed results. Kokawa et al [64] observed that liquid penetration at large angle grain boundaries was much more pronounced than at low angle ones. Thus, a decrease in grain boundary energy will slow down the development of liquid penetration. Kokawa et al [64] also found liquid penetration at grain boundary regions would also increase isothermal solidification rate due to the increase in total solid/liquid interfacial area. Nakagawa et al [43] similarly found that the formation of a non-planar solid/liquid interface due to grain boundary penetration increased the effective solid/liquid interfacial

area and accelerated the diffusion of MPD solute into the base metal. In their review, Gale and Butts [46] reported that the effect of grain boundary dissolution is often attributed incorrectly to preferential diffusion of solute along the grain boundary. In fact, the use of higher temperatures (close to melting point of base alloy) during TLP bonding renders grain boundary diffusion no faster than that of lattice bulk diffusion.

In their work, Kokawa et al [64] reported that the rate of isothermal solidification was greater when fine grained nickel was used during TLP brazing using Ni-P filler alloy. They attributed their findings to an increase in the overall interfacial area created by the penetration of liquid at grain boundary regions. The fine grained nickel contained a larger fraction of grain boundary sites, thus it increased the overall solid/liquid interfacial area and the rate of isothermal solidification. Saida et al [65] reported that the completion time for isothermal solidification decreased in the order of single crystal, course-grained, and fine grained nickel using the same Ni-P filler alloy. In their study of TLP bonding of CMSX-2 superalloy using Ni-Cr-B filler alloy, Kim et al [66] reported that dissolution rate could also be affected by grain size. They reported that base metal dissolution width decreased with a decrease in grain size, however, grain boundary penetration was more significant with decreasing grain size. Similarly in an earlier work by Tuah-Poku et al [39] it was suggested that liquid penetration at grain boundary regions could be a factor contributing to marked differences between their calculated and experimental isothermal solidification completion times.

2.5.7 Transient Liquid Phase Bonding Applications and Anomalies

A number of studies have been done on TLP bonding including those focused on modeling, microstructural development, and process parameter selection. As discussed, there are a number of different models used to describe certain stages during TLP bonding. New numerical and hybrid type modeling solutions have become more accurate in quantifying these stages, however a remnant problem persists in the availability of reliable data such as diffusion coefficients, solubilities, and partitioning data [46]. Binary phase diagram data, Ni-B in this study, can be difficult to apply to higher order systems owing to differences in reported data and unknown effect of secondary base alloy elements. Data such as maximum solubility of MPD element in base alloy can be very significant in modeling of certain time dependent stages of TLP bonding, especially isothermal solidification. A number of different values of solubility of boron in nickel have been reported in literature [37, 67, 68]. One solution to the unavailability of reliable phase diagrams of multi-element alloys has been the use of calculated diagrams. Campbell and Boettinger [69] used this approach to evaluate TLP bonding in the Ni-Al-B system. In a different approach Sinclair et al. [6, 7] actually suggested that in the case where two solutes are removed from the liquid at very different rates, due to a significant difference in their respective solubilities and/or diffusion coefficients, that isothermal solidification stage could be divided into two parabolic regimes, the first regime being dominated by the “faster” solute, and the second by the slower of the two. They suggested that a deviation from isothermal solidification rate predicted by conventional TLP diffusion models, which are normally based on binary systems, could be encountered during bonding of multicomponent alloys.

Work done by Natsume et al [70] using phase-field simulation found that reduction in liquid width during isothermal solidification stage may be difficult to identify at temperatures relatively higher than the melting point of filler alloy. They reported that in pure nickel bonded with 50 μm Ni-P interlayer at 1200°C, the liquid width increased to 115 μm during dissolution stage, reduced to 105 μm during 1 hour at bonding temperature, and finally reduced to 40 μm during cooling stage. Eutectic type microstructure was only visible in a thickness of 40 μm therefore attributing around 65 μm of reduction in liquid thickness to cooling. This could be expected where the bonding temperature used is much higher than melting temperature of the interlayer such that $C_{L\alpha}$, the equilibrium liquidus concentration, could increase significantly during cooling stage causing a reduction in the volume of liquid present at equilibrium.

A number of quantitative and microstructural studies have been done on TLP bonding of nickel and nickel-base superalloys. Work by Nakao et al [71] on a number of different superalloy and interlayer compositions found that a linear relationship occurred between the liquid width and the square root of holding time during bonding. They suggested that isothermal solidification was controlled by solid state diffusion of MPD in the superalloys. Successful joining or repair of superalloys by TLP bonding method has been reported in a number of studies. High-quality TLP joints were reported by Yeh and Chuang [72] in the repair of Inconel 718SPF superalloy with Ni-P and Ni-Cr-P as well as by Le Blanc and Mevrel [73] on bonding of DS 247 to Astrolloy using Ni-Si-B interlayer. Jung and Kang [74] explored the use of thin boron interlayer in the bonding of nickel-

base superalloy Rene80. They found that the width of the eutectic layer had a linear relationship with the square root of holding time and that microstructures free of eutectic constituents could be achieved. Recently, Jalilian et al [75] successfully bonded Inconel 617 using Ni-Si-B interlayer. Saha et al [76] also reported that TLP bonding was a successful method for joining oxide dispersion strengthened (ODS) superalloy MA758 using both Ni-Cr-Fe-B-Si and Ni-P interlayers.

In addition to TLP bonding of polycrystalline superalloy materials, successful joining of a number of single crystal alloys has been reported. Nishimoto et al [77, 78, 79] bonded single crystal superalloys CMSX-2 and CMSX-4 using Ni-Cr-B and Ni-Cr-Co-W-Al-Ta-B interlayers. They found that the γ solid solution phase grew epitaxially into the liquid phase from the substrate during isothermal solidification. More importantly they reported that single crystallinity was maintained in the joints and tensile properties of the joint were almost identical to the base metal. W. Li et al [80, 81] studied TLP bonding of an unnamed Ni-Co-Cr-W-Mo-Al-Ti superalloy with 45 μm thick Ni-Co-Cr-W-Mo-B interlayer. They reported that bonding could be accomplished and crystallographic orientation was maintained along the joint. Their selection of interlayer composition was such that the interlayer was very similar to the base metal, however γ' forming elements aluminum and titanium were specifically excluded while boron was added as a MPD. Complete isothermal solidification was reported to be achieved in 35 hours at 1220°C, which is an especially long time considering the temperature used. They attributed this effect to the absence of high-diffusivity grain boundary paths in the base material. In a different work, X. Li et al [82] bonded single crystal superalloy DD6 with an interlayer of

almost identical composition with addition of MPD element boron. They also reported excessively long times of 24 hours for a complete isothermal solidification at 1290°C with a gap size of 40 μm . The result of extended solidification time for these systems suggests that either the absence of grain boundary regions and/or selection of high operating temperatures could cause sluggish isothermal solidification rate behavior.

Microstructural development of TLP bonds in real systems can be complex, and deviation from conventional expectations may be observed. Gale and Wallach [57] in their work on joining of pure nickel using Ni-Si-B interlayer found that diffusion of boron into the solid substrate before equilibration of the liquid and solid phases could result in development of significant boron concentrations immediately adjacent to the solid/liquid interface. Similar effect of departure from equilibrium at solid/liquid interface was found using Ni-P interlayers by Natsume et al [70]. The influx of boron could thus lead to the precipitation of boride phases in the substrate at bonding temperatures below the binary nickel-boron eutectic temperature, which was not predicted by conventional models. Gale and Wallach [57] suggested that continuous distributions of these stable phases may be detrimental to in-service properties of the joint. Xie et al [83] reported formation of borides at interfacial zone of IC6 superalloy even at higher bonding temperatures of 1220°C. Idowu et al. [84] also reported that precipitation of a complex cubic Cr-, Mo-, and W-based $\text{M}_6(\text{C},\text{B})$ phase in Inconel 738 TLP bonded joints was observed in the base metal adjacent to bond centerline. Formation of stable borides were found on the Ni side while bonding NiAl to Ni using Ni-Si-B interlayer by Orel et al [85] at temperatures below the Ni-B eutectic temperature.

Furthermore, they reported that a rapid increase in aluminum content was observed in the eutectic with increase in brazing time. Using a filler metal originally void of aluminum, bonding done at 1065°C for only 1 (one) minute revealed a eutectic with average aluminum concentration of 6 (six) at.%. Dissolution of NiAl substrate was observed to occur rapidly and extensively even at this relatively low temperature, and was suggested to be responsible for the rapid increase in aluminum content present in the liquid state at the bond centerline. Gale and Guan [86] also found that significant diffusion of Al from NiAl side of Ni/Cu/NiAl bond formed stable γ' (Ni_3Al) on the opposite pure Ni side during bonding at 1150°C (Cu interlayer thickness = 50 μm). It is clear that compositional modification of liquid and/or a second phase formation within the substrate could occur due to significant base metal diffusion of alloying element during TLP bonding of some systems.

2.5.8 Scope of the Present Investigation

Proper selection of various process parameters is paramount to achieve reliable TLP bonded joints in both Inconel 738LC and Waspaloy systems. A number of TLP bonding models, which are normally based on binary alloy systems, have been developed to explain the process mechanisms and simulate the production of joints devoid of any harmful phases. However, the phase relationships that are actually encountered in commercial joining of complex multicomponent alloys may not always lend themselves to an extrapolation of the binary analysis. Recent studies have suggested that the presence of a second solute introduction into liquated insert during bonding process may affect isothermal solidification kinetics.

In view of this, the present study was initiated to further investigate the effect of bonding parameters, namely temperature and time, on microstructure of TLP bonded nickel-base superalloys. Inconel 738LC was bonded using Amdry DF-3 (Ni-Cr-La-B) filler alloy and Waspaloy with Microbraz 150 (Ni-Cr-B) filler alloy. The results of the study are presented and discussed in Chapter 3 and 4 of this thesis.

CHAPTER 3

EXPERIMENTAL TECHNIQUES

3.1 Materials

The base alloys used in this study were as-cast Inconel 738 sectioned into 6.0 x 6.0 x 12.0 mm coupons, and wrought Waspaloy sectioned into 7.0 x 8.0 x 10 mm coupons. Inconel 738 was supplied by Hitchiner Manufacturing Co. and was used in as-cast condition, while Waspaloy was supplied by Allvac Inc., and was used in both wrought and heat-treated form. Commercial interlayer metals Amdry DF-3 (Ni-Cr-Co-Ta-La-B) and Microbraz 150 (Ni-Cr-B), whose compositions are given in Table 3.1, were used as filler alloy.

3.2 Sample Preparation

The base metal coupons were sectioned from as-received plates by using a numerically controlled wire electro-discharge machine (EDM). EDMed surfaces were subsequently polished to 600 grit using SiC grinding paper to remove the re-cast layer formed through the EDM process, and were ultrasonically cleaned in acetone for 15 minutes. The filler alloy was thereafter placed between the cleaned surfaces and the couple tack welded to ensure minimal movement during brazing operation. The sides of the base metal were coated with Microbraz green "stop off" to prevent liquid flow out of joint area during bonding.

Table 3.1: Composition of interlayer filler alloys (wt. %).

Element	Amdry DF-3	Nicrobraz 150
Ni	Bal.	Bal.
Cr	20	15
Co	20	-
Ta	3.0	-
La	0.05	-
B	3.0	3.5

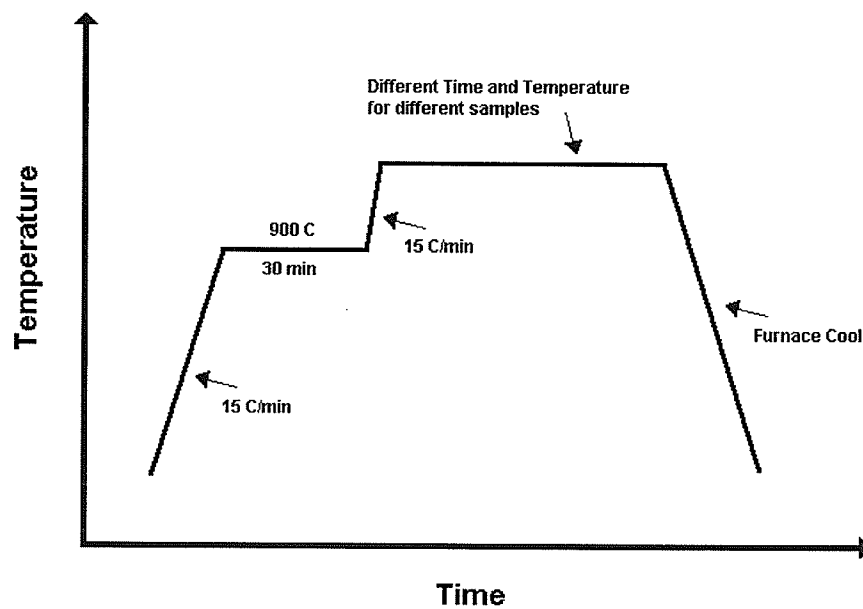


Figure 3.1: TLP bonding cycle used for all samples.

TLP bonding was carried out in a LABVAC II brazing furnace under a vacuum of 10^{-4} to 10^{-5} torr at a variety of temperatures and for various holding times. The brazing cycle employed is shown in Figure 3.1. Bonded samples were sectioned using EDM due to the brittle nature of the brazement and prepared by standard metallographic techniques for microstructural assessment. Polished Inconel 738 samples were electro-etched in 12 ml H_3PO_4 + 40 ml HNO_3 + 48 ml H_2SO_4 solution for 6 V for 5 seconds. Waspaloy samples were either electro-etched using same solution or etched using Kalling's reagent.

3.3 Microscopic Examination

Preliminary general assessment of the joint microstructure was performed by an inverted-reflected light microscope equipped with a CLEMEX Vision 3.0 image analyzer. Scanning electron microscopic microstructural examination, using secondary and backscatter electron image modes, and compositional analysis of brazement were conducted by a JEOL 5900-LV scanning electron microscope, equipped with a thin window Oxford energy dispersive spectrometer (EDS) system equipped with INCA software. Microhardness of centerline region of the bonded joint was determined by Leitz microhardness tester at 100 gram load.

CHAPTER 4

RESULTS AND DISCUSSION

4.1 TLP Bonding of Inconel 738 With Amdry DF-3

4.1.1 Microstructure of As-Received Inconel 738 Base Alloy

An optical micrograph of as-received cast IN-738 LC is shown in Figure 4.1. As shown in this figure, electro-etched as-received samples showed a cored dendritic structure which is typical of a cast alloy. The microstructure of the as-received material is also shown in Figure 4.2 which was obtained by SEM operated in secondary electron mode. As seen in this figure the microstructure consisted of unimodal γ' phase within the γ matrix and also contained randomly dispersed intragranular MC carbides. The average grain size of the material was determined to be about 750 μm .

4.1.2 Effect of Diffusion Time on Bond Microstructure

To study the effect of holding time on the microstructure of Inconel 738 bonded with 75 μm Amdry DF-3 filler alloy, brazing was done at 1120°C and 1160°C for 30, 290, and 420 minutes. The microstructures of the samples joined at these temperatures, as obtained by SEM operated in secondary electron mode, are shown in Figures 4.3 and 4.4., and 4.5. The microstructure of the joint produced after 30 minutes holding at both the temperatures showed the existence of continuous distributions of centerline eutectic-type constituent. The average eutectic thickness, after this holding time, decreased from 20.3 μm in the 1120°C sample to 14.9 μm in the 1160°C sample. EDS compositional analysis of the three main phases observed within the eutectic, given in Table 4.1,

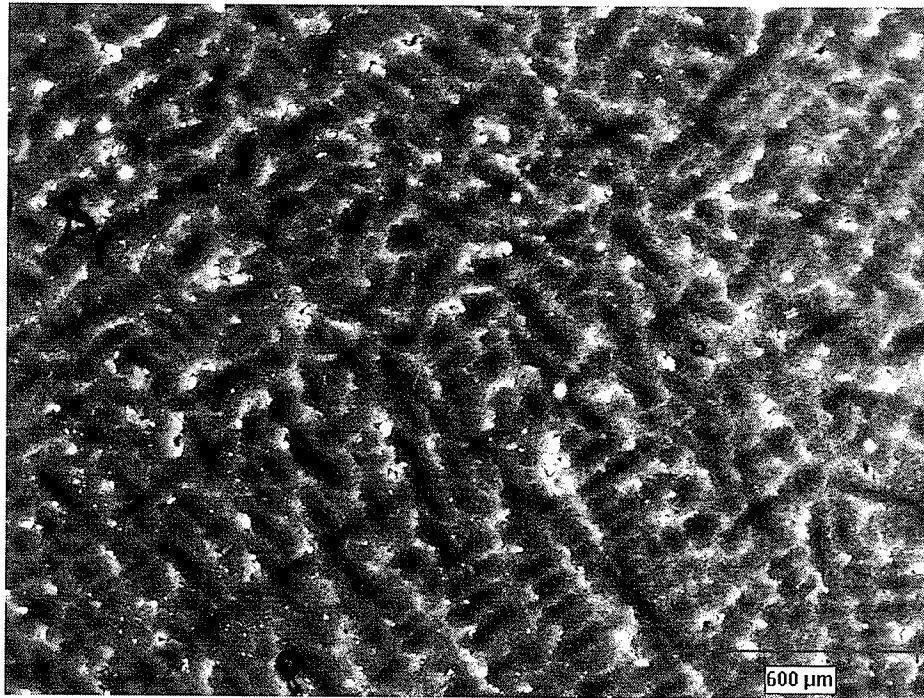


Figure 4.1: Optical micrograph of as-received Inconel 738 showing dendritic structure (X50 mag).

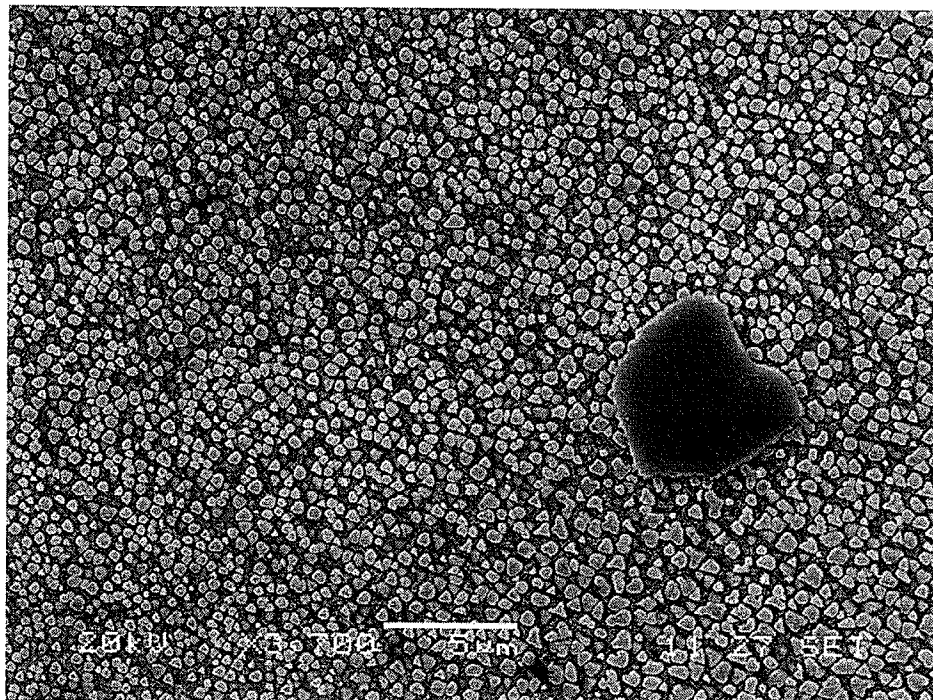


Figure 4.2: SEM micrograph of as-received Inconel 738 showing uniformly dispersed γ' particles within γ matrix and MC carbide.

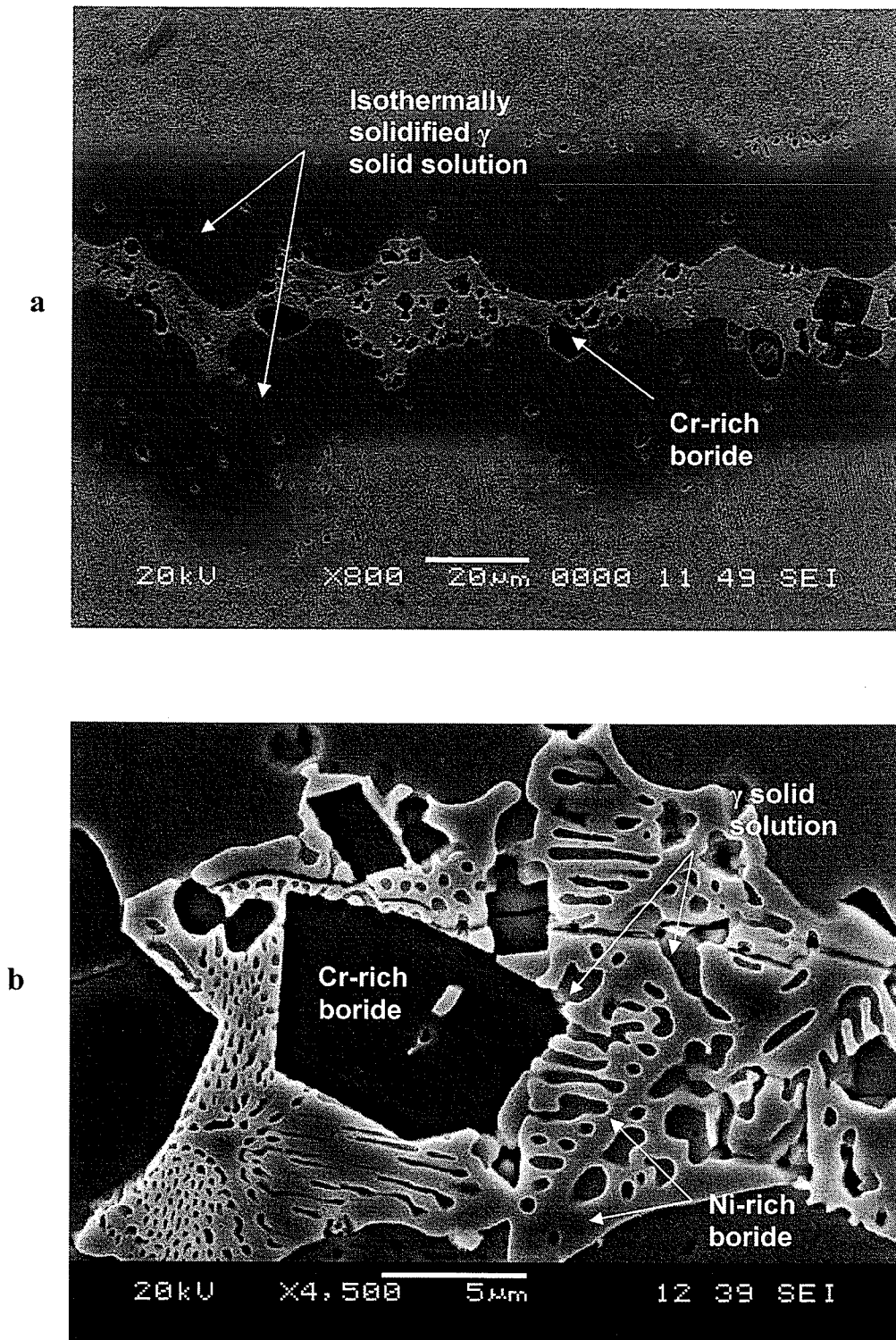


Figure 4.3: SEM micrograph of Inconel 738 bonded with Amdry DF-3 at 1120°C for 30 minutes at (a) X800 and (b) X4500.

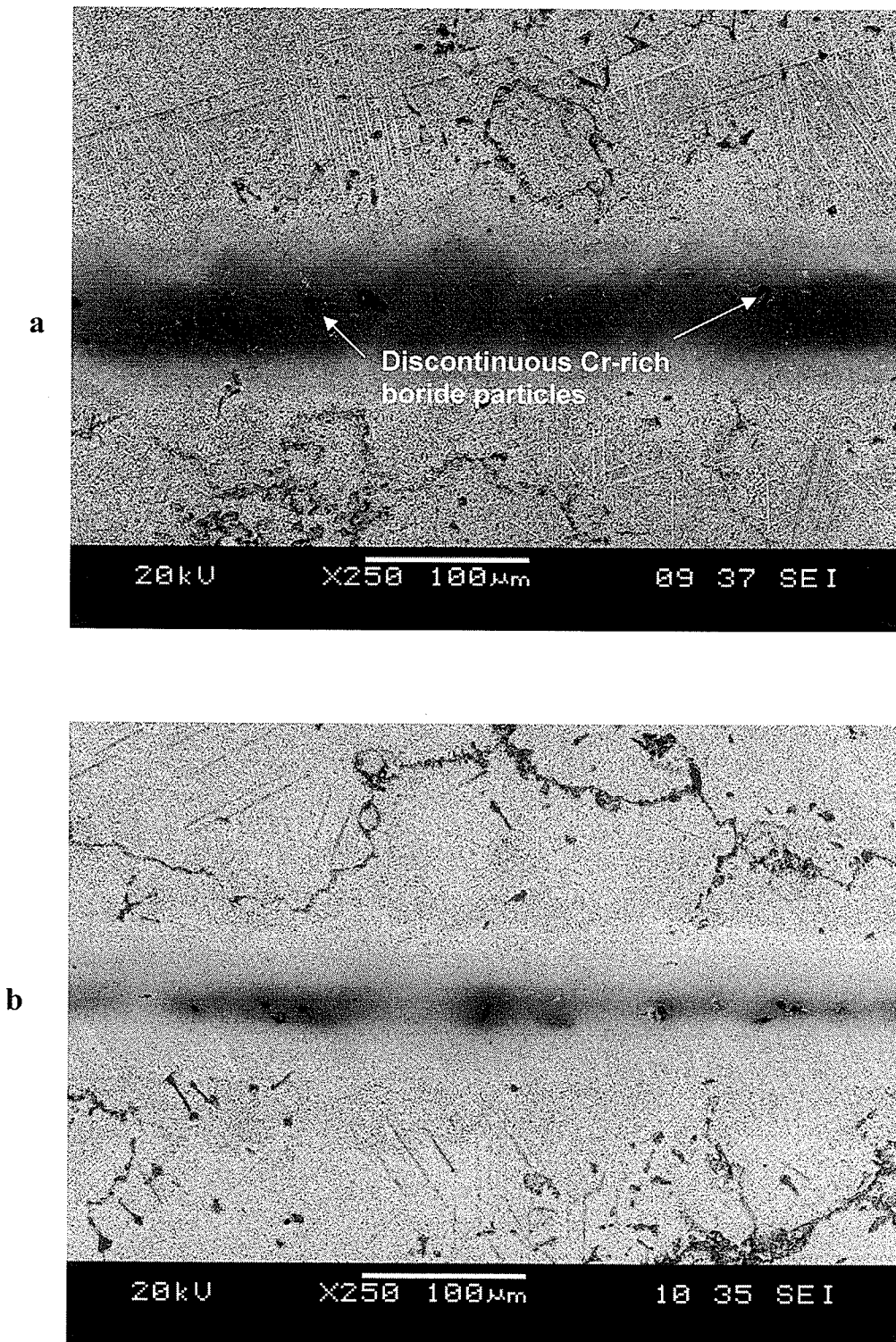
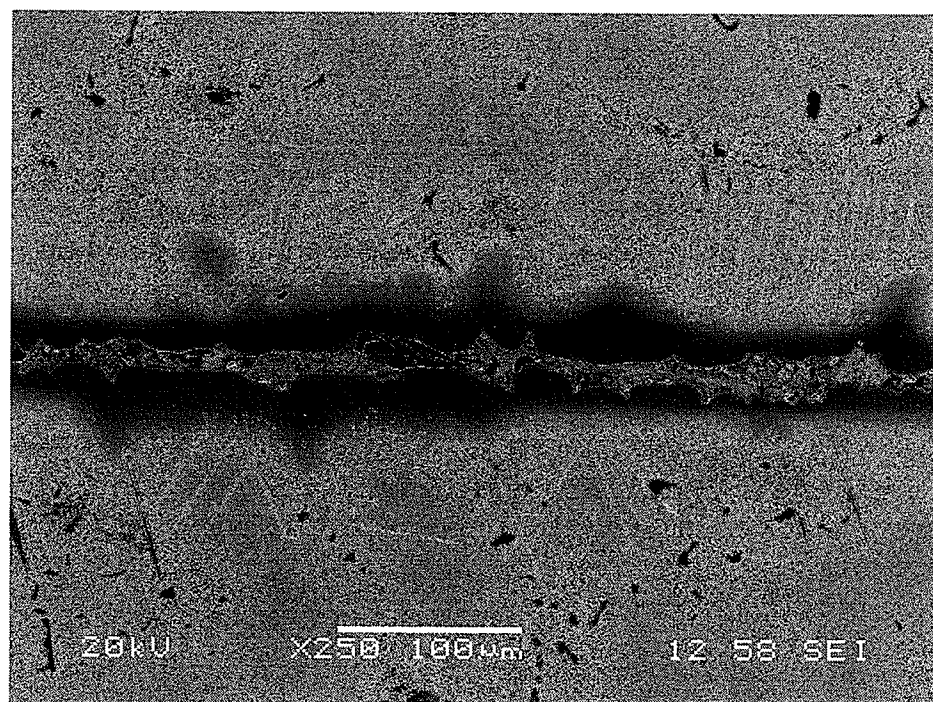


Figure 4.4: SEM micrograph of Inconel 738 bonded with Amdry DF-3 at 1120°C for (a) 290 minutes and (b) 420 minutes.

a



b

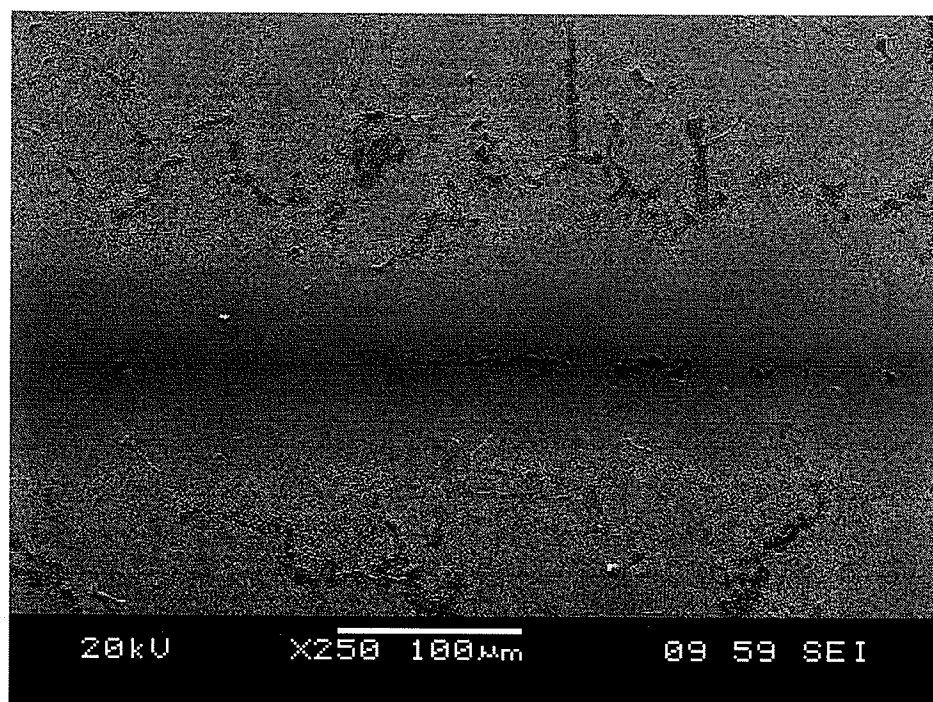
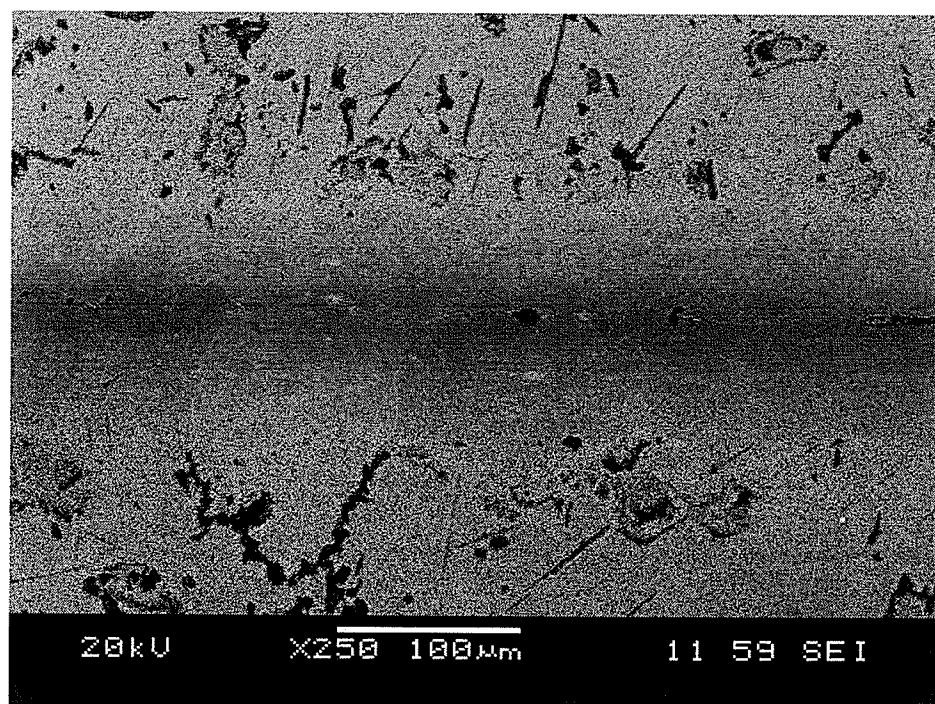


Figure 4.5: SEM micrograph of Inconel 738 bonded with Amdry DF-3 at 1160°C for (a) 30 minutes (b) 290 minutes and (c) 420 minutes.

c



suggested them to be nickel base solid solution phase, which was similar to the phase adjoining the eutectic product, a nickel rich boride phase and chromium rich boride phase. Figures 4.6, 4.7, and 4.8 show typical EDS spectra of these phases. On increasing the holding time at both bonding temperatures there was a considerable reduction in the width of the eutectic constituent such that after both 290 and 420 minutes only a discontinuous distribution of chromium rich particles was observed at bond centerline (Fig. 4.4 and Fig. 4.5b,c). Boron was detected in all boron rich particles but could not be measured due to the inability of the software to quantify light elements accurately. It can be seen that bonding of Inconel 738 with 75 μm Amdry DF-3 at 1120°C and 1160°C for 30, 290, and 420 minutes is insufficient for complete isothermal solidification of the liquated interlayer. Similar eutectic microstructure in the centerline of TLP bonded Ni alloy has been observed by other researchers. For example, by the use of Scheil simulations Ohsassa et al. [50] studied the solidification behavior of residual liquated insert during TLP bonding of pure nickel with Ni-B-Cr ternary filler alloy, and reported the formation of a ternary centerline eutectic consisting of nickel base solid solution (γ), nickel boride (Ni_3B) and chromium boride (CrB) at 997°C. For samples initially held at 1100°C they showed that solidification of the residual liquid initially formed γ , followed by the eutectic reaction $\text{L} \rightarrow \gamma + \text{Ni}_3\text{B}$ at 1042°C. Completion of solidification was reported to be at 997°C with a ternary eutectic reaction $\text{L} \rightarrow \gamma + \text{Ni}_3\text{B} + \text{CrB}$. Gale and Wallach [57] in their work on TLP bonding of pure nickel using Ni-Si-B filler alloy similarly reported the formation of a deposit of $\text{Ni} + \text{Ni}_3\text{B}$ eutectic mixture in a sample brazed at 1150°C for 5 minutes. In the present work the centerline eutectic constituent is suggested to be formed by the solidification of liquated filler during cooling from the

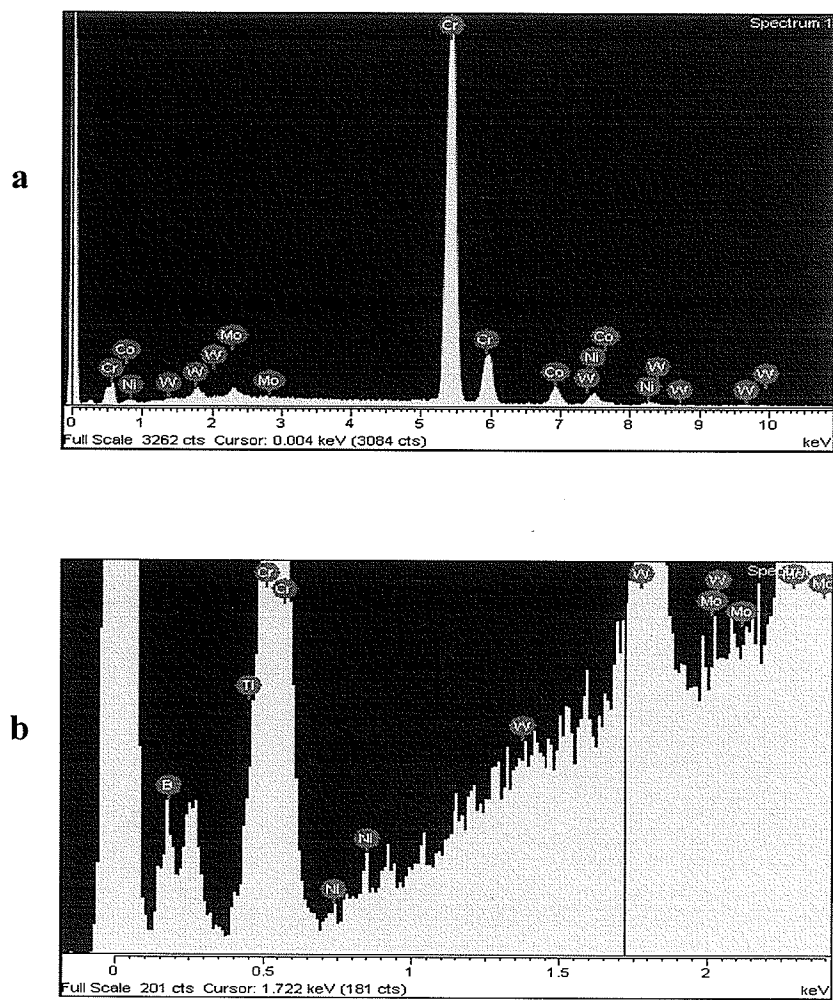


Figure 4.6: EDS spectra of Cr-rich boride particle at bond centerline for (a) entire spectra and (b) boron peak.

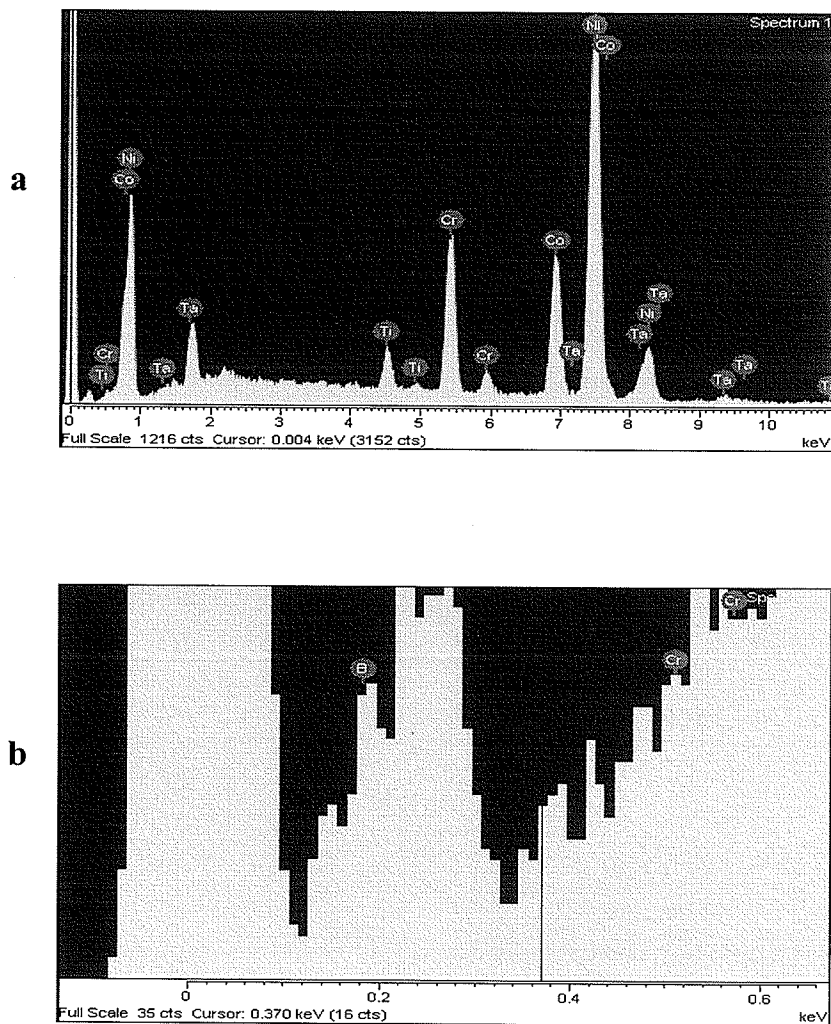


Figure 4.7: EDS spectra of Ni-rich boride particle at bond centerline for (a) entire spectra and (b) boron peak.

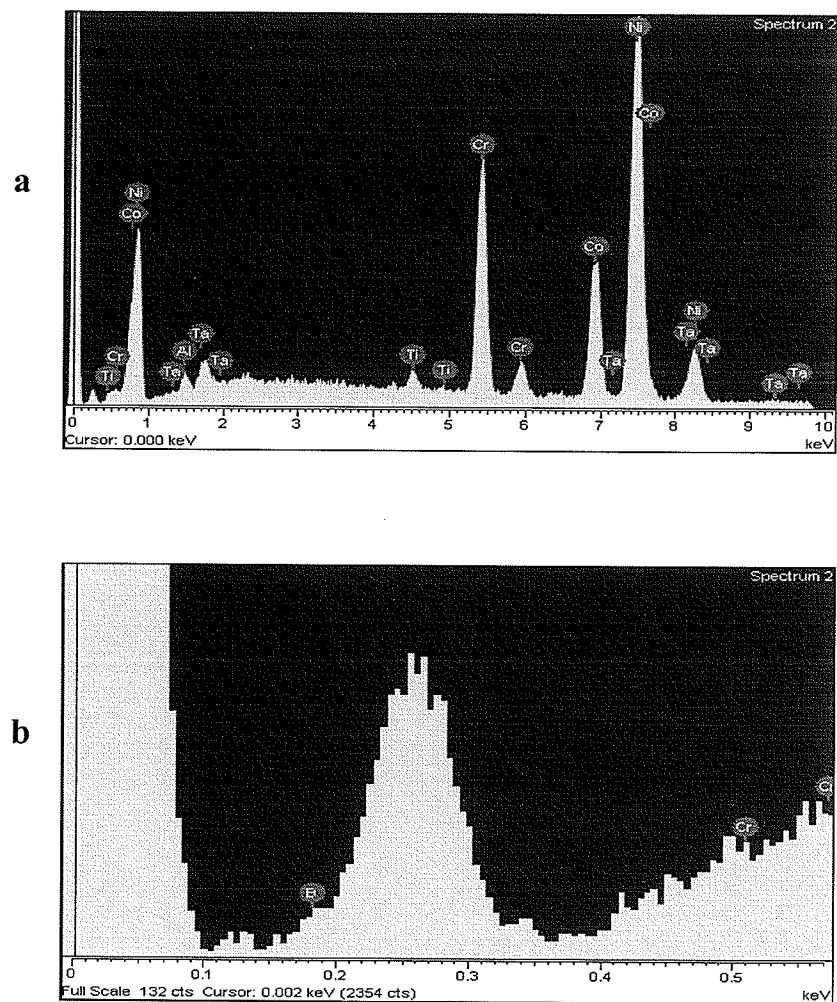


Figure 4.8: EDS spectra of γ solid solution phase at bond centerline for (a) entire spectra and (b) absence of boron peak.

Table 4.1: Composition of eutectic phases present for Inconel 738 joints bonded at 1120°C and 1160°C.

Element	Cr-rich boride (at%)	Ni-rich boride (at.%)	Gamma (γ)
Ni	4.87	62.35	57.63
Cr	86.09	10.41	18.64
Co	7.86	19.96	17.99
Al	-	-	1.42
Ti	-	3.42	1.86
Nb	-	0.62	0.30
Ta	-	2.77	1.29
W	0.54	0.47	0.39
Mo	0.64	0	0.48

brazing temperature when a sufficient hold time for complete isothermal solidification was not allowed. The formation of these eutectic constituents, especially in a continuous fashion along braze centerline, would be deleterious to the mechanical properties of the bond joint as their existence could provide a low resistance path for crack propagation.

4.1.3 Effect of Gap Size on Bond Microstructure

As mentioned earlier, migration of solid-liquid interface, i.e. isothermal solidification of liquid insert during TLP bonding occurs by diffusion of melting point depressing solute away from the liquid into solid base alloy. At constant temperature and holding time, the amount of boron diffusion and, thus, extent of isothermal solidification would be the same independent of gap size. Therefore, the width of residual liquid, which transformed during cooling into centerline eutectic, is expected to decrease with a decrease in the initial filler gap size, as was observed in Figure 4.9. This implies that a longer time will be required to achieve complete isothermal solidification in larger gap size samples compared to smaller gap size samples. Models based on the diffusion induced solid-liquid interface motion have been used in estimating the time, t_f , that is required to produce a single phase microstructure during TLP bonding through a complete isothermal solidification of liquated insert. Generally, in these models, the time t_f is approximated by:

$$t_f^{1/2} = \frac{2h}{\gamma 4D^{1/2}} \quad (17)$$

where, D is diffusion coefficient of the melting point depressant in the solid base alloy, and $2h$ is the maximum width of the braze insert following its equilibration at solid-liquid

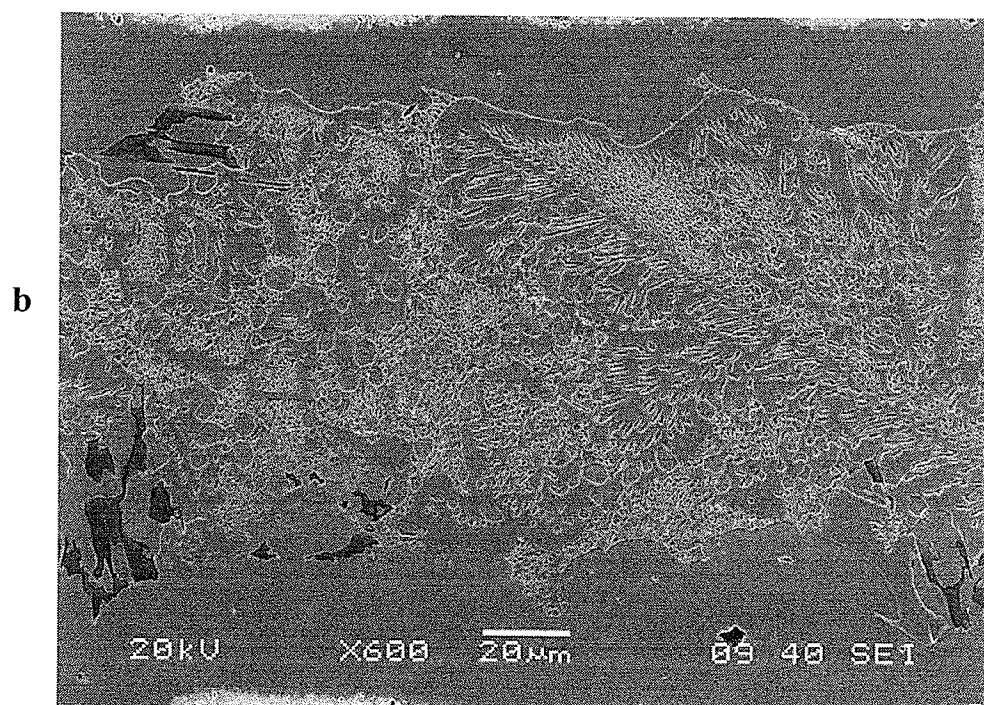
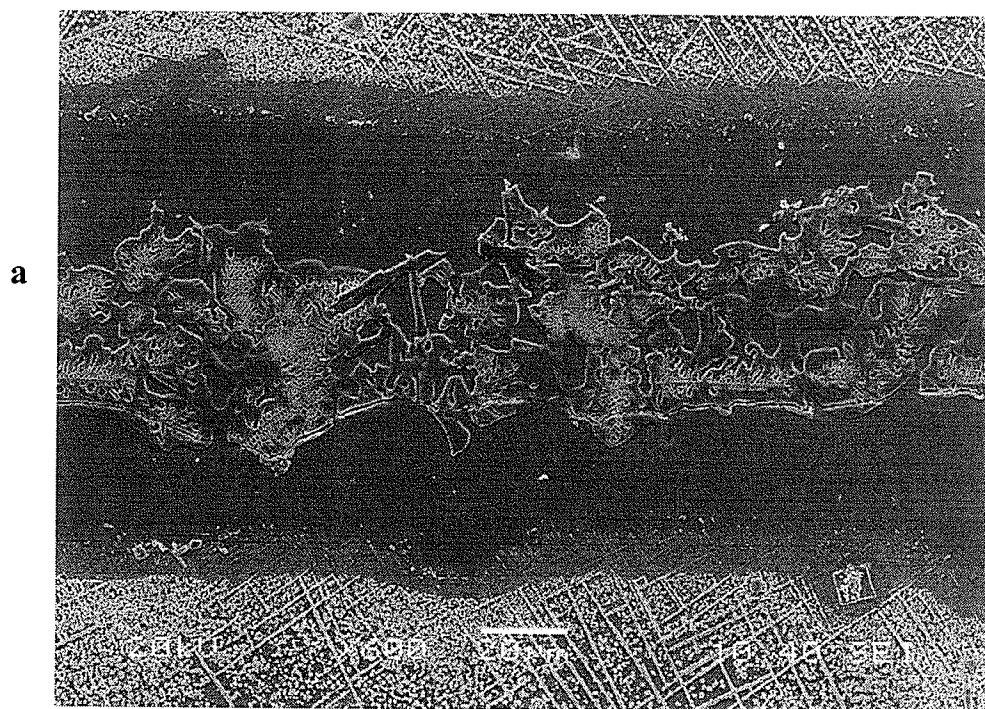


Figure 4.9: SEM micrograph of Inconel 738 bonded with Amdry DF-3 at 1100°C for 1 hour at a gap size of (a) 100 µm and (b) 200 µm.

interface. γ is a dimensionless parameter, which is estimated by solving the following equation numerically:

$$\frac{C_{\alpha} - C_m}{C_{\beta} - C_{\alpha}} = \gamma \sqrt{\pi} \exp(\gamma^2 (1 + \operatorname{erf} \gamma)) \quad (18)$$

where, C_{α} and C_{β} are solute concentration in the solid and liquid phase at the migrating interface, respectively, and C_m is the initial solute concentration in the base alloy. The maximum width, $2h$, of the braze insert after equilibration depends strongly on the initial width (W) of the interlayer employed. Thus, it can be seen from equation 17, and as indicated by the present observation, that the time, t_f , for full migration of the solid-liquid interface to prevent formation of the centerline eutectic will increase with increase in gap size for at given temperature.

4.1.4 Effect of Diffusion Temperature on Bond Microstructure

To study the effect of temperature on bond microstructure of Inconel 738 with 75 μm thick Amdry DF-3 filler alloy, brazing was done at 1175°C and 1190°C for 290 and 420 minutes. SEM micrographs of these brazed joints are shown in Figures 4.10 and 4.11. It can be seen that almost complete isothermal solidification was achieved in the sample brazed at 1175°C for 420 minutes. It can be seen that an almost complete isothermal solidification was achieved in the sample brazed at 1175°C for 420 minutes. This is as predicted by the TLP bonding model that an increase in the rate of isothermal solidification would occur with an increase in brazing temperature.

The isothermal solidification is considered to be complete when the concentration of the melting point depressant solute at center of the liquated interlayer is reduced to the value

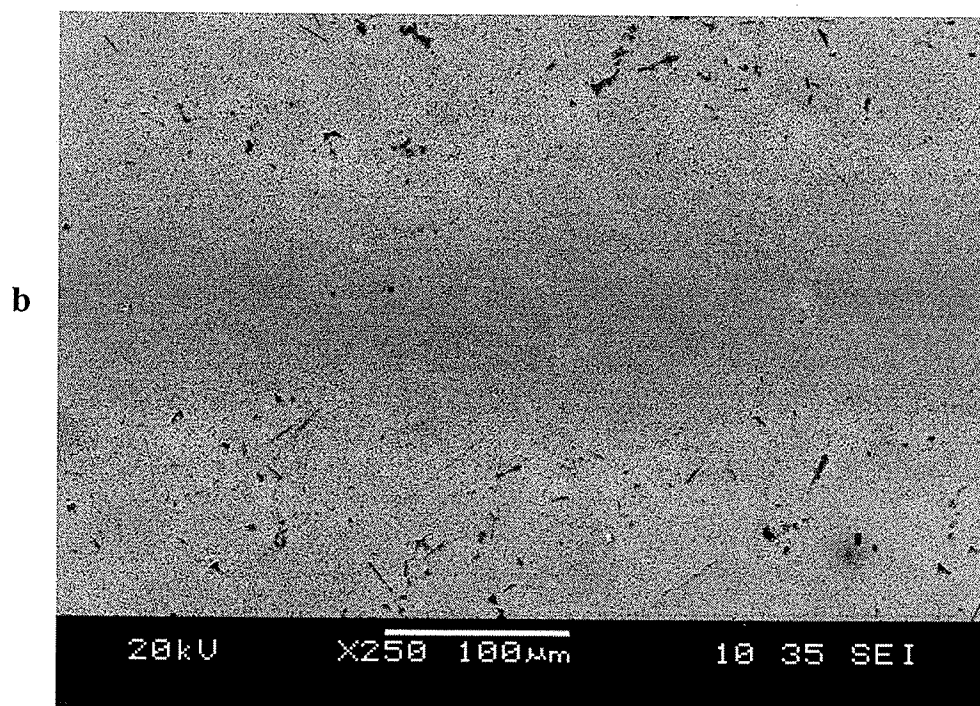
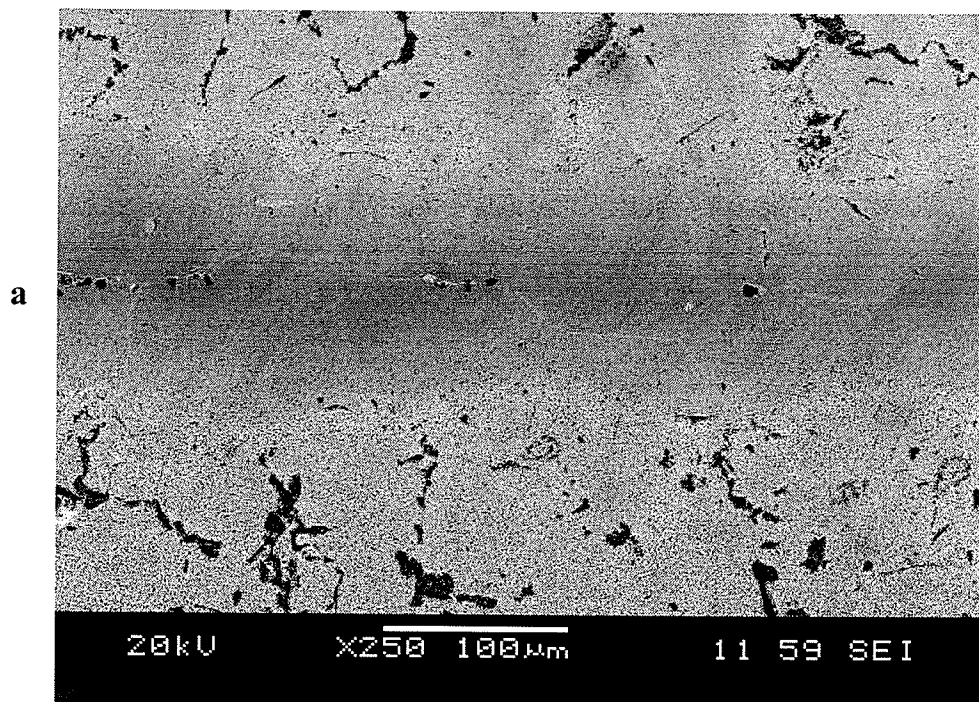


Figure 4.10: SEM micrograph of Inconel 738 bonded with Amdry DF-3 at 1175°C for (a) 290 minutes and (b) 420 minutes.

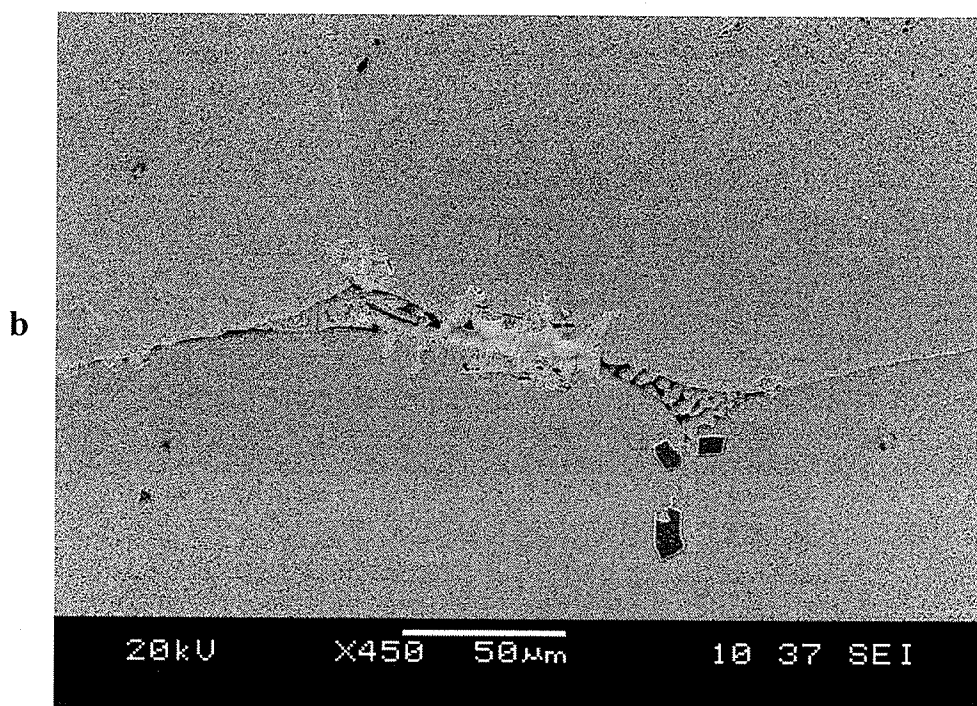
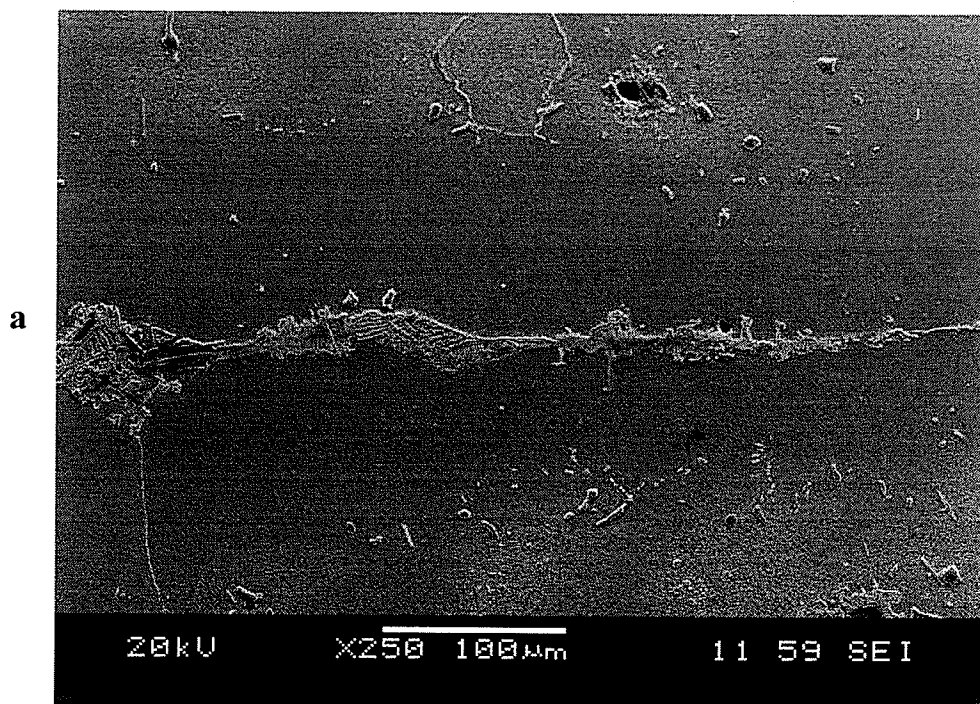


Figure 4.11: SEM micrograph of Inconel 738 bonded with Amdry DF-3 at 1190°C for (a) 290 minutes and (b) 420 minutes.

of the concentration of the melting point depressant solute at the solvus, C_s . Gale and Wallach [58] and Ojo et al. [56] have shown that the time required to achieve a complete isothermal solidification can be predicted by the following equation:

$$C_s - C_m = C_0 - C_m \left(\operatorname{erf} \frac{w}{\sqrt{4Dt_f}} \right) \quad (19)$$

where C_m is the initial solute concentration in the base metal, C_0 is the initial solute concentration in the interlayer, w is one half the initial thickness of the braze interlayer, D is the diffusion coefficient of the solute in the substrate and t_f is the time required to achieve complete isothermal solidification. Ojo et al. [56] used an alternative approach based on a moving solid-liquid interface boundary model to reasonably estimate the value of t_f by the following expression:

$$t_f^{1/2} = J \left(\frac{2h}{D^{1/2}} \right) \quad (20)$$

where, J is a constant, $2h$ is the maximum width of the liquid insert following homogenization of the liquid. Eqs. (19) and (20) suggest that the time required for a complete isothermal solidification is expected to be strongly dependant on the diffusion coefficient, which in turn is dependent upon bonding temperature. An increase in bonding temperature is expected to significantly reduce t_f and produce joints without detrimental centerline eutectic phases.

However, on increasing the bonding temperature to 1190°C (Fig. 4.11) a significant departure in the microstructure of the joint was observed to occur compared from that predicted by the conventional TLP bonding models. Continuously distributed centerline eutectic constituents were observed to have formed in samples brazed for both 290 and

420 minutes at this temperature. This implied that more residual liquid was present in these joints than that was present after the equivalent holding times at lower temperature (1120°C, 1160°C, and 1175°C). Analytical SEM-EDS examination showed that the eutectic product contained a Ni-Ti-rich intermetallic particle at 1190°C (Fig. 4.12 and Table 4.2) that was not previously observed at lower temperatures. This suggests that significantly more enrichment of residual liquid with Ti atoms occurred at 1190°C than that occurred at lower temperatures. Fine γ/γ' eutectic constituents, which are known to form due to the enrichment of liquid by Ti [87], were also observed as part of the re-solidified product. Also, fine γ' particles were observed in both 1175°C and 1190°C samples within the isothermally solidified γ matrix (Fig. 4.13). These particles would have formed by solid state precipitation during cooling due to an increased concentration of Ti in the bond region. The average concentration of Ti present at the centerline of joints bonded for 290 minutes at various temperatures is shown in Figure 4.14. It is seen from this plot that the Ti concentration in the centerline region of the joint increased considerably above 1175°C. This temperature is close to the solvus temperature of Ti-rich γ' precipitate particles in Inconel 738 [87], and their dissolution in the base metal would allow more Ti atoms to be available for diffusion into the brazed joint. Correspondingly, the increase in concentration of Ti, which is one of the main constituents of the principal hardening phase of this alloy, γ' , is corroborated by the observed increase in hardness of the centerline region of the joint with an increase in temperature, as shown in Figure 4.14.

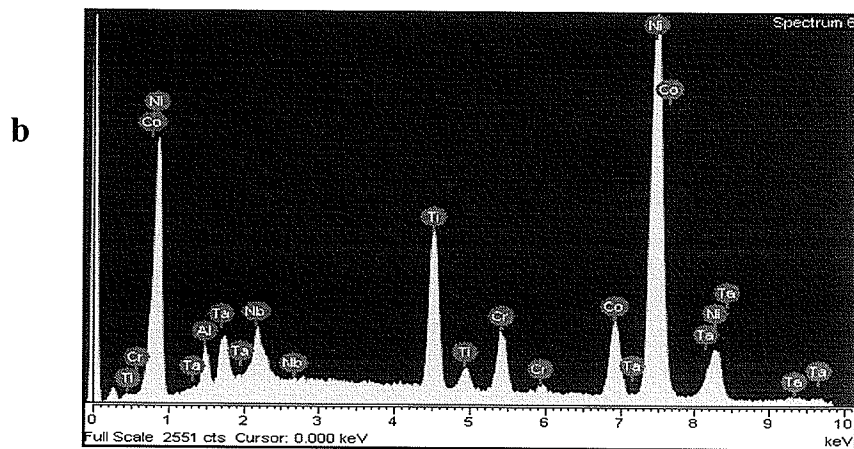
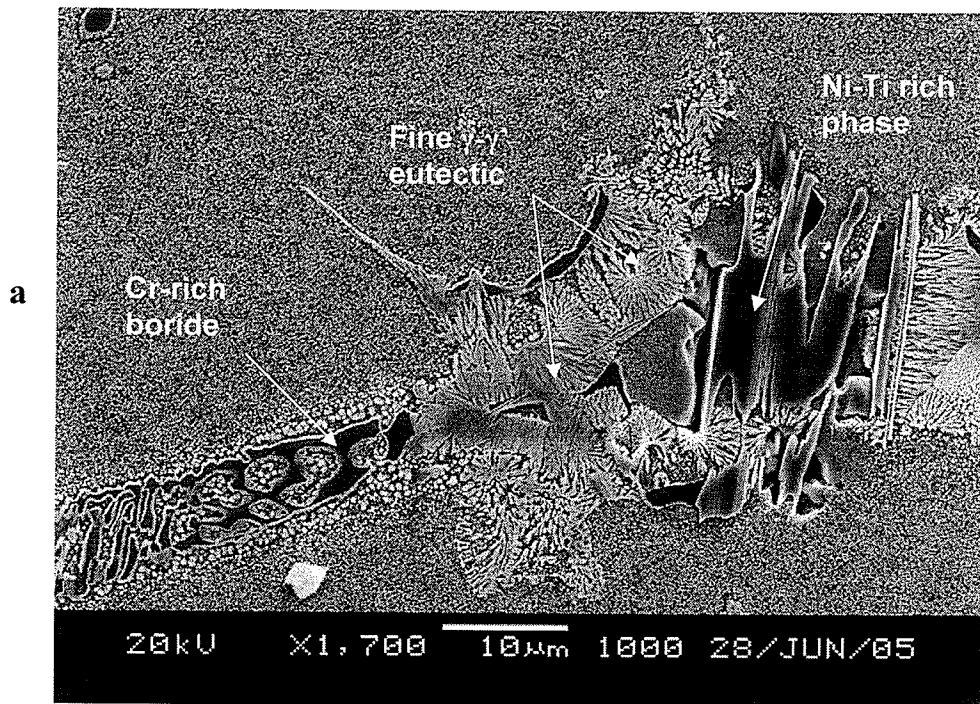


Figure 4.12: (a) SEM micrograph of Inconel 738 bonded with Amdry DF-3 at 1190°C for 290 minutes showing phases present and (b) EDS spectra of Ni-Ti rich phase.

Table 4.2: Composition of Ni-Ti rich phase present at 1190°C.

Element	Ni-Ti rich phase (at%)
Ni	63.04
Cr	5.11
Co	10.66
Al	4.35
Ti	11.63
Nb	2.27
Ta	2.00
W	0.63
Mo	0.31

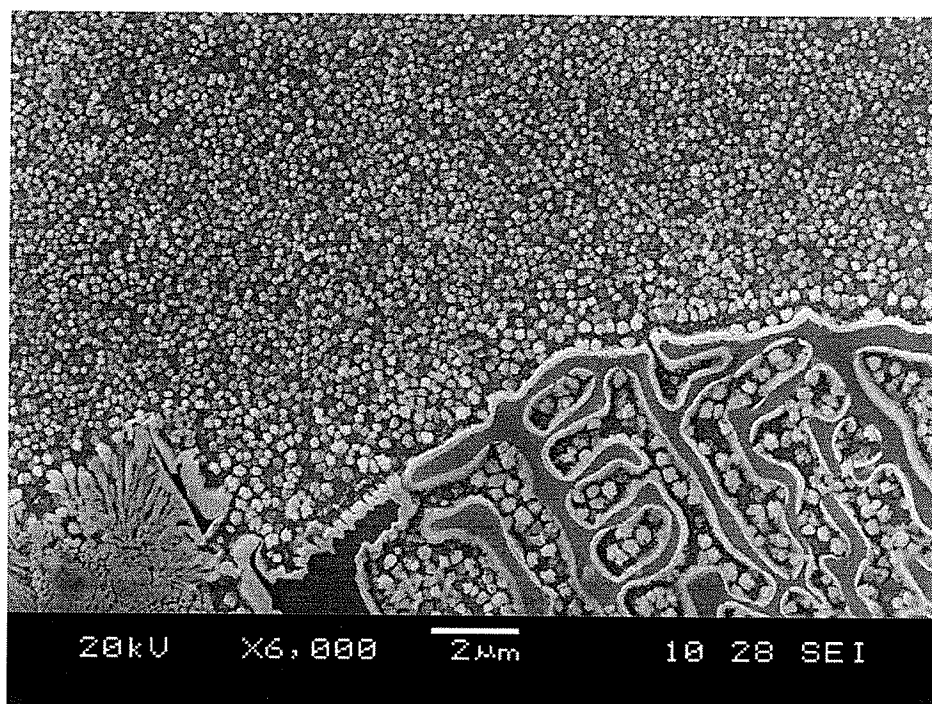


Figure 4.13: Fine γ' particles formed within γ matrix Inconel 738 bonded with Amdry DF-3 at 1190°C for 290 minutes

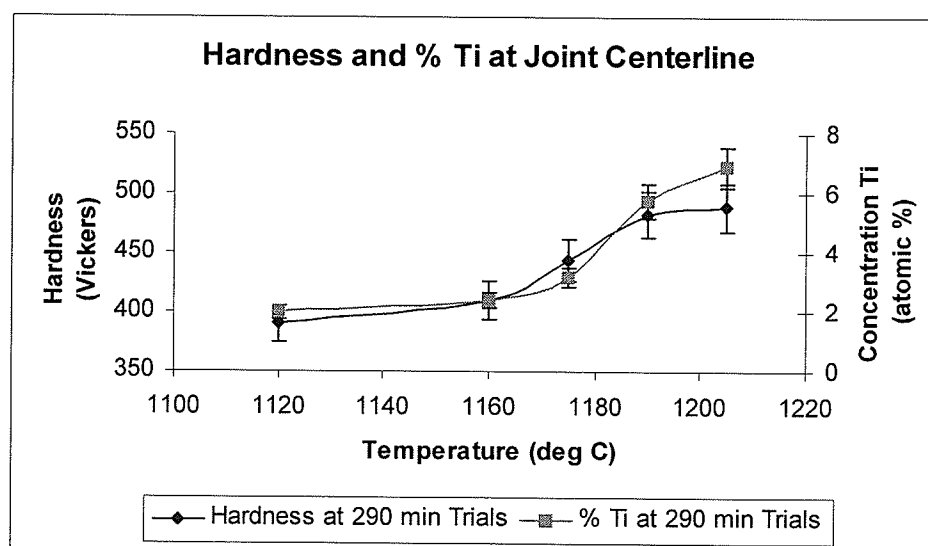


Figure 4.14: Variation in concentration of Ti and microhardness of centerline region of bonded region with temperature.

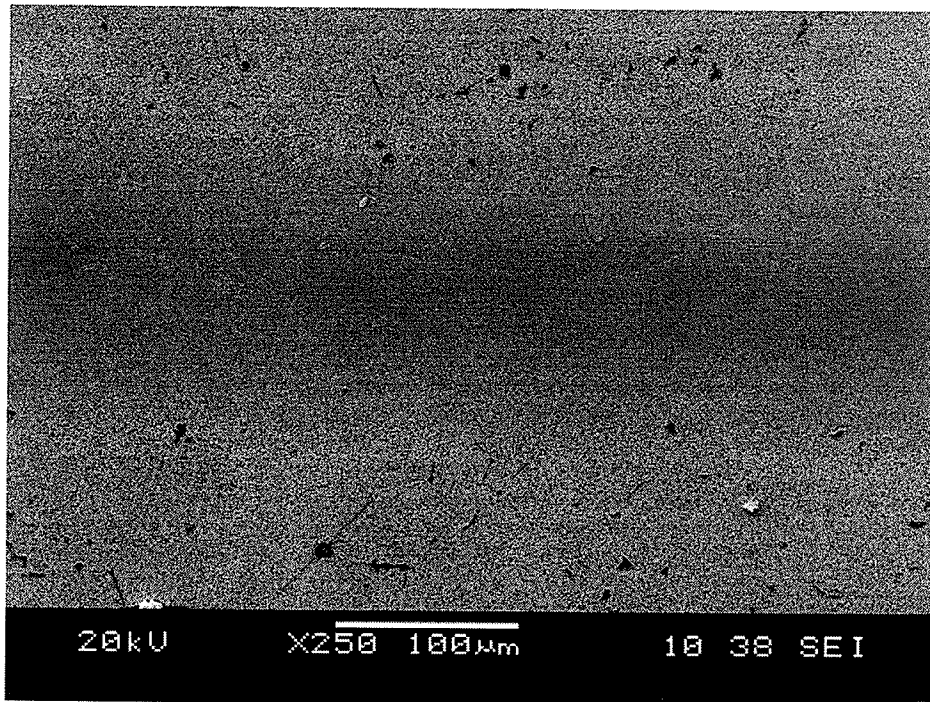
In order to investigate further the effect of bonding temperature on the change in isothermal solidification rate, specimens were bonded at 1175°C and 1225°C for 12 hours. As can be seen in Figure 4.15 a complete isothermal solidification occurred in specimens bonded at 1175°C for 12 hours, while the same brazing time resulted in an incomplete isothermal solidification in 1225°C specimens. Again, this is a significant departure from conventional expectation than an increase in bonding temperature would produce more diffusion of MPD boron into the base metal and thus result in a higher isothermal solidification rate. A further discussion of the seemingly anomalous behavior, eg., a decrease in isothermal solidification rate with increase in bonding temperature beyond 1175°C, will be presented in section 4.2.3.

4.1.5 Interface Precipitates

Besides the influence of diffusion temperature on the formation of centerline eutectic, it was also observed, qualitatively, in the present work that an increase in temperature from 1120°C to 1190°C resulted in a decrease in the precipitation of chromium rich particles within the base alloy grains adjacent to the brazed joint (Figs.4.4, 4.5 and 4.11). Extensive precipitation of globular and acicular particles was observed in the brazed samples within the base alloy grains and intergranular regions adjacent to the joint interface. Quantitatively, the number density of these particles was observed to decrease in a gradual fashion with increasing distance from the joint interface.

As was stated in the literature review section, the analytical models of TLP bonding treat the joining process to be consisting of a number of sequential discrete steps, viz., melting

a



b

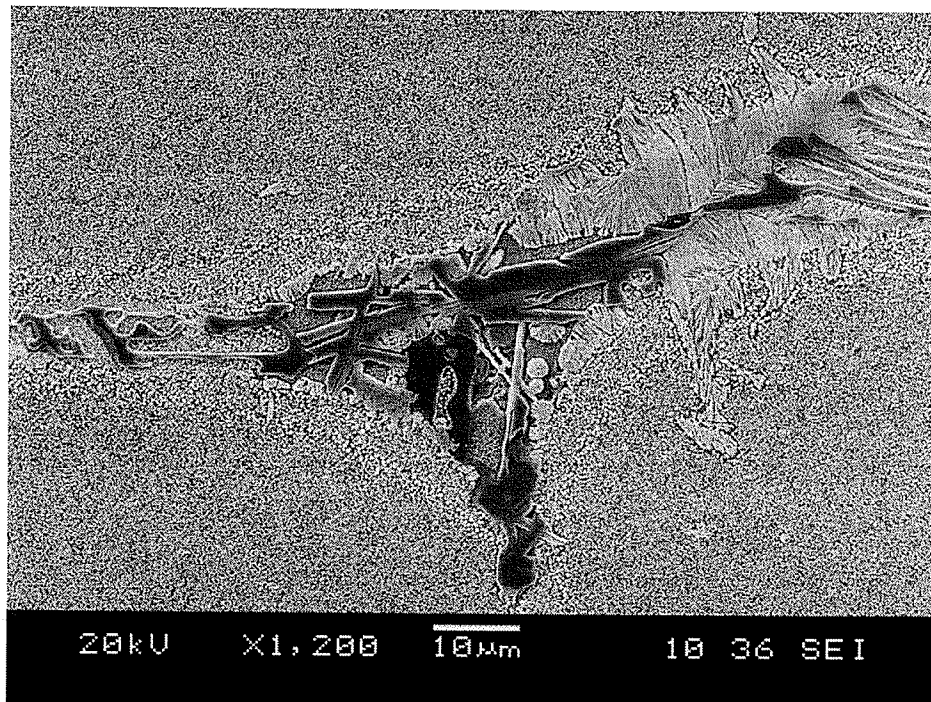


Figure 4.15: SEM micrograph of Inconel 738 bonded with Amdry DF-3 for 720 minutes (12 hours) at (a) 1175°C and (b) 1225°C.

of the interlayer, base metal dissolution, isothermal solidification, and homogenization stages. It is assumed that due to orders of magnitude of difference in diffusivity of solute on the two sides of the solid-liquid interface, dissolution of the base metal into the liquid layer occurs at a much faster rate than the solid-state diffusion of the MPD in the base metal. Hence, the interlayer alloy upon melting rapidly attains equilibrium with the solid base metal, which involves base alloy dissolution, following which the solid-state diffusion of MPD commences. Under this condition, boron rich second phase particles are not expected to form during the TLP bonding process, since it is assumed that solid-state diffusion in the base metal takes place under equilibrium condition subsequent to liquid-solid equilibration involving base metal dissolution. However, it has been suggested that the two processes occur simultaneously rather than sequentially [88], in which case the boride precipitation would be expected to occur within a region of the base alloy where solute solubility is exceeded as a result of substantial solid-state diffusion of the solute during base metal dissolution stage. It has recently been reported by Idowu et al. [84], that precipitation of a complex cubic Cr-, Mo-, and W-based $M_6(C,B)$ phase in Inconel 738 TLP bonded joints was observed in the base metal adjacent to bond centerline. Nakao et al. [41] modeled the base metal dissolution in nickel-base superalloys for a Ni-B filler using the Nerst-Brunner theory. Their results indicated that the time required for the base metal dissolution stage reduced with an increase in the bonding temperature. Accordingly, increase in the bonding temperature could reduce the time available for solid-state solute diffusion during the liquid-solid equilibration process. Perhaps this could be contributing to the observed decrease in the extent of precipitation of chromium rich particles with increase in brazing temperature in the base metal region

adjacent to the joint. Considering the high chromium content of the particles, this would lead to a significant depletion of chromium around this region of the substrate, which may result in a decrease in the region's corrosion resistance.

4.2 TLP Bonding of Waspaloy with Nicrobraz 150

Subsequent work was done to determine if the anomalous effect of increase in bonding temperature beyond a critical temperature on the reduction in isothermal solidification rate, as observed in IN738-DF3 brazed joints, also occurred in other superalloys. For this, Waspaloy, a different nickel-base superalloy also precipitation hardened by γ' , was bonded with Nicrobraz 150 filler alloy and the results are presented in this section.

4.2.1 Microstructure of As-Received Waspaloy Base Alloy

An optical micrograph of as-received wrought Waspaloy is shown in Figure 4.16. It shows that the material grains elongated along the direction of rolling. The microstructure of the material is also shown in Figure 4.17 which was obtained by SEM operated in secondary electron mode. The microstructure consisted of γ' precipitates within the γ matrix and some randomly dispersed MC carbide particles. The average grain size was determined to be about 8-10 μm .

4.2.2 Effect of Diffusion Time on Bond Microstructure

To study the effect of holding time on TLP bond microstructure in Waspaloy, 125 μm thick Nicrobraz 150 filler alloy was used in joining the material at 1100°C for 60, 360, and 480 minutes. The microstructures of these specimens as observed by SEM operated

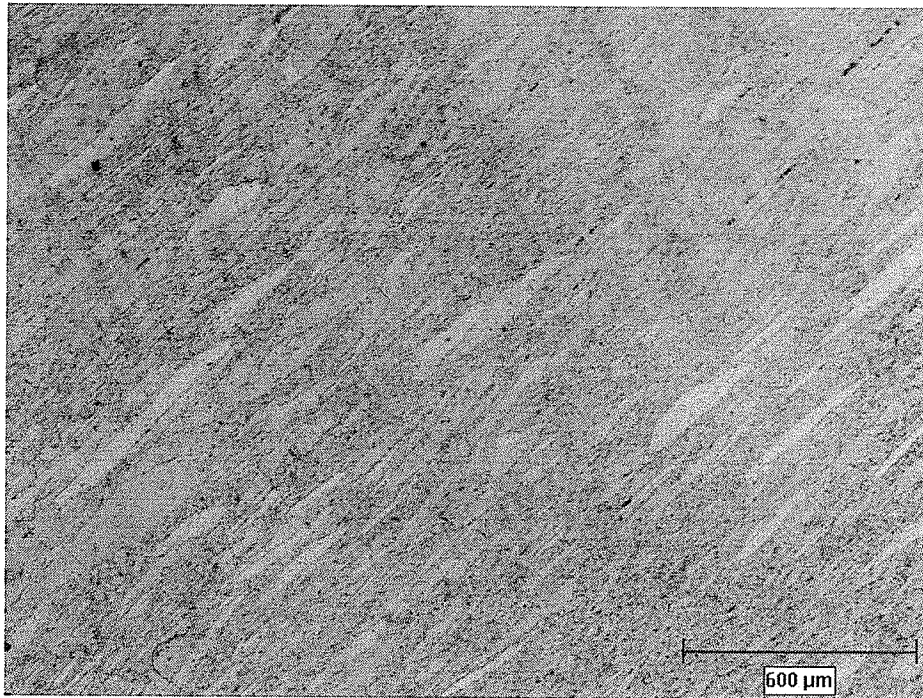


Figure 4.16: Optical micrograph of as-received Waspaloy showing grain extension in rolling direction (X50 mag).

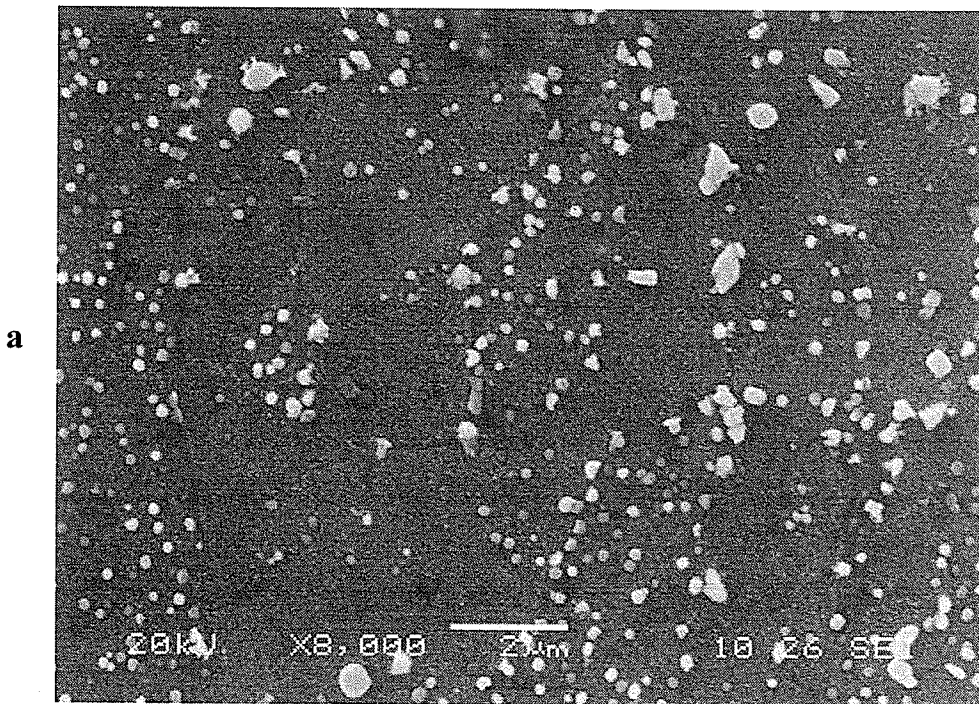
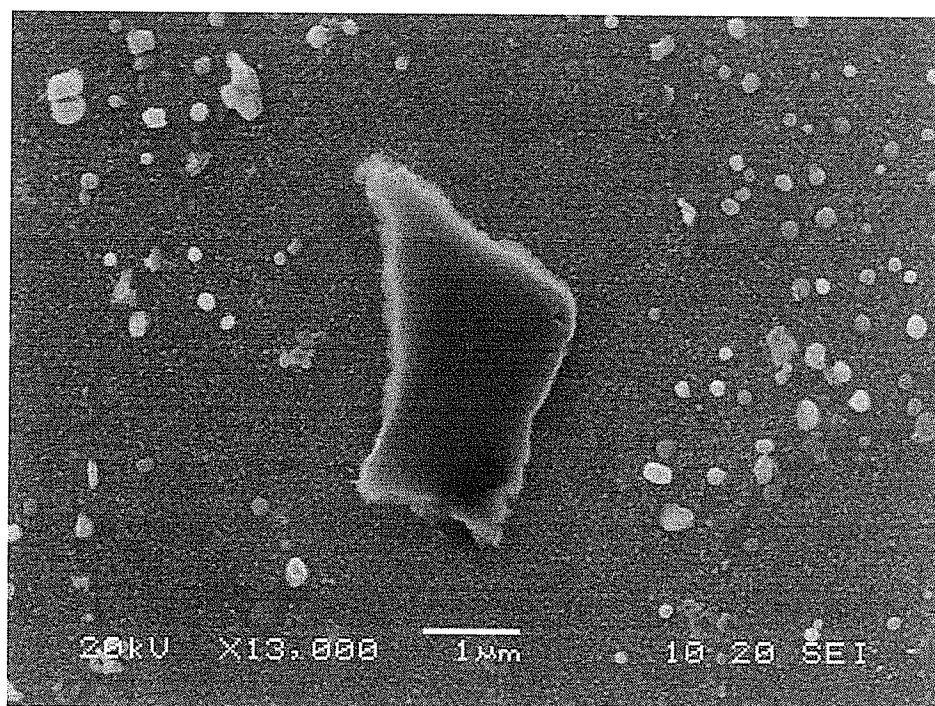
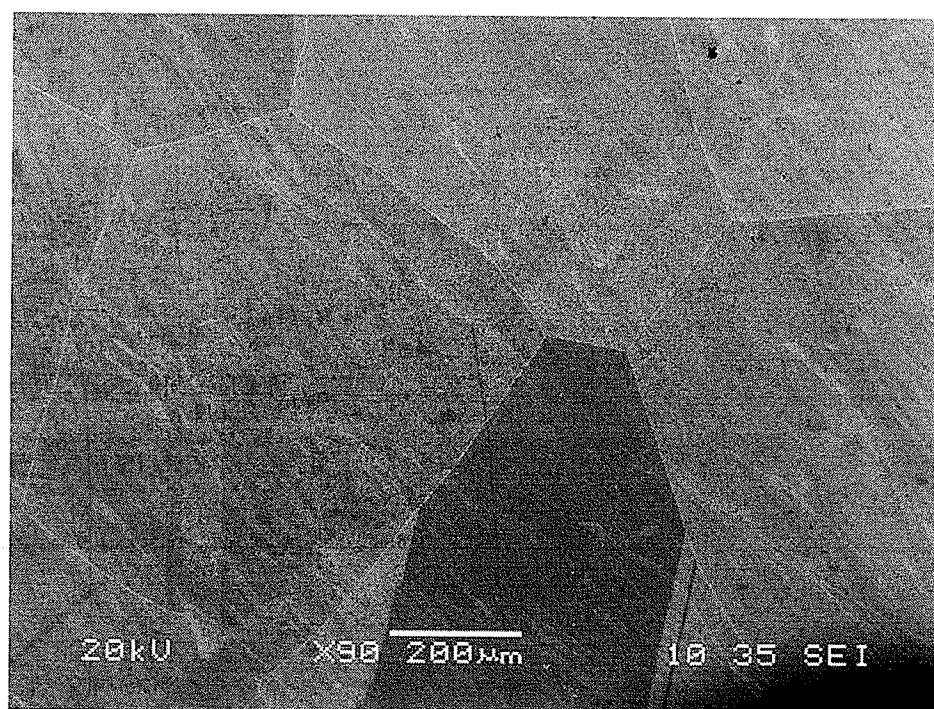


Figure 4.17: SEM micrographs of (a) as-received Waspaloy showing primary and secondary γ' within γ matrix (b) MC carbide in as-received Waspaloy showing reduction in γ' particles immediately adjacent to carbide and (c) heat treated Waspaloy at 1200°C for 30 minutes showing extensive grain growth.

b



c



in secondary electron mode are shown in Figure 4.18. The microstructure of the joint bonded for 60 minutes consisted of a continuously distributed eutectic constituent with an average thickness of 32 μm (Fig. 4.18a). A decrease in average eutectic thickness to 10 μm was observed in 360 minute samples, while a holding time of 480 minutes resulted in complete elimination of the centerline eutectic (Figs. 4.18b,c). EDS compositional analysis of the three main phases observed within the eutectic suggests them to be nickel base solid solution, nickel rich boride phase, and chromium rich boride phase (Table 4.3), similar to those observed in the Inconel 738/DF-3 joint produced at temperature $\leq 1175^\circ\text{C}$.

4.2.3 Effect of Diffusion Temperature on Bond Microstructure

To study the effect of temperatures on joint microstructure Waspaloy samples were bonded at 1145°C for 360 minutes. In contrast to the situation at 1100°C , a holding time of 360 minutes at 1145°C resulted in a joint that was entirely free of centerline eutectic (Fig. 4.19). This observation suggests that there is an increase in isothermal solidification rate with increase in bonding temperature from 1100°C to 1145°C . Similar to the situation in IN-738, the increase in rate can be attributed to increase in solid-state diffusion of MPD boron in the base metal at higher bonding temperatures. However, a further increase in temperature resulted in the formation of centerline eutectic in joints produced at 1175°C and 1225°C (Fig. 4.20) after 360 minutes of hold time, which had precluded their formation at a lower temperature of 1145°C . That is, the anomalous effect of increase in temperature beyond some critical temperature was also observed in a different nickel-base superalloy, Waspaloy, bonded with a different filler alloy, Nicrobraz

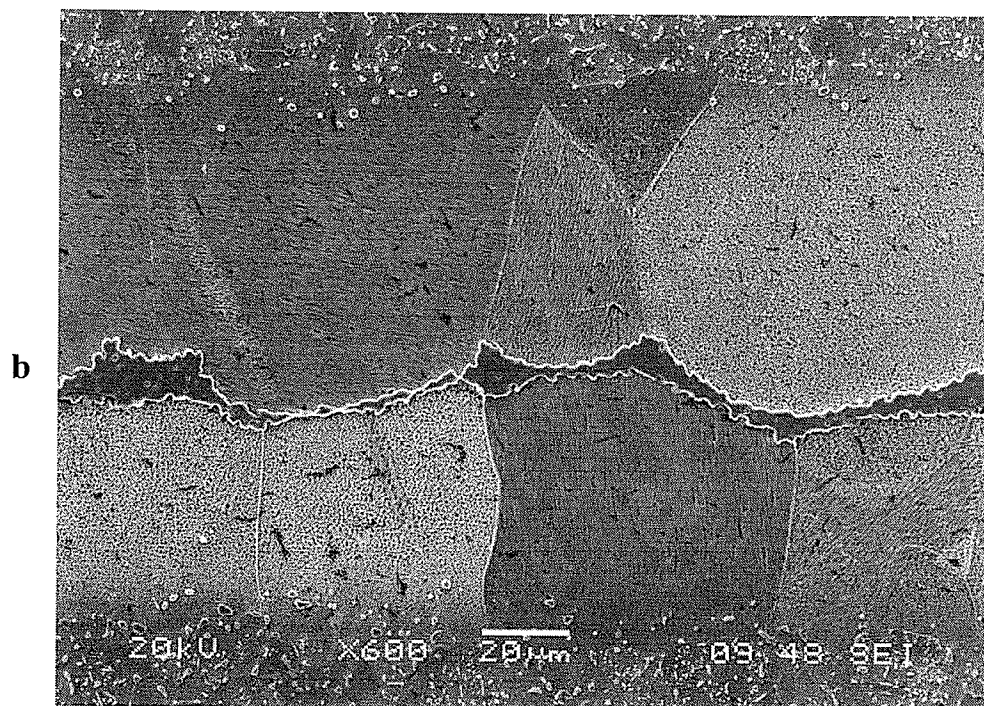
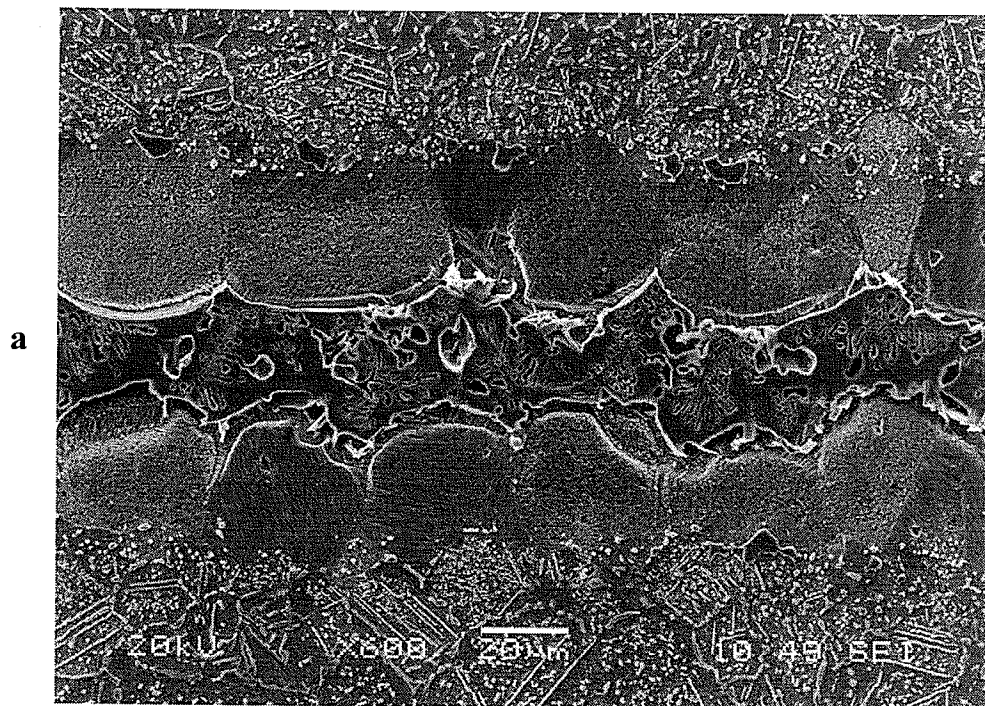


Figure 4.18: SEM micrograph of Waspaloy bonded with Nicrobraz 150 at 1100°C for (a) 30 min (b) 360 min and (c) 480 min.

c

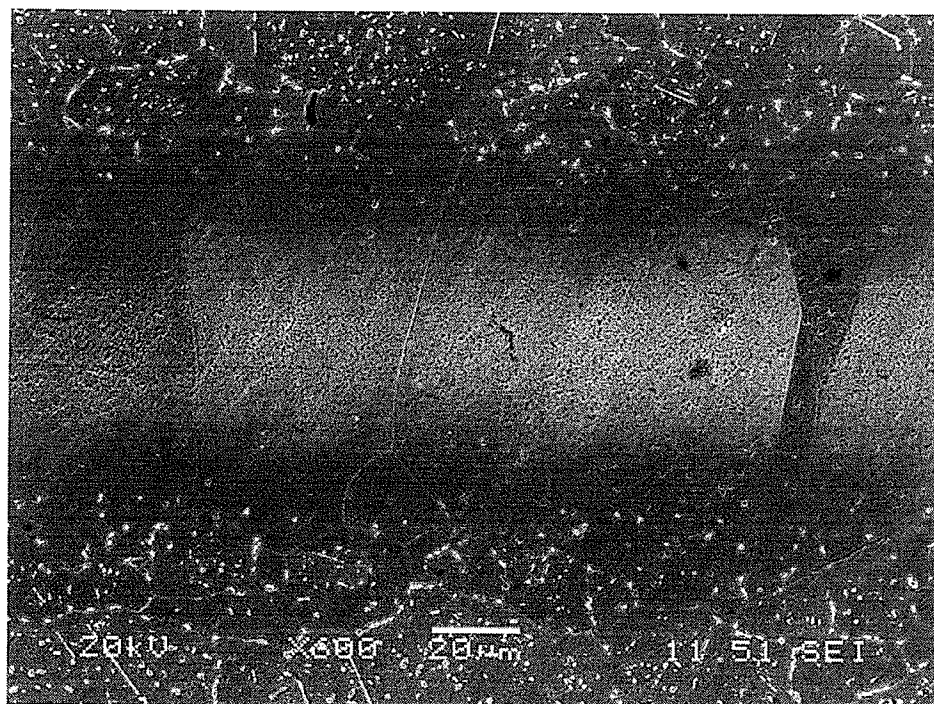


Table 4.3: Composition of eutectic phases present in Waspaloy joints.

Element	Cr-rich boride (at%)	Ni-rich boride (at.%)	Gamma (γ)	Ni-Ti rich phase
Al	-	0.72	1.30	4.07
Co	-	1.82	1.79	7.79
Cr	94.10	9.71	16.50	4.33
Mo	2.05	-	0.28	-
Nb	-	0.38	-	2.91
Ni	2.69	84.58	79.04	67.73
Ta	-	0.31	0.15	0.76
Ti	0.35	2.30	0.66	10.84
W	0.80	0.18	0.29	0.36

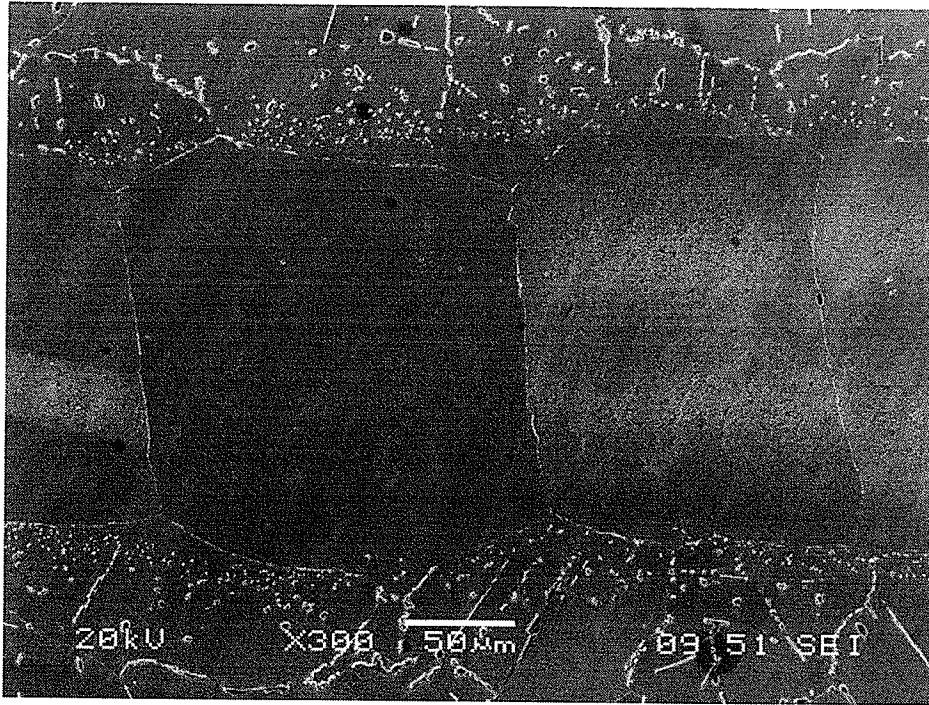


Figure 4.19: SEM micrograph of Waspaloy bonded with Nicrobraz 150 at 1145°C for 360 min.

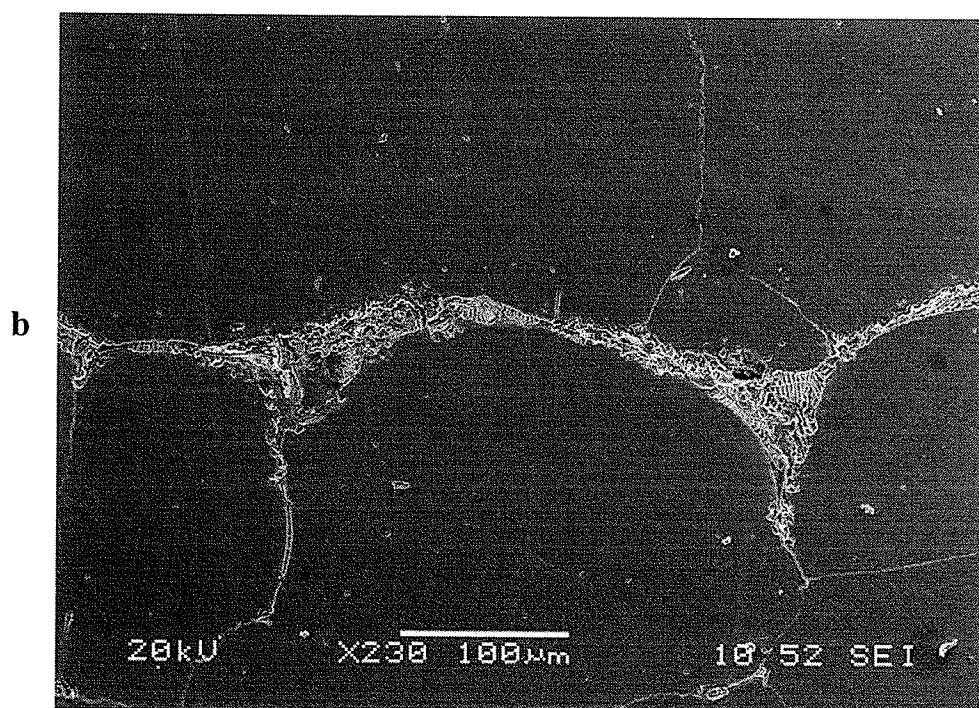
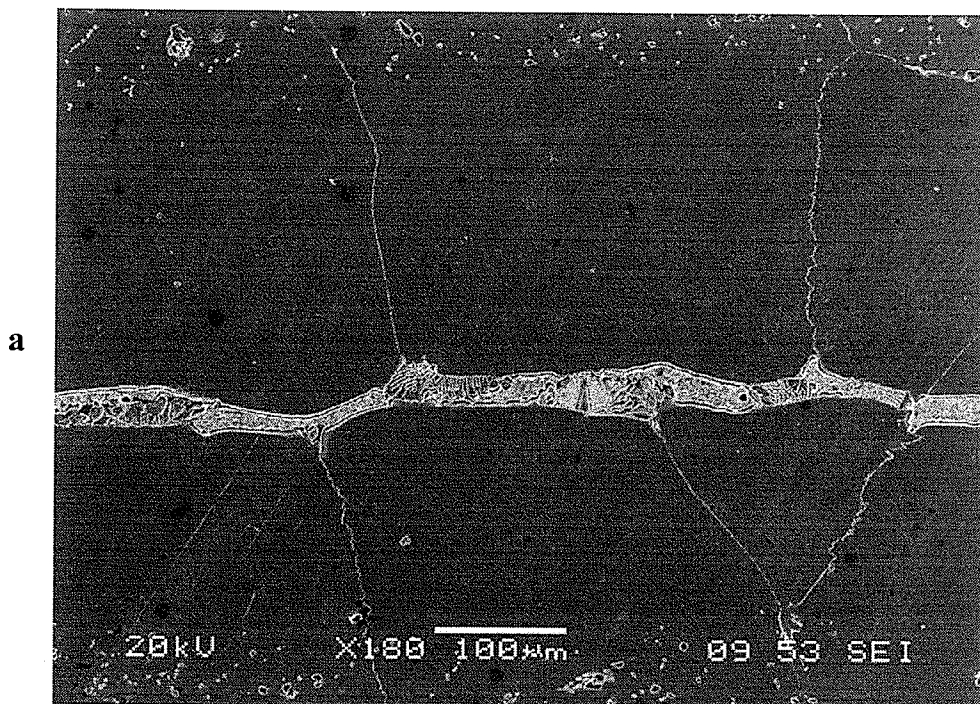


Figure 4.20: SEM micrograph of Waspaloy bonded with Nicrobraz 150 for 360 min at (a) 1175°C and (b) 1225°C.

150. Akin to the Inconel 738/DF-3 joint, the eutectic product in 1175°C and 1225°C bonded specimens was observed to contain a Ni-Ti rich intermetallic phase that was not present at lower temperatures. Compositions of all the phases observed within the eutectic are shown in Table 4.3. Extensive precipitation of globular and acicular particles was also observed in brazed samples of Waspaloy within base alloy grains adjacent to the joint interface.

A number of models used to explain TLP bonding process are based on the use of binary phase relationships, often hypothetical, and depend on classical solutions to Fick's diffusion equations. In these situations the process is considered to be controlled exclusively by the solid-state diffusion of MPD element out of liquated insert away from the joint region. According to these models, complete isothermal solidification is strongly dependent on the bonding temperature. An increase in bonding temperature is expected to increase the isothermal solidification rate and produce a joint without centerline eutectic at a reduced value of bonding time as compared to the ones obtained at lower temperatures. In agreement with these models an increase in isothermal solidification rate with increase in temperature was observed in Inconel 738 samples bonded at 1120°C to 1175°C and in Waspaloy samples bonded at 1100°C and 1145°C.

However, in contrast to predictions based on these models a decrease in isothermal solidification rate was observed in Inconel 738 samples bonded at 1190°C and 1225°C and in Waspaloy joints prepared at 1175°C and 1225°C. Sinclair et al. [6, 7] have suggested that a deviation from isothermal solidification rate predicted by conventional

TLP diffusion models, which are normally based on binary systems, can be encountered during bonding of multicomponent alloys. It was noted that if the solubilities and/or diffusion coefficients of the two diffusing solutes which are capable of controlling isothermal solidification process during TLP bonding (normally MPD elements) are very different, isothermal solidification stage can be divided into two parabolic regimes. The first regime being dominated by the “faster” solute, and the second by the slower of the two. In extreme cases a complete isothermal solidification may not be realized in experimentally feasible times.

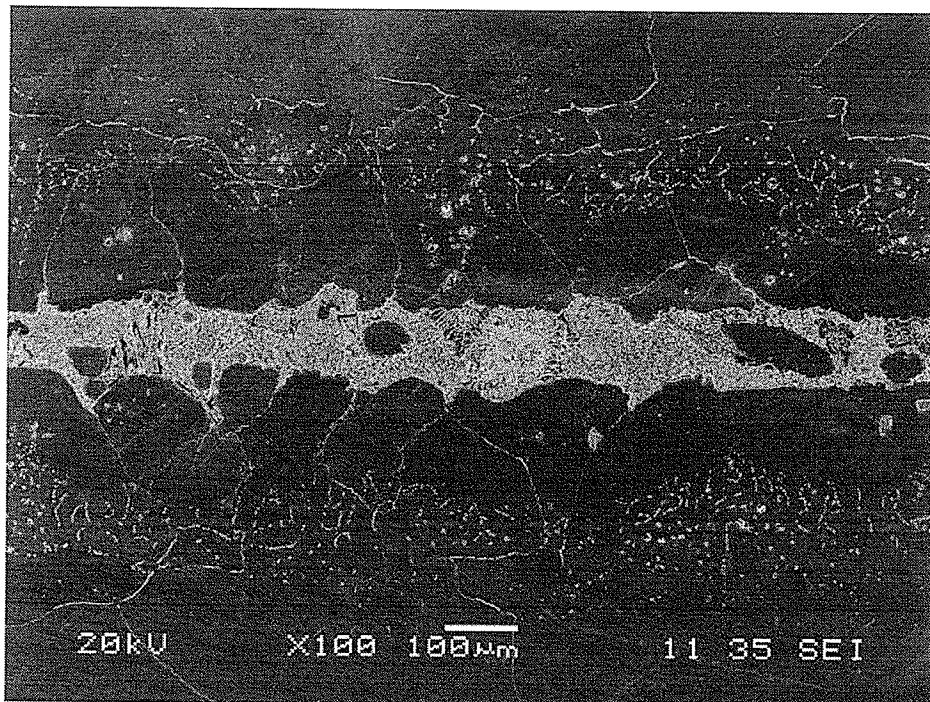
In the present work, diffusion of MPD element boron, which is essentially an interstitial atom in nickel and has a higher diffusivity as compared to substitutional solutes, is believed to be controlling the isothermal solidification process in the first regime (1120°C - 1175°C for Inconel 738/DF-3 system and 1100°C - 1160°C for Waspaloy/NB 150 styem). However, during the bonding process continual interdiffusion of elements between the liquid insert and base metal would cause the composition of the liquid to be continually modified as solidification progresses. At higher temperatures, the concentration gradients of Ti between the base alloy γ matrix and the liquated insert is expected to be very steep, since the later is enriched with Ti atoms owing to the dissolution of γ' (Ni_3Ti , Al) at this temperature [87], while they are absent in the filler alloy. This would result in a considerable enrichment of the liquated insert with base metal alloy Ti due to an increased diffusion of this element caused by its high concentration gradient and increased diffusion coefficient with increased temperature. The solidification partition coefficient (k) of Ti in nickel alloys is less than 1 (one),

therefore an increase in its concentration would result in a depression of the solidification temperature [89]. Consequently, a considerable enrichment of this element in the liquated insert during high temperature TLP bonding of multicomponent superalloys could lead to the commencement of a second solidification regime, which is characterized by a slower isothermal solidification rate, as suggested by Sinclair et al. [6, 7]. A similar deviation in isothermal solidification rate during brazing of Inconel 738LC at higher temperatures, but using Nicrobraz 150, has also been reported recently by Idowu et al. [90].

4.3 Effect of Pre-Bond Heat Treatment of Waspaloy

A unique observation was made in Waspaloy samples bonded at temperatures above 1175°C. Significant grain boundary liquation occurred which rendered measurement of centerline eutectic extremely difficult (Figs. 4.21b and 4.22). In order to prevent this occurrence, pre-bond heat treatment at 1200°C for 30 minutes was performed to increase the grain size of the base material (Fig. 4.17c). This heat treatment increased the grain size of the material to about 500 μm . Microstructural examination of sample bonded in this heat treated condition showed a considerable reduction in the grain boundary liquation (Fig. 4.21a). As previously stated in the literature review isothermal solidification during TLP bonding can be significantly influenced by grain boundary phenomenon. Kokawa et al. specifically [64] reported that the rate of isothermal solidification was greater when fine grained nickel was used during TLP brazing using Ni-P filler alloy as compared to larger grained material. Saida et al [65] also reported that the completion time for isothermal solidification decreased in the order of single

a



b

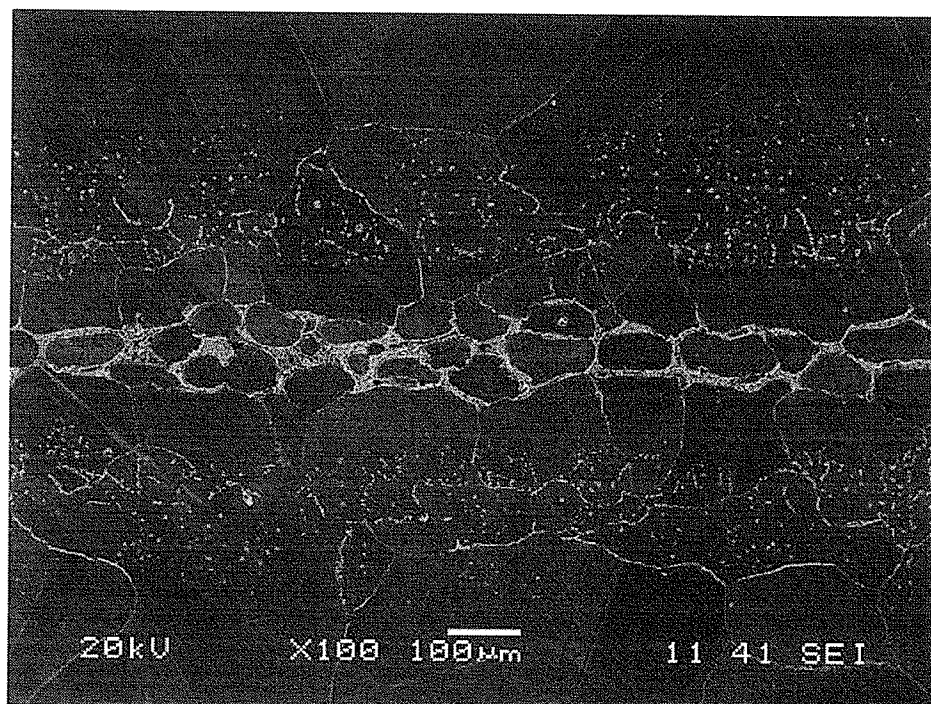
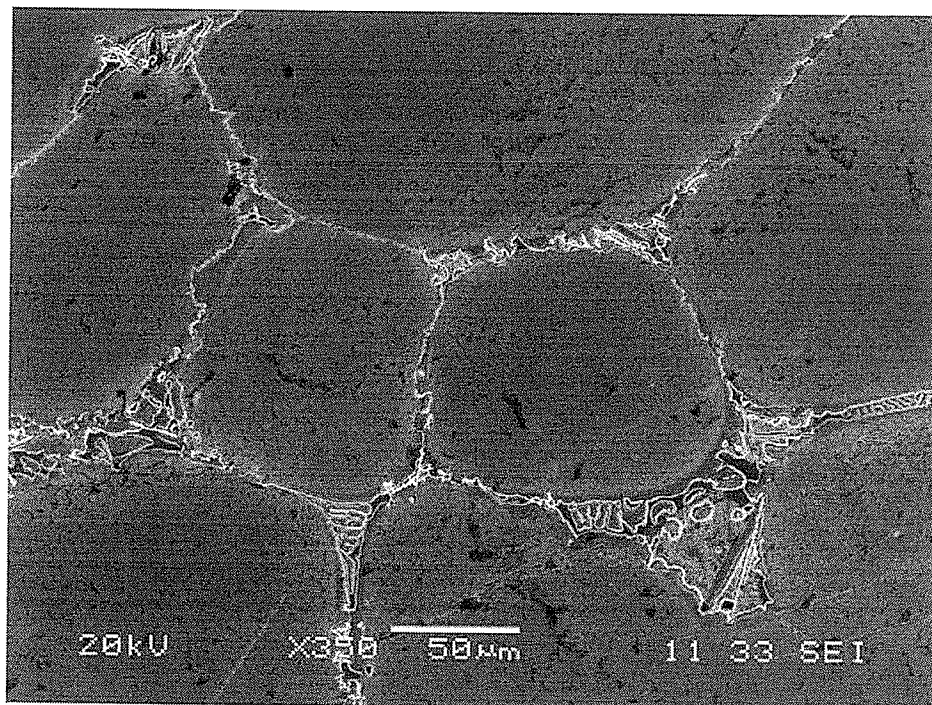


Figure 4.21: SEM micrograph of Waspaloy bonded with Nicrobraz 150 at 1175°C for 1 hour with (a) pre-bond heat treatment and (b) as-received.

a



b

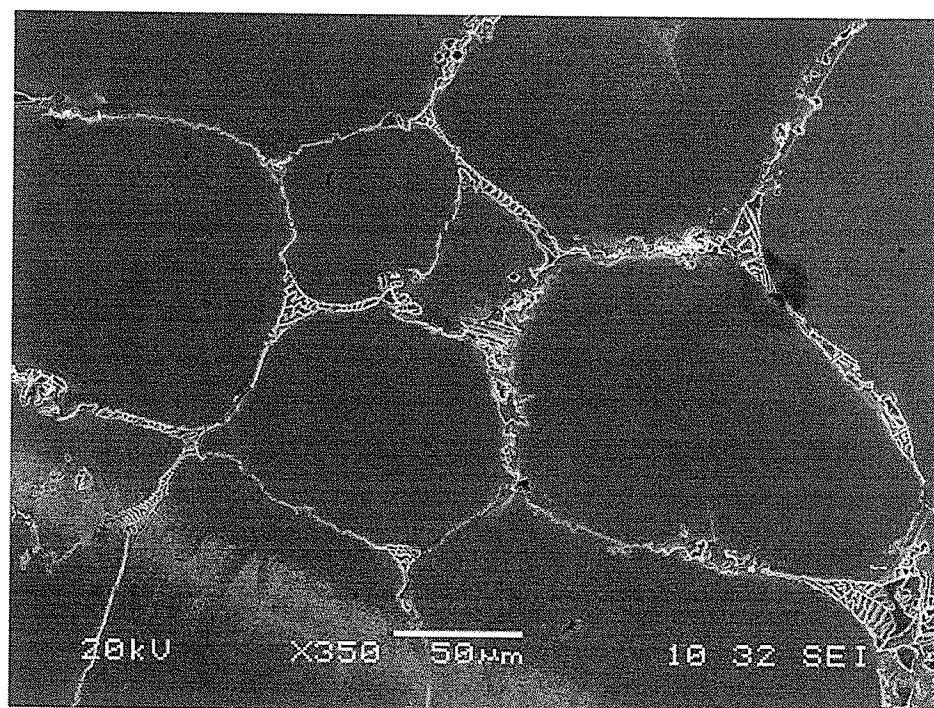


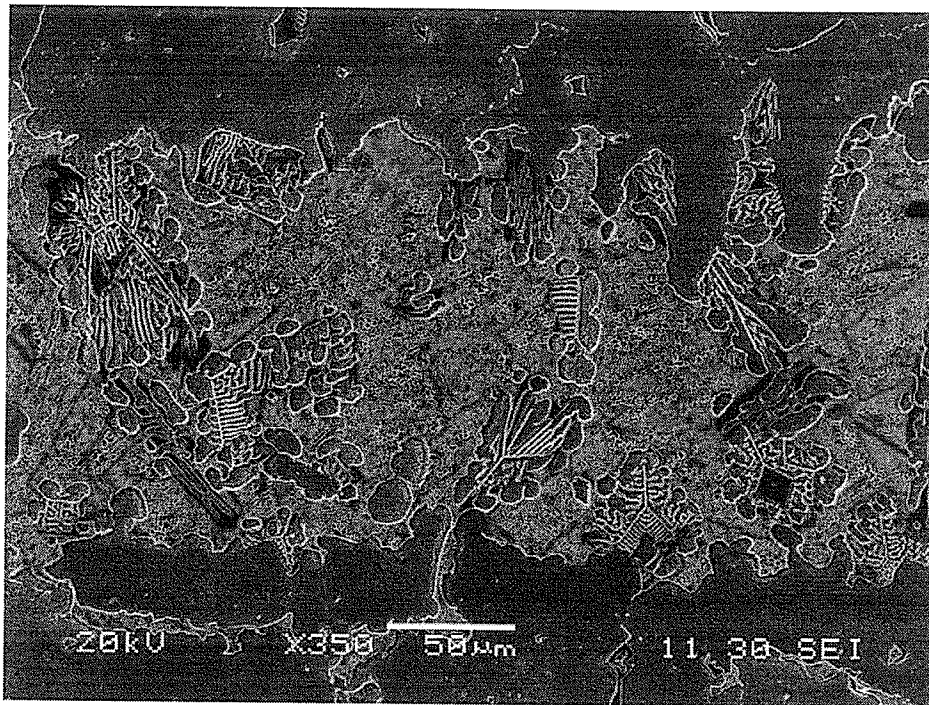
Figure 4.22: SEM micrograph of as-received Waspaloy for 360 minutes at (a) 1200°C and (b) 1225°C.

crystal, coarse-grained, and fine grained nickel using the same Ni-P filler alloy. In the present work, the samples used to study the effect of increase in temperature on TLP joint microstructure as discussed in the following section, were subjected to the pre-bond heat treatment.

4.4 High Temperature Isothermal Solidification Kinetics

To further investigate the effect of high temperature on isothermal solidification rate during brazing of Waspaloy, TLP bonding was performed at 1175°C for 10, 60, and 360 minutes (Fig 4.23) to investigate the effect of time on joint microstructure and at 1200°C and 1225°C for 360 minutes (Fig. 4.24). The microstructure of the joint produced in all samples showed the existence of continuous centerline eutectic-type constituent. The average eutectic thickness of joints produced at 1175°C decreased from 152 μm after 10 minutes to 101 μm after 60 minutes, and was finally reduced to 17.0 μm after 360 minutes. Boron containing particles were observed within the centerline eutectic product in all the samples even after 6 hours of holding time. Figure 4.25 shows the boron concentration profile across the joint produced at 1175°C for 360 minutes. In contrast however, complete isothermal solidification was achieved at 1145°C for 360 minutes (Fig 4.19) with no formation of B containing particles along the joint. The presence of boron rich particles along the centerline region of the samples bonded for the same holding time of 360 minutes, suggests that boron diffusion out of liquated insert was reduced at 1175°C, 1200°C, and 1225°C.

a



b

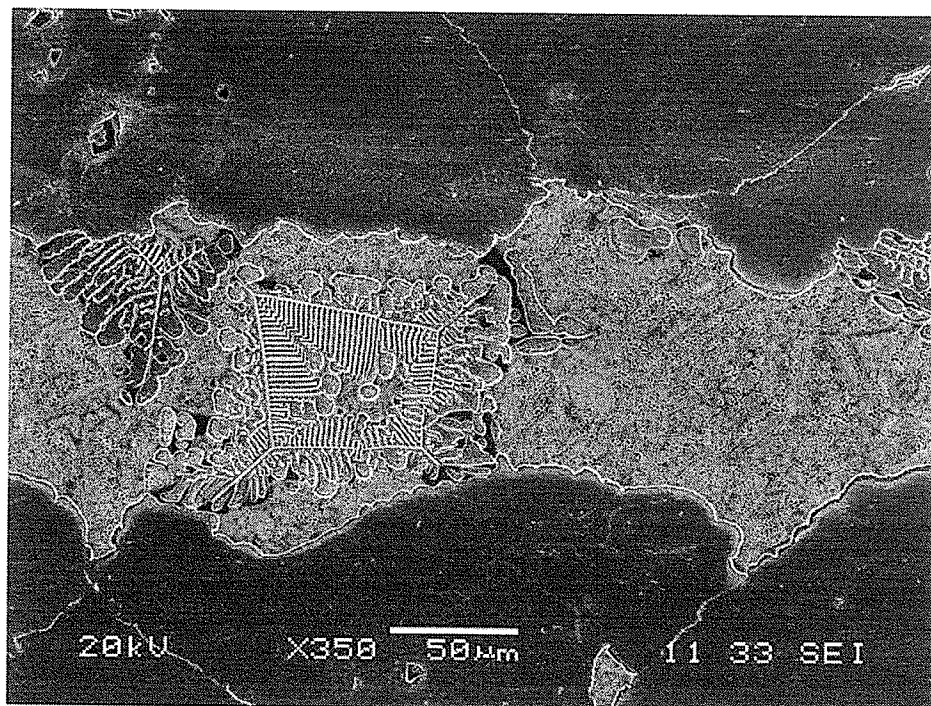
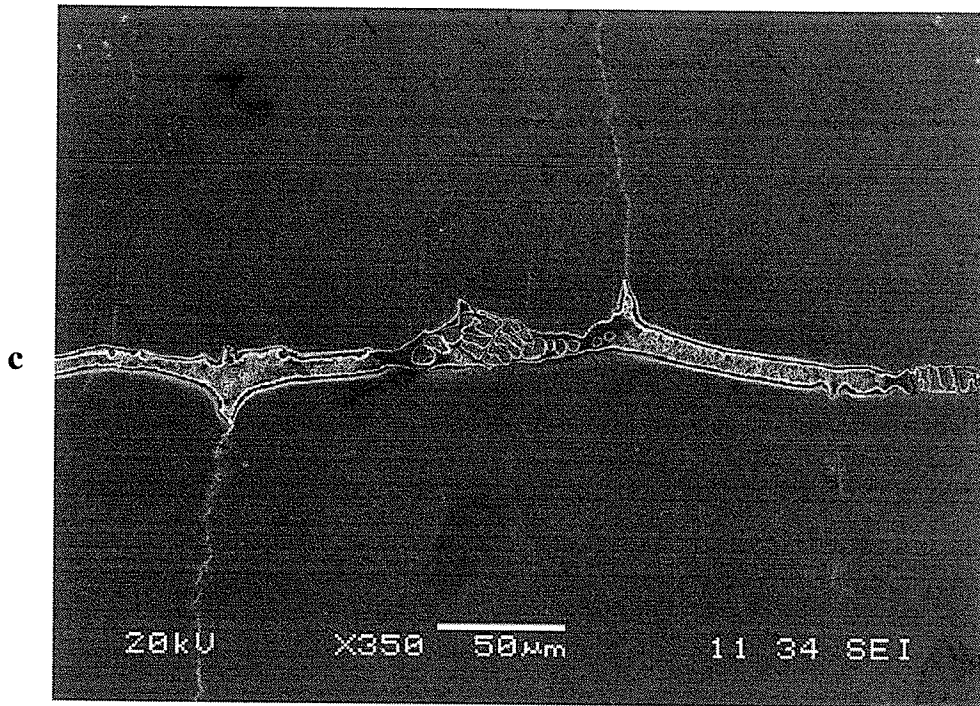
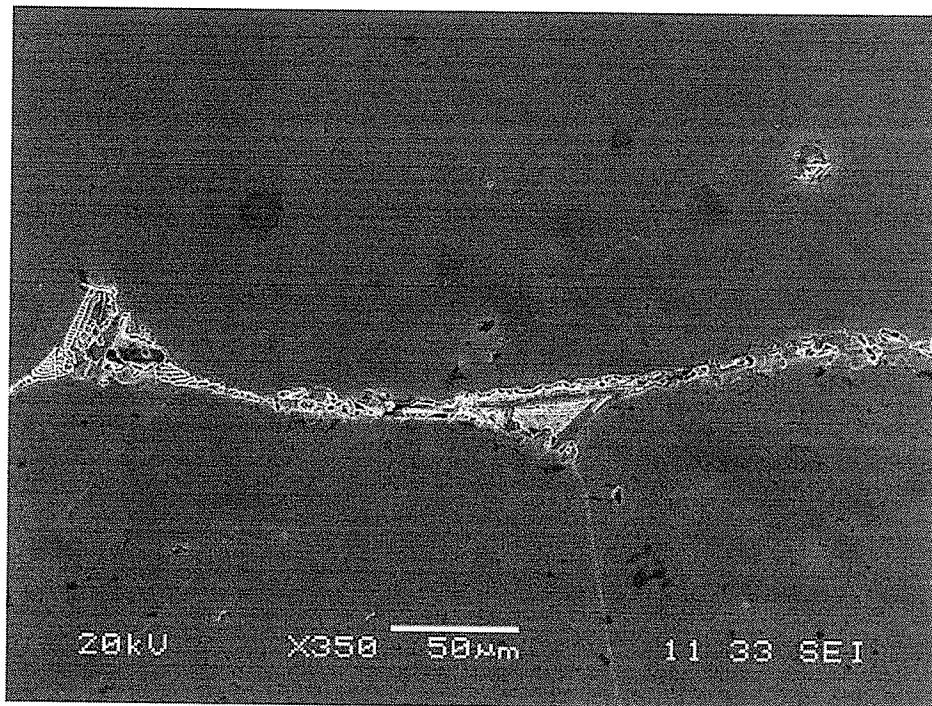


Figure 4.23: SEM micrograph of Waspaloy bonded with Microbraz 150 at 1175°C for (a) 10 min (b) 60 min and (c) 360 min.



a



b

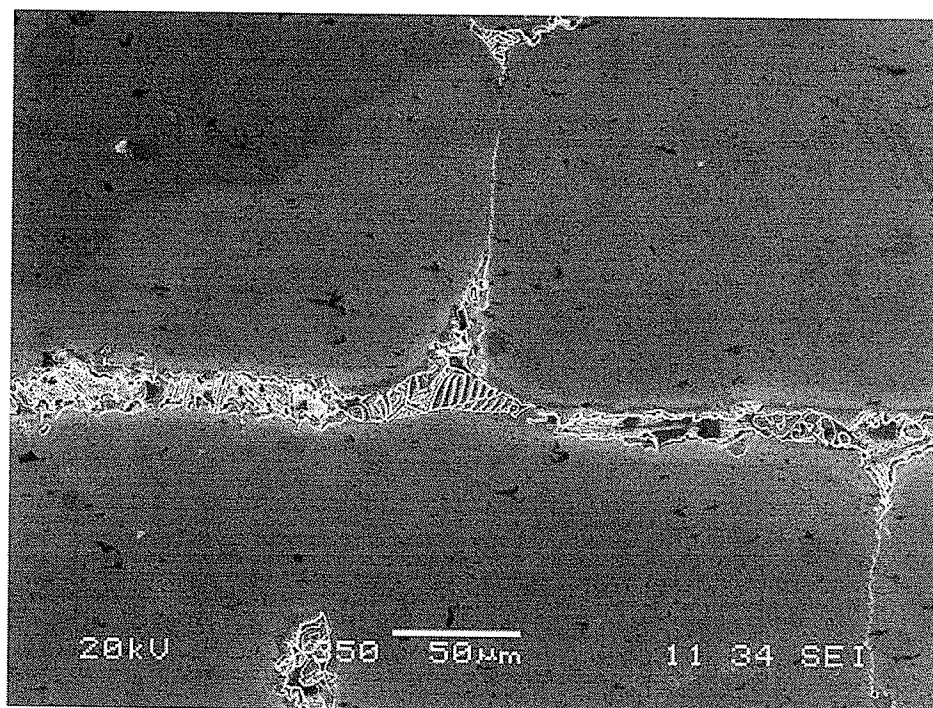


Figure 4.24: SEM micrograph of Waspaloy bonded with Microbraz 150 for 360 minutes at (a) 1200°C and (b) 1225°C.

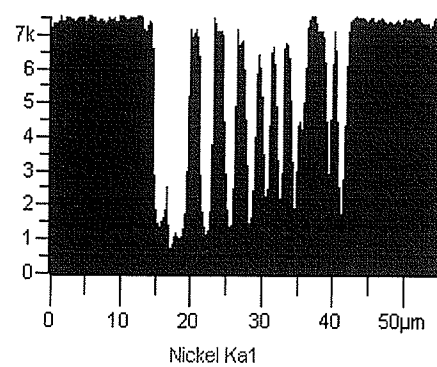
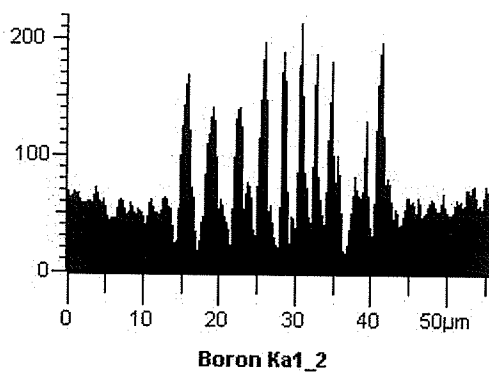
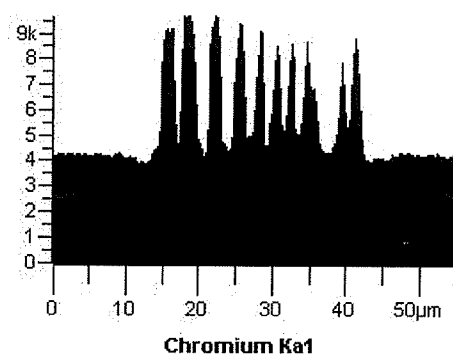
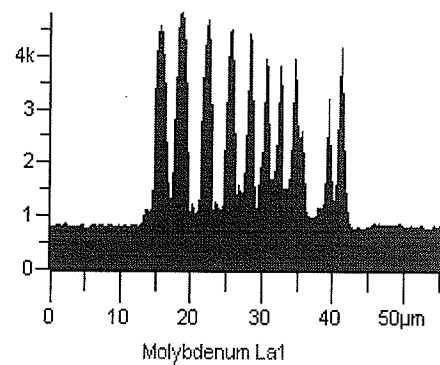
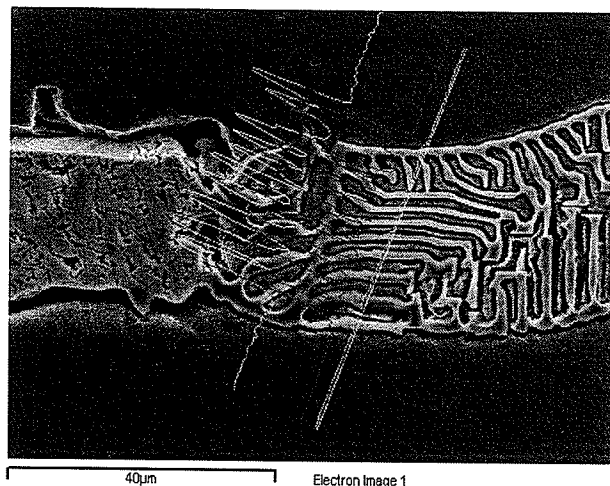


Figure 4.25: EDS spectra of eutectic cross section of Waspaloy bonded at 1175°C for 6 hours showing existence of Cr, Mo rich boron containing phase.

In addition to the formation of boride particles the average eutectic thickness did not appear to have reduced with increase in temperature from 1175°C to 1225°C. Assuming that at temperatures where reduction in isothermal solidification rate occurred was controlled by diffusion of second solute, as suggested by Sinclair et al. [6,7], a decrease in eutectic thickness with increase in temperature should be expected. This is based on the consideration that diffusivity of the second solute would increase with temperature. The observation made in the present work, however, is contrary to this concept.

According to Fick's 2nd law of diffusion, and assuming a constant diffusion coefficient,

$$\frac{\partial C}{\partial t} = D \frac{\partial^2 C}{\partial x^2} \quad (21)$$

where, $\partial C/\partial t$ is the rate of change in solute concentration with time at a given position in the base metal, which is an indication of isothermal solidification rate, D is the diffusion coefficient, and $\partial^2 C/\partial x^2$ is the rate of change in concentration gradient with distance. At any given instant, the concentration gradient ($\partial C/\partial x$) of a diffusing solute in the base metal is influenced by the solute solubility limit and thus $\partial^2 C/\partial x^2$ is also dependent on maximum solubility. Therefore, it can be seen from this equation that the diffusion controlled isothermal solidification rate is not only dependent on diffusion coefficient, but also on solubility, both of which are controlled differently by bonding temperature. An increase in temperature will cause an exponential increase in solute diffusivity according to Arrhenius relation:

$$D = D_0 e^{-\frac{Q}{RT}} \quad (22)$$

where, D is the diffusion coefficient (diffusivity), D_0 is a constant, Q is the activation energy, R is the universal gas constant, and T is the bonding temperature. However, according to the Ni-B phase diagram the solubility of boron in nickel decreases with increase in temperature above the eutectic temperature, as seen in Figure 4.26 [67]. A reduction in the solubility of boron at higher temperatures in the nickel-base superalloys used in the present work could cause a decrease in the rate of change of concentration gradient ($\partial^2 C / \partial x^2$) in the base metal during bonding. This may, according to Fick's 2nd law, decrease the rate of isothermal solidification at these higher temperatures. A decrease in solubility of boron in nickel from 320 ppm at 1125°C to 210 ppm at 1225°C has been related to reduction in isothermal solidification kinetics during diffusion brazing of pure Ni [47]. Likewise, based on analytical study of TLP bonding of binary systems, Tuah-Poku et al. [39] developed the following equation to express the dependence of isothermal solidification completion time, t , on bonding temperature:

$$t = \frac{\pi W_0^2}{16 D_0} \left[\frac{\exp\left(\frac{Q}{RT}\right)}{(C_{as})^2} \right] \quad (22)$$

where, W_0 is the initial liquid width, D_0 is the diffusion coefficient, Q is the activation energy, T is the temperature of bonding, and C_{as} is the equilibrium solidus composition of the MPD. They showed that qualitatively, as the temperature increases, t will decrease via the exponential term. However, an increase in bonding temperature simultaneously reduces the solidus composition (solid solubility), C_{as} , and hence will tend to raise t . This suggests that time, t , may not continue to monotonically decrease with increase in temperature but instead will tend to increase as the temperature reaches and exceeds a

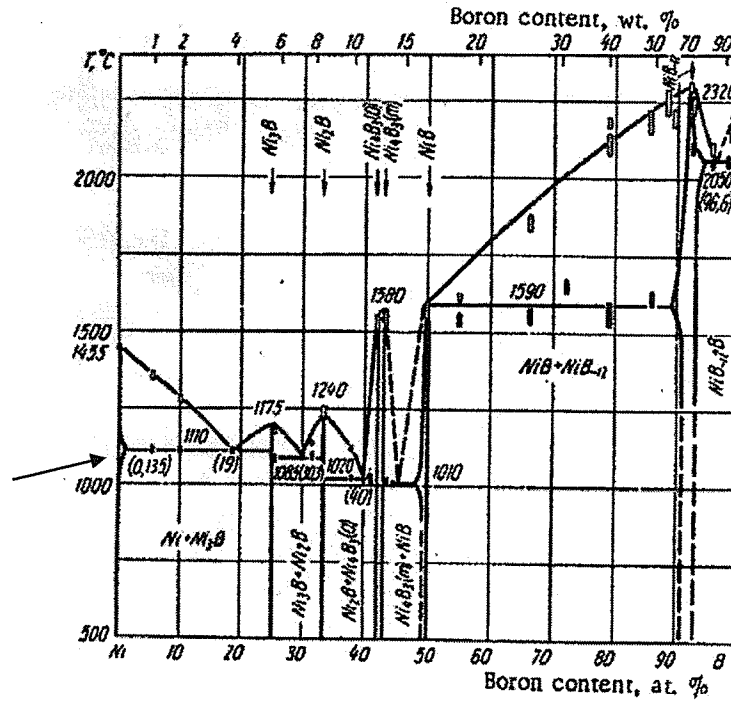


Figure 4.26: Phase diagram of nickel-boron system showing small solid solubility region of boron in nickel [67].

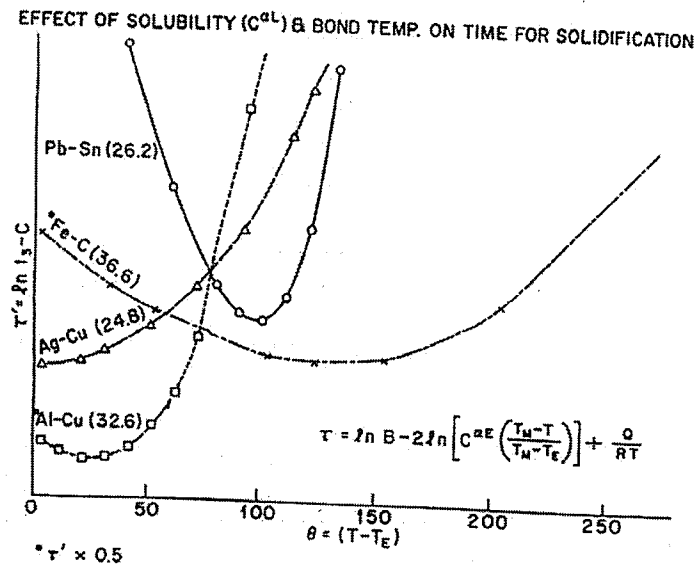


Figure 4.27: Effect of bonding temperature and solubility on total time for complete isothermal solidification for different eutectic systems [39].

critical value where the influence of reduced solubility overrides higher diffusivity. This interplay between the two opposing terms offers the possibility of minimizing the time required for a complete isothermal solidification by an appropriate selection of bonding temperature, interlayer composition, and interlayer thickness. Tuah-Poku et al. [39] calculated the temperature dependence on time, t , required for complete isothermal solidification for several systems (Fig. 4.27), however, no experimental verification of this behavior was presented. Recently, Chukwukaeme et al. [91] have also observed a reduction in isothermal solidification rate with increase in temperature above a critical value during TLP bonding of an essentially Ni-Fe-Cr ternary alloy that contained no titanium. This implies that the concept of diffusion of slower second solute that was based on the suggestion by Sinclair et al. [6,7] may not be solely responsible for the reduction in isothermal solidification rate during TLP bonding of nickel base superalloys.

An interplay between increase in diffusivity and decrease in solubility of MPD boron with increase in temperature could be an important factor contributing to the observed isothermal solidification behavior in the present work. It is plausible that the slower rate of isothermal solidification at the higher temperatures (above 1175°C) was a consequence of overriding effect of lower solubilities of boron relative to its higher diffusivity at these temperatures.

CHAPTER 5

SUMMARY AND CONCLUSIONS

Diffusion based TLP bonding of Inconel 738 with Amdry DF-3 filler alloy, and that of Waspaloy with Microbraz 150 filler alloy was carried out to study the effect of process parameters, namely temperature and time, on the joint microstructures. The results of this investigation showed that:

1. Isothermal solidification of the liquated filler metal occurred during holding at the bonding temperatures, the extent of which increased with increase in time.
2. Almost complete isothermal solidification, which precluded the formation of centerline eutectic constituent, was observed in Inconel 738 using Amdry DF-3 filler alloy at 1175°C for 420 minutes and was fully realized after 720 minutes. Complete isothermal solidification was observed in Waspaloy using NB 150 at 1145°C for 360 minutes.
3. A deviation from conventional TLP bonding diffusion models was observed in Inconel 738 samples bonded at 1190°C and 1225°C, and in Waspaloy samples bonded at 1175°C, 1200°C and 1225°C. In these samples, an increased amount of liquid, and hence the amount of centerline eutectic, was

present in the joints produced at these temperatures than that present after an equivalent hold time at lower temperatures ($<1175^{\circ}\text{C}$).

4. Increased diffusion of Ti from the base metal into the liquated filler metal at the temperatures where reduction in isothermal solidification rate occurred, was observed in Inconel 738 and Waspaloy. This may suggest that enrichment of this element in the liquated interlayer could lead to a second solidification regime controlled by the base metal and thus responsible for the slower solidification rate observed at the higher bonding temperatures.
5. However, boron rich particles were also observed among the eutectic product formed in joints prepared at the high temperatures which suggested a reduction in diffusion of boron from the liquated insert towards the base metal. In addition, the eutectic thickness did not decrease with an increase in temperature during the sluggish solidification rate regime, as would be expected even if the process was controlled by a slower diffusing second solute as suggested by Sinclair et al. Therefore, it is suggested that an increase in temperature reduced the solubility of boron in the base alloy, which in accordance with Fick's 2nd law reduced the diffusion of boron from the interlayer into the base metal. This is likely to be also a reason for reduction in isothermal solidification rate observed at higher temperatures in the present work.

6. In addition to the formation of centerline eutectic product in bonded samples, precipitation of chromium rich particles was observed in the base metal regions adjacent to the joint interface in both Inconel 738 and Waspaloy. Increase in the bonding temperature resulted in a considerable decrease in the extent of the interface precipitation.

CHAPTER 6

SUGGESTIONS FOR FUTURE WORK

1. A large amount of discussion about change in isothermal solidification rate has been related to the effect of the presence of a second solute element in the liquid interlayer. Current developments have led to the understanding that certain fundamental concepts involved in diffusional process are probably more important in controlling this rate. Further understanding of what factors, and to what extent, play roles in influencing isothermal solidification rate with increase in bonding temperature should be explored. Detailed application of computational numerical analysis of the Fick's second law to isothermal solidification of the TLP process may provide valuable understanding of this phenomenon.
2. Observation of boron containing particles at bond centerline at higher bonding temperatures in the present work suggested that there is a reduction in the amount of MPD boron diffused out of liquated region. Quantitative analysis of diffusion of MPD out of liquated insert during bonding should be explored. Diffusion of MPD during TLP bonding plays an integral role in solidification kinetics, and as such quantitative knowledge of its dependence on bonding parameters should be investigated.

3. TLP bonding of multicomponent systems inherently adds complexity in the analysis of isothermal solidification kinetics. It is suggested that simplified systems should be investigated to attribute or dispute the effect of second solute on reduction in isothermal solidification rate. Simple systems would also provide an easier approach to model the isothermal solidification rate, and allow for the use of predetermined material constants that are often difficult to obtain for more complex systems. This could be useful in comparing the effect of second solute and that of fundamental diffusional concepts (decrease in solute solubility with increase in temperature) on reduction in isothermal solidification rate at higher temperatures.
4. A systematic study of the influence of post-bond heat treatment(s) in modifying as-bond microstructure and achieving homogenization of bonded materials is necessary. This is essential in producing sound and reliable TLP joints in commercial nickel-base superalloys.

REFERENCES

- [1] Beiber, G.C., and Hihalisin, R.J., 2nd International Conf. on the Strength of Metals and Alloys, Asilomer, ASM, vol. 4, p. 1031.
- [2] Penkalla, H.J., Wosik, J., and Czystka-Filemonowicz, A., Metals and Chemistry Physics, vol. 81, 2003, p. 417.
- [3] Duvall, D.S., and Owczarski, W.A., Weld. J., vol. 46, no. 9, 1967, p. 423.
- [4] Duvall, D.S., Owczarski, W.A., and Paulonis, D.F., Weld. J., vol. 53, no. 4, 1974, p. 203.
- [5] Lugsscheider, E., Schmoor, H., Eritt, U., High Temperature Brazing and Diffusion Welding, Germany, 1995, p. 259.
- [6] Sinclair, C.W., J. Phase Equilibrium, vol. 20, no. 4, 1999, p. 361.
- [7] Sinclair, C.W., Purdy, G.R., and Morral, J.E., Metall. Trans. A., vol. 31A, 2000, p. 1187.
- [8] "Alloy IN-738: Technical Data", INCO, New York, p. 1.
- [9] Fahrman, M., et al., Acta. Metall., vol. 43, no. 3, 1995, p. 1007.
- [10] "Udimet Waspaloy", Alloy Digest, 1978, p. 1.
- [11] "Waspaloy", Special Metals, Publication Number SMC-011, 2004, p. 1.
- [12] Krieger, O.H., and Baris, J.M., Trans. Am. Soc. Met., vol. 62, 1969, p. 195.
- [13] Goken, M., and Kempf, M., Acta. Mater., vol. 47, no. 3, 1999, pg. 1043.
- [14] Chang, K-M, and Liu, X., Mat. Sci. Eng. A, vol. 308, 2001, pg. 1.
- [15] Deye, D.J., and Coutts, W.H., MiCon 78: Optimization of Processing, Properties, and Service Performance Through Microstructural Control, ASTM, 1979, p. 601.

- [16] Donachie, M.J., and Donachie, S.J., Superalloys – A Technical Guide, 2nd ed., ASM International, 2002.
- [17] Meetham, G.W., Metals Technology, vol. 11. 1984, p. 414.
- [18] Decker, R.F., and Sims, C.T., *in* The Superalloys, Sims, C.T., and Hagel, W.C., New York, 1972.
- [19] Holt, R.T., and Wallace, W., Int. Met. Rev., 1976, p. 1.
- [20] McKamey, C.G., et al., 9th International Conf. on Creep and Fracture of Engineering Materials and Structures, UK, 2001, p. 459.
- [21] Kennedy, R.L., Cao, W.D., Superalloys 1996, Pennsylvania, USA, 22-26 Sept. 1996, p. 589.
- [22] Benhaddad, S., Richards, N.L., Prasad, U., Guo, H., Chaturvedi, M.C., 9th International Symposium on Superalloys, Seven Springs, PA, USA. 17-21 Sept. 2000, p. 703.
- [23] Jena, A.K., and Chaturvedi, M.C., J. Mat. Sci., vol. 19, 1984. p. 3121.
- [24] Garosshen, T.J., and McCarty, G.P., Metall. Trans., vol. 16A, 1985, p. 1213.
- [25] Fayman, Y.C., Mat. Sci. Eng., vol. 82, 1986, p. 203.
- [26] Qiu, Y.Y., Scripta. Mater., vol. 33, no. 12, 1995, p. 1961.
- [27] Collins, H.E., and Quigg, R.J., Trans. ASM, vol. 61, 1968, p. 139.
- [28] Decker, R.F., Proceedings of Steel Strengthening Mechanism Symposium, Switzerland, 1969, p. 1.
- [29] Kotval, P.S., Venables, J.D., and Calder, R.W., Met. Trans., vol. 3, 1972, p. 453.
- [30] Okerblom, N., Institut De Soudure, Report No. 807, Paris, 1964.
- [31] Cam, G., and Kocak, M., Int. Mat. Rev., vol. 43, no. 1, 1998, p. 1.

- [32] Prager, M., and Shira, C.S., Weld. Res. Counc. Bull., no. 128, 1968.
- [33] Kelly, T.J., Proc. Symp. on Weldability of Materials, ASM International, Detroit, 1990, p. 151.
- [34] Ojo, O.A., Richards, N.L., and Chaturvedi, M.C., Scripta Mater., vol. 50, 2004, p. 641.
- [35] Ojo, O.A., Richards, N.L., and Chaturvedi, M.C., Scripta Mater. Vol. 51, 2004, p. 141.
- [36] Zhang, L., Gobbi, S.L., Loreau, J.H., J. Mat. Proc. Tech., vol. 65, 1997, p. 183.
- [37] Massalski, T.B., Binary Phase Diagrams, Vol. 1, Ni-B Phase Diagram, 1990, p. 508.
- [38] Nakao, Y., Nishimoto, K., Shinozaki, K., and Kang, C., International Institute for Welding, Document no. IA-334-86-OE, UK, 1986.
- [39] Tuah-Poku, I., Dollar, M., and Massalski, T.B., Metall. Trans. A, vol. 19A, 1988, p. 675.
- [40] MacDonald, W.D., and Eager, T.W., Annu. Rev. Mater. Sci., vol. 22, 1992, p. 23.
- [41] Nakao, Y., Nishimoto, K., Shinozaki, K., and Kang, C, Schweissen und Schneiden (Germany), vol. 44, no. 2, 1992, p. 87.
- [42] Nakagawa, H., et al., Metall. Trans., vol. 22A, 1991, p. 543.
- [43] Nakagawa, H., et al., Schweissen und Schneiden (Germany), vol. 43, no. 7, 1991, p. 140.
- [44] Zhang, X.P., and Shi, Y.W., Scripta Mater., vol. 50, 2004, p. 1003.
- [45] Lashko, N.F., Metallurgical Processes in Soldering Metals, Moscow, Metallurgy Press, 1977.

- [46] Gale, W.F., and Butts, D.A., *Sci. Tech. W. Join.*, vol. 9, no. 4, 2004, p. 283.
- [47] Ramirez, J.E., and Liu, S., *Weld. J.*, vol. 71, 1992, p. 365s.
- [48] Liu, S., Olson, D.L., Martin, G.P., and Edwards, G.R., *Weld. J.*, vol. 70, 1991, p. 207s.
- [49] Lesoult, G., *Center for Joining of Materials Report*, Carnegie Mellon University, Pittsburg, PA, 1976.
- [50] Ohsassa, K., Shinimura, T., Narita, T., *J. Phase Equilibria*, vol. 20, 1999, p. 199.
- [51] Zhou, Y., and North, T.H., *Z. Metallkd*, vol. 85, no. 11, 1994, p. 775.
- [52] Zhou, Y., *J. Mater. Sci. Letters*, vol. 20, no. 8, 1991, p. 207s.
- [53] Cain, S.R., Wilcox, J.R., and Venkatraman, R., *Acta Mater.*, vol. 45, no. 2, 1997, p. 701.
- [54] Illingworth, T.C., Golosnoy, O., Gergely, V., and Clyne, T.W., *J. Mater. Sci.*, vol. 40, 2005, p. 2505.
- [55] Shewmon, P., *Diffusion in Solids*, 2nd ed., 1989.
- [56] Ojo, O.A., Richards, N.L., and Chaturvedi, M.C., *Sci. Tech. W. Join.*, vol. 9, no. 6, 2004, p. 532.
- [57] Gale, W.F., and Wallach, E.R., *Metall. Trans. A*, vol. 22A, 1991, p. 2451.
- [58] Gale, W.F., and Wallach, E.R., *Mater. Sci. Tech.*, vol. 7, 1991, p. 1143.
- [59] Ikawa, H., Nakao, Y., and Isai, T., *Trans. Jpn. Weld. Soc.*, vol. 10, 1979, p. 24.
- [60] Nakao, Y., Nishimoto, K., Shinozaki, K., Kang, C., Shigeta, H., *Trans. Jpn. W. Soc.*, vol. 23, no. 2, 1992, p. 26.
- [61] Mishin, Y.M., and Razumovskii, I.M., *Acta Metall.*, vol. 40, 1992, p. 839.
- [62] Suto, H., and Sato, S., *Trans. JIM*, vol. 21, 1980, p. 83.

- [63] Ikeuchi, K., Zhou, Y., Kokawa, H., and North, T.H., Metall. Trans. A, vol. 23A, 1992, p. 2905.
- [64] Kokawa, H., Lee, C.H., and North, T.H., Metall. Trans. A., vol. 22A, 1991, p. 1627.
- [65] Saida, K., Zhou, Y., and North, T.H., J. Mater. Sci., vol. 28, 1993, p. 6427.
- [66] Kim, D., Kang, C., and Lee, W., Met. & Mater., vol. 5, no. 5, 1999, p. 477.
- [67] Portnoi, K.I., et al., Soviet Powder Met. Ceram., no. 2, 1967, p. 99.
- [68] Schobel, J., and Stadelmaier, H.H., Z. Metallkde, vol. 56, no. 12, 1965, p. 856.
- [69] Campbell, C.E., and Boettinger, W.J., Metall. Mater. Trans. A, vol. 31A, 2000, p. 2835.
- [70] Natsume, Y., Ohsasa, K., and Narita, T., Mater. Trans., vol. 44, no. 5, 2003, p. 819.
- [71] Nakao, Y., Nishimoto, K., Shinozaki, K., and Kang, C., Trans. Jpn. Weld. Soc., vol. 20, no. 1, 1989, p. 60.
- [72] Yeh, M.S., and Chuang, T.H., Weld. J., vol. 76, no. 12, 1997, p. 517s.
- [73] Le Blanc, A., and Mevrel, R., High Temperature Materials for Power Engineering, Belgium, 1990, p. 1451.
- [74] Jung, J.C., and Kang, C.S., Mater. Trans., vol. 37, no. 5, 1996, p. 1008.
- [75] Jalilian, F., Jahazi, M., Drew, R.A.L., Mater. Sci. Eng. A, vol. 423, 2006, p. 269.
- [76] Saha, R.K., Wei, S., and Khan, T.I., Mater. Sci. Eng. A, vol 406, 2005, p. 319.
- [77] Nishimoto, K., Saida, K., Kim, D., and Nakao, Y., ISIJ International, vol. 35, no. 10, 1995, p. 1298.

- [78] Nishimoto, K., Saida, K., Kim, D., Asai, S., Furukawa, Y., and Nakao, Y.,
Welding in the World, vol. 41, 1998, p. 121.
- [79] Kim, D., and Nishimoto, K., Metals and Materials International, vol. 8, no. 4,
2002, p. 403.
- [80] Li, W., et al., Scripta Mater., vol. 48, 2003, p. 1283.
- [81] Li, W., et al., J. Mater. Sci. Tech., vol. 18, no. 1, 2002, p. 54.
- [82] Li, X., et al., China Welding, vol. 14, no. 1, 2005, p. 19.
- [83] Xie, Y., et al., Trans. Nonferrous Met. Soc. China, vol. 13, no. 4, 2003, p. 885.
- [84] Idowu, O.A., Ojo, O.A., and Chaturvedi, M.C., Met. and Mat. Trans. A, vol. 37A,
2006, p. 2787.
- [85] Orel, S.V., Parous, L.C., and Gale, W.F., Weld. J., June 1995, p. 319s.
- [86] Gale, W.F., and Guan, Y., Metall. Mater. Trans. A, vol. 27A, 1996, p. 3621.
- [87] Rosenthal, R., West, D.R.F., Mater. Sci. Tech., vol. 15, no. 12, 1999, p. 1387.
- [88] Lee, C.H., and North, T.H., 71st American Welding Society Convention, April
1990, p. 273.
- [89] Taha, M.A., and Kurz, W., Z. Metallkd, vol. 72, no. 8, 1981, p. 546.
- [90] Idowu, O.A., Richards, N.L., and Chaturvedi, M.C., Mat. Sci. Eng. A, vol. 397,
2005, p. 98.
- [91] Chukwukaeme, C., Ojo, O.A., and Chaturvedi, M.C., University of Manitoba,
Unpublished Work.

CONTRIBUTIONS TO RESEARCH FROM THE PRESENT DISSERTATION

Articles Published in Refereed Journals

Wikstrom, N.P., Ojo, O.A., and Chaturvedi, M.C. (2006) Influence of Process Parameters on Microstructure of Transient Liquid Phase Bonded Joints of IN 738LC Superalloy using Amdry DF-3 Interlayer. *Materials Science and Engineering: A*. 417: 299-306.

Other Refereed Contributions

1. **Wikstrom, N.P.**, Idowu, O.A., Ojo, O.A., and Chaturvedi, M.C., (2006) Deviation from Conventional Transient Liquid Phase Bonding Models During Diffusion Brazing of Nickel-Based Superalloys. *Proceedings of the 3rd International Brazing and Soldering Conference*. April 23-26, 2006, San Antonio, TX, USA. pg. 6-11.
2. Idowu, O.A., **Wikstrom, N.P.**, Ojo, O.A., and Chaturvedi M.C., (2006) Transient Liquid Phase Bonding of a Nickel-base Superalloy: Effects of Process Variables. *Proceedings of the 3rd International Conference of Metallurgists: Aerospace Materials and Manufacturing*. October 1-4, 2006, Montreal, PQ. pg. 289-299.

Non-Refereed Contributions (Presentations)

1. **Wikstrom, N.P.**, Ojo, O.A., and Chaturvedi, M.C., (2006) Diffusion Brazing of Waspaloy Nickel-based Superalloy. 18th Canadian Materials Science Conference. June 19-21, 2006, Montreal, PQ.

2. **Wikstrom, N.P.**, Idowu, O.A., Ojo, O.A., and Chaturvedi, M.C., (2006) Deviation from Conventional Transient Liquid Phase Bonding Models During Diffusion Brazing of Nickel-Based Superalloys. 3rd International Brazing and Soldering Conference. April 23-26, 2006, San Antonio, TX, USA.
3. Chaturvedi, M.C., **Wikstrom, N.P.**, and Ojo, O.A. (2005) Diffusion Brazing of Inconel 738 Superalloy. European Congress on Advanced Materials and Processes. September 5-8, 2005, Prague, Czech Republic.
4. **Wikstrom, N.P.**, Ojo, O.A., and Chaturvedi, M.C., (2005) Influence of Diffusion of Elements on the Evolution of Microstructures in Transient Liquid Phase Bonded Joints of Inconel 738 LC. 17th Canadian Materials Science Conference. June 12-14, 2005, Vancouver, BC.